University of Ghana http://ugspace.ug.edu.gh

DESIGN AND FABRICATION OF A CONTROL SYSTEM FOR A PHOTOVOLTAIC-GREENHOUSE SOLAR DRYER AND PERFORMANCE EVALUATION OF THE DRYER

BY

MARY AFENYIE-ABEKAH

(10340096)

THIS THESIS IS SUBMITTED TO THE UNIVERSITY OF GHANA, LEGON IN PARTIAL FULFILMENT OF THE REQUIREMENT FOR THE AWARD OF MPHIL FOOD PROCESS ENGINEERING DEGREE

JULY 2019

University of Ghana http://ugspace.ug.edu.gh

DECLARATION

This dissertation is presented by Mary Afenyie-Abekah as a product of my research undertaken under the supervision of Professor Samuel Sefa-Dedeh of the Department of Food Process Engineering, University of Ghana.

…… …….

Mary Afenyie-Abekah DATE

(Student)

…… ……

Prof. Samuel Sefa-Dedeh DATE

(Supervisor)

University of Ghana http://ugspace.ug.edu.gh

ABSTRACT

Solar dryers have become important components for the delivery of dried agricultural products of high quality. They generally are designed to maximize the production of a heating system based on solar radiation. This study involved the design, building and testing of a control system to allow the monitoring of temperature, solar radiations and control of humidity in a Photovoltaic (PV)-Greenhouse Solar Dryer (PVGSD). This was accomplished by assembling a solar charge controller, three solar panels, a power inverter, and a battery system. An Arduino UNO Rev3, DHT22-sensor, solderless breadboard, Liquid Crystal Display (LCD) screen, jumper cables, Light-Emitting Diode (LED) red, Global System for Mobile (GSM) communication module, 10k Ω, 220 Ω and 1k Ω resistors and two 5V one channel relays formed the control system. These were assembled in a multi-functional workstation linked to the solar dryer. The GSM communication module was an innovation to allow connection to the internet over General Packet Radio Service (GPRS) network and send/receive SMS. It was used to control the fans remotely and further allowed logging of periodic sensor data (temperature, humidity, voltage and solar radiation values) by sending SMS to a phone number and server. Dryer and product characteristics were measured including temperature, humidity, solar radiation and moisture content.

The temperature and humidity profile were monitored for 11 days in the empty PVGSD without the workstation and Open Sun Drying (OSD) showed that the PVGSD recorded the highest temperature of 69^{o}C occurring between 12:00 and 14:00 hours GMT while the OSD recorded at 41.5^{o}C. The highest relative humidity recorded in the PVGSD was 75.5% and 83% for OSD observed at night from 20:00 hours to 5:00 hours GMT.

Two commodities, cassava (slices and chunks) and red pepper were dried to evaluate the dryer efficiency, and this was compared with OSD and existing greenhouse type solar dryer (GSD). The

University of Ghana http://ugspace.ug.edu.gh

cassava slices dried faster than the cassava chunks in all the drying methods indicating that sample size influenced drying rate. PVGSD had a faster drying rate for cassava slices of 0.0732g/g.h compared to 0.04908g/g.h for GSD and 0.02074g/g.h for OSD, while drying rate of PVGSD, GSD and OSD for cassava chunks were 0.0457g/g.h, 0.0355g/g.h and 0.01667g/g.h respectively. Similarly, PVGSD was observed to obtain the highest rate of drying for red pepper of 0.097g/g.h compared to GSD of 0.094g/g.h and OSD of 0.047g/g.h. The drying method, time and sample size were found to have statistical significance ($p<0.05$) on temperature, moisture content, humidity and drying rate. The PVGSD dryer with the workstation was able to keep the humidity conditions in the dryer low to prevent moisture uptake during the night. The samples in this dryer showed consistent drop in moisture content throughout the drying period.

To further evaluate the drying effect on the samples, laboratory analyses such as water activity, color profile and particle size determination were performed on the resultant dried cassava flour samples and red pepper (whole). The color profile of red pepper flour and cassava flour from the PVGSD was observed to be better in terms of the redness (a^*) for red pepper, lightness (L^*) for cassava, browning index (BI) and color change (ΔE). The color change of red pepper for PVGSD, GSD and OSD were 11.94, 16.43 and 25.25 respectively. The color change of cassava slices for PVGSD, GSD and OSD were 10.49, 10.84 and 11.59 respectively, while that for cassava chunks recorded at 10.60, 12.09 and 12.11 respectively for PVGSD, GSD and OSD. The SD_{50} values for flours from the slices were finer than those from the chunks. The SD_{50} values for cassava slices under PVGSD, GSD and OSD were 62 µm, 76 µm and 78 µm respectively, while SD_{50} values for cassava chunks under PVGSD, GSD and OSD recorded at 80 µm, 92 µm and 106 µm respectively. In general, cassava slices under the three drying methods demonstrated a better quality than the chunks in terms of color and particle size. All samples were dried to a water activity below 0.500

University of Ghana http://ugspace.ug.edu.gh

to prevent microbial spoilage. Final water activity for red pepper was 0.384, 0.388 and 0.414 respectively for PVGSD, GSD and OSD, while that for cassava slices and chunk for PVGSD was 0.361 and 0.415 respectively, GSD was 0.384 and 0.446 respectively and OSD recorded at 0.421 and 0.490 respectively.

To further understand and describe the drying curves for the samples under the three drying methods, 12 Thin Layer Mathematical models were evaluated. The best model under this study for red pepper is the Midilli and Kucuk model under both PVGSD and GSD while Logarithmic model describes best under OSD. Approximation of diffusion model can be used for cassava slices under PVGSD and GSD, while Midilli and Kucuk model for OSD. These models were selected according to the lowest Root Mean Square Error (RMSE) and chi square (χ^2) and highest correlation coefficient (R^2).

University of Ghana http://ugspace.ug.edu.gh

DEDICATION

I devote this research to my parents Mr. John Kojo Abakah and Mrs. Mary Afenyie-Abekah. I have reached this level of education because of their sacrifices, love, emotional and financial support and most importantly their prayers. I pray for God's everlasting grace and blessings upon their lives. Thank you all abundantly.

University of Ghana http://ugspace.ug.edu.gh

ACKNOWLEDGEMENTS

I am forever grateful to God for his abundant grace, strength and wisdom to come this far and seeing me through this entire research study.

My sincere appreciation also goes to Prof. Samuel Sefa-Dedeh, for his tremendous supervision, guidance, financial support and constructive criticisms throughout this project and a mentor throughout my career journey and Prof. F. K. Saalia for his assistance. Many thanks also go to Ghana Energy Commission for providing the solar panels and its accessories and Carnegie for partially funding this research.

My final thanks go to all friends and colleagues who helped in diverse ways especially Mr. Delali Kanda and Mr. Bernard Kuditchar for their selfless provision of assistance. God bless you all.

University of Ghana http://ugspace.ug.edu.gh

TABLE OF CONTENTS

DECLARATION ii
ABSTRACT iii
DEDICATION vi
ACKNOWLEDGEMENT vii
LIST OF FIGURES xi
LIST OF TABLES xiii
LIST OF ILLUSTRATIONS xv
LIST OF ABBREVIATIONS xvi
CHAPTER ONE 1
1.0 INTRODUCTION 1
1.1 Drying 1
1.2 Objectives 3
1.3 Specific Aims 3
CHAPTER TWO 5
2.0 LITERATURE REVIEW 5
2.1 Drying 5
2.1.1 Mechanism of drying 5
2.1.2 Drying Rate 7
2.1.3 Water activity, α_w 8
2.2 Open sun drying 9
2.2.1 Drying of Red Pepper 9
2.2.2 Drying of Cassava (*Kokonte*) 10
2.3 Solar Dryer 10
2.3.1 Greenhouse Solar Dryer 11
2.4 Thin layer solar drying 13
2.4.1 Mathematical models 14
2.4.2 Determination of the moisture effective diffusivity coefficients 15
2.5 Process control system 16
CHAPTER THREE 18
3.0 MATERIALS AND METHODS 18
3.1 MATERIALS 18
3.1.1 Multi-Function Control System 18

University of Ghana http://ugspace.ug.edu.gh

3.1.2 PV-Greenhouse Solar Dryer, Drying Rack and Trays 27
3.1.3 Food Samples for Dehydration 27
3.2 METHODS 27
3.2.1 Multi-Function Control System 27
3.2.2 PV-Greenhouse Solar Dryer Drying rack and Trays 41
3.2.4 Drying Experiment of Red Pepper 48
3.2.5 Drying Experiment of Cassava samples 50
3.2.6 Laboratory Analysis 52
3.2.7 Size Reduction 54
3.2.8 Particle Size Distribution 54
3.3 STATISTICAL DATA ANALYSIS 55
CHAPTER FOUR 56
4.0 RESULTS AND DISSCUSSIONS 56
4.1 Multi-Function Control System 56
4.1.1 Control system function – Simulation output 56
4.1.2 Development of Control system function – Prototype stage 58
4.1.3 Development of Control system function – Actual design 58
4.2 Design characteristics and construction of the multifunction workstation 59
4.3 Design, construction and evaluation of performance of the PV-greenhouse solar dryer. 61
4.3.1 Design and construction of the dryer 61
4.3.2 Temperature and relative humidity profile of the empty PV greenhouse solar dryer and open sun drying 62
4.4 Drying of Red Pepper and Cassava samples in the PV-Greenhouse Solar Dryer (PVGSD), Greenhouse Type Solar Dryer (GSD) and Open Sun (OSD) 65
4.4.1 Climate variation 65
4.5.2 Drying Kinetics 75
4.6 Mathematical modelling for the drying process of red pepper and cassava using the three drying methods, PVGSD, GSD and OSD. 90
4.6.1 Mathematical modelling for red pepper 90
4.6.2 Mathematical modelling for Cassava slices and chunks. 95
4.7 Moisture effective diffusivity 112
4.7.1 Moisture effective diffusivity of Red pepper 112

University of Ghana http://ugspace.ug.edu.gh

4.7.2 Moisture effective diffusivity of Cassava slices and chunks 113
4.8 Post Drying Evaluation by Analyzing Quality Indices of the Dried Samples 115
4.8.1 Water Activity, a_w 115
4.8.2 Color Profile 117
4.8.3 Particle Size Distribution (PSD) 122
CHAPTER FIVE 125
5.0 CONCLUSION AND RECOMMENDATION 125
5.1 CONCLUSIONS 125
5.2 RECOMMENDATIONS 126
REFERENCES 127
APPENDICES 131
APPENDIX 1: PROGRAM CODE FOR THE ARDUINO UNO 131
APPENDIX 2: TEMPERATURE AND RELATIVE HUMIDITY PROFILE 136
APPENDIX 3: TEMPERATURE, RELATIVE HUMIDITY (RH) AND SOLAR RADIATION DATA FOR PVGSD, GSD AND OSD. 139
APPENDIX 4: MOISTURE CONTENT VARIATION OF RED PEPPER 140
APPENDIX 5: DRYING RATE OF RED PEPPER 141
APPENDIX 6: MOISTURE CONTENT OF CASSAVA USING 80WATTS BATTERY 142
APPENDIX 7: DRYING RATE OF CASSAVA USING 80WATTS BATTERY 143
APPENDIX 8: MOISTURE CONTENT OF CASSAVA USING 1200WATTS BATTERY 144
APPENDIX 9: DRYING RATES OF CASSAVA USING 1200WATTS BATTERY 145
APPENDIX 10: ANALYSIS OF VARIANCE (ANOVA) ON COLOR PROFILE FOR RED PEPPER 146
APPENDIX 11: ANALYSIS OF VARIANCE (ANOVA) ON COLOR PROFILE FOR CASSAVA 147
APPENDIX 12: PARTICLE SIZE DISTRIBUTION OF CASSAVA FLOUR 148

University of Ghana http://ugspace.ug.edu.gh

LIST OF FIGURES

Figure **Title** **Page**

1: Representative drying curve showing periods of drying (Source: Mercer, 2018) 7
2: Classification of solar dryers (source: (Hage *et al.*, 2018)) 11
3: Classification of greenhouse solar dryer (Source: Singh et al., 2018) 12
4: Block diagram of the energy generation function 28
5: Wiring diagram of DHT22-sensor to Arduino 30
6: Wiring diagram of LCD screen to Arduino 31
7: Wiring diagram of the relays to the Arduino and fans 32
8: Wiring diagram of the Arduino to GSM communication module. 33
9: Block diagram for the Arduino to voltage divider 34
10: The wiring diagram for the connection for solar radiation measurement 35
11: Complete wiring diagram of the control system function using Fritz software. 36
12: Circuit diagram of the control system function using Proteus 8 Professional. 37
13: The Simulation Circuit 39
14: Modification based on the classification of greenhouse solar dryer 44
15: The simulation virtual terminal output 56
16: Day 1 Changes in temperature of empty PVGSD and OSD 62
17: Day 6 Changes in temperature of empty PVGSD and OSD 63
18: Day 11 Changes in temperature of empty PVGSD and OSD 63
19: Day 1 Changes in relative humidity in the empty PVGSD and OSD 64
20: Day 6 Changes in relative humidity in the empty PVGSD and OSD 64
21: Day 11 Changes in relative humidity in the empty PVGSD and OSD 65
22: Changes in ambient temperature and solar radiation during drying of red pepper 66
23: Comparison of the temperatures of PVGSD, GSD and OSD during drying of red pepper 67
24: Comparison of the relative humidity of PVGSD, GSD and OSD during drying of red pepper. 67
25: Changes in ambient temperature and solar radiation during drying of cassava 69
26: Comparison of the temperatures of PVGSD, GSD and OSD during drying of cassava samples 70
27: Comparison of the relative humidity of PVGSD, GSD and OSD during drying of cassava samples 70
28: Comparison of the temperatures of PVGSD, GSD and OSD during drying of cassava samples 72
29: Comparison of the relative humidity of PVGSD, GSD and OSD during drying of cassava samples 73
30: Moisture content variation with time for red pepper 76
31: Changes in drying rate with time for red pepper in PVGSD, GSD and OSD. 78
32: Changes in moisture content with time of red pepper at various shelf position inside the PVGSD. 79
33: Changes in drying rate with time of red pepper at various shelf position inside the PVGSD. 80

University of Ghana http://ugspace.ug.edu.gh

34: Changes in content with time of cassava slices in PVGSD GSD and OSD. 82
35: Changes in moisture content with time of cassava chunks in PVGSD GSD and OSD..... 82
36: Changes in moisture content with time of cassava slices under PVGSD, GSD and OSD 85
37: Changes in moisture content with time of cassava chunks under PVGSD, GSD and OSD.. 85
38: Variations in drying rate with time for cassava slices in PVGSD, GSD and OSD. 87
39: Variations in drying rate with time for cassava chunks in PVGSD, GSD and OSD..... 87
40: Variations in drying rate with time for cassava slices in PVGSD, GSD and OSD. 89
41: Variations in drying rate with time for cassava chunks in PVGSD, GSD and OSD..... 89
42: Experimental Midilli and Kucuk model curve for red pepper under PVGSD..... 92
43: Experimental Midilli and Kucuk model curve for red pepper under GSD..... 92
44: Experimental Logarithmic model curve for red pepper under OSD. 93
45: Experimental Approximation of diffusion model curve for Cassava slices under PVGSD.. 99
46: Experimental Approximation of diffusion model curve for Cassava slices under GSD..... 99
47: Experimental Midilli and Kucuk model curve for Cassava slices under OSD..... 100
48: Experimental Verma et. al model curve for Cassava Chunks under PVGSD. 104
49: Experimental Midilli and Kucuk model curve for Cassava chunks under GSD. 104
50: Experimental Logarithmic model curve for Cassava chunks under OSD. 105
51: Experimental Midilli and Kucuk model curve for Cassava slices under PVGSD..... 109
52: Experimental Midilli and Kucuk model curve for Cassava slices under GSD..... 109
53: Experimental Midilli and Kucuk model curve for Cassava slices under OSD..... 110
54: Experimental Wang and Singh model curve for Cassava chunks under PVGSD. 111
55: Experimental Midilli and Kucuk model curve for Cassava chunks under GSD. 111
56: Experimental Midilli and Kucuk model curve for Cassava chunks under OSD. 112
57: Variation of logarithm of red pepper moisture ratio with time for PVGSD..... 113
58: Variation of logarithm of cassava slices moisture ratio with drying time for PVGSD. 114
59: Variation of logarithm of cassava chunks moisture ratio with drying time for PVGSD..... 115
60: Cumulative frequency plot for PSD of PVGSD slices and chunks 123
61: Cumulative frequency plot for PSD of GSD slices and chunks 123
62: Cumulative frequency plot for PSD of OSD slices and chunks 124

University of Ghana http://ugspace.ug.edu.gh

LIST OF TABLES

Tables **Title** **Page**

1: Mathematical models for describing the drying kinetics 15
2: Specifications of solar panel 19
3: Specification of solar charge controller. 20
4: Specification of the Power Inverter 21
5: Specification of Delkor HICA80 battery 22
6: Specification of Sunfit 6GFM100 battery 22
7: Technical specification of Arduino UNO Rev3 23
8: Specification of DHT22-sensor 24
9: Specification of relay. 25
10: Key features of SIM900 26
11: Analysis of Variance (ANOVA) of Temperature variations of Red Pepper during drying. . 68
12: Analysis of Variance (ANOVA) of Humidity variations of Red Pepper 68
13: Analysis of Variance of (ANOVA) Temperature variations of Cassava samples during drying. 71
14: Analysis of Variance (ANOVA) of Humidity variations of Cassava samples during drying. 71
15: Analysis of Variance of (ANOVA) Temperature variations of Cassava samples during drying. 73
16: Analysis of Variance (ANOVA) of Humidity variations of Cassava samples during drying. 74
17: ANOVA of Moisture Content changes for Red Pepper 77
18: ANOVA of Drying rates changes for Red Pepper 78
19: Analysis of Variance (ANOVA) of Moisture Content changes at different shelf position for Red Pepper 80
20: Analysis of Variance (ANOVA) of Moisture Content changes at different shelf position for Red Pepper 81
21: ANOVA of Moisture Content changes for Cassava samples 83
22: ANOVA for Moisture Content changes for Cassava samples 86
23: Analysis of Variance (ANOVA) of Drying rate changes for Cassava samples 88
24: Mathematical models and respective constants for PVGSD of Red Pepper. 93
25: Mathematical models and respective constants for GSD of Red Pepper. 94
26: Mathematical models and respective constants for OSD of Red Pepper. 95
27: Mathematical models and respective constants for PVGSD of Cassava Slices. 96
28: Mathematical models and respective constants for GSD of Cassava Slices 97
29: Mathematical models and respective constants for OSD of Cassava Slices. 97
30: Mathematical models and respective constants for PVGSD of Cassava Chunks. 101
31: Mathematical models and respective constants for GSD of Cassava Chunks. 102
32: Mathematical models and respective constants for OSD of Cassava Chunks. 103
33: Mathematical models and respective constants for PVGSD of Cassava Slices. 106
34: Mathematical models and respective constants for GSD of Cassava Slices. 107

University of Ghana http://ugspace.ug.edu.gh

35: Mathematical models and respective constants for OSD of Cassava Slices. 108
36: Values of moisture effective diffusivities for different drying methods of red pepper. 113
37: Values of moisture effective diffusivities for different drying methods for cassava slices and chunks. 114
38: Final average water activity of dried samples 116
39: Analysis of Variance (ANOVA) of Water Activity changes for Red Pepper 117
40: Analysis of Variance (ANOVA) of Water Activity changes for Cassava samples 117
41: The color indicators of fresh and dried red pepper under the PVGSD, GSD and OSD. 119
42: The color indicators of fresh and dried cassava slices and chunks under the PVGSD, GSD and OSD. 119

University of Ghana http://ugspace.ug.edu.gh

LIST OF ILLUSTRATIONS

Illustrations **Title** **Page**

1: Open sun drying of pepper (a and b) and cassava (c) 2
2: Front view of the workstation 40
3: Back view of the workstation 40
4: Left view (left) and Right view (right) of the workstation 41
5: The front view of the PV-Greenhouse solar dryer 42
6: The side view of the Greenhouse solar dryer 42
7: Existing greenhouse type solar dryer (Source: Obimpeh, 2018) 43
8: Front view of the PV-greenhouse solar dryer 45
9: Side view of the PV-greenhouse solar dryer 45
10: Back view of the PV-greenhouse solar dryer 46
11: Three-dimensional view of the rack (left) and sieve (right) 46
12: Drying of red pepper samples under GSD (a), OSD (b) and PVGSD (c) 49
13: Drying of cassava slices and chunks under GSD (a), OSD (b) and PVGSD (c) 51
14: Measured parameters sent via SMS 57
15: Prototype of the control system component 58
16: Shows the control system component opened (left) and cased (right) inside the workstation 59
17: Front view (left) and back view (right) of the multifunction workstation 60
18: Inside the multifunction workstation 60
19: Complete experimental set-up of the PV-greenhouse solar dryer and the multifunction workstation 61
20: Accumulation of moisture on the surface of the polycarbonate sheet inside the GSD 74
21: No accumulation of moisture on the surface of the polycarbonate sheet inside the PVGSD 75
22: Dried red pepper under PVGSD (a), GSD (b) and OSD (c). 120
23: Dried red pepper powder under PVGSD (a), GSD (b) and OSD (c). 120
24: Dried cassava slices under PVGSD (a), GSD (b) and OSD (c). 121
25: Dried cassava slices flour under PVGSD (a), GSD (b) and OSD (c). 121
26: Dried cassava chunks under PVGSD (a), GSD (b) and OSD (c). 122

University of Ghana http://ugspace.ug.edu.gh

LIST OF ABBREVIATIONS

PVGSD – Photovoltaic- greenhouse solar dryer

GSD – Greenhouse solar dryer

OSD – Open sun drying

M_o – initial moisture content

M_t – moisture content at time t (d. b)

M_e – equilibrium moisture content (d. b)

MR – moisture ratio

DR – drying rate (d. b)

W_w – weight of wet material

W_d – weight of dried material

a, b, c, g, h, k, n – empirical constants in drying models

n – number of constants

N – number of observations

A_w – water activity

D_{eff} – Moisture effective diffusivity

ΔE – total color change

BI – browning index

H^0 – hue angle

P – power

V – voltage

t – time (s)

w. b – wet basis

d. b – dry basis

Subscripts

exp – experimental

pre – predicte

University of Ghana http://ugspace.ug.edu.gh

CHAPTER ONE

1.0 INTRODUCTION

1.1 Drying

The reasons for food losses include improper cultivation, lack or improper application of technology for post-production handling, improper transportation and marketing within the food system. Food preservation can reduce post-harvest food losses (Tiwari *et al*., 2016). There are several food preservation methods including food drying or dehydration. Dehydration turns perishable food materials into shelf-stable products and avoids microbial spoilage by reducing their water activity to appropriate safe levels (Marques *et al.*, 2009). This in many cases reduces packaging and transportation costs and improving product quality and availability.

Drying is an energy-intensive method contributing to 10-25% of the entire energy utilized in the food industries globally (Strumillo and Adamiec, 1996). The four major drying techniques are identified mainly by the energy source used. These include open air (sun), electrical, firewood/fuel and solar drying (Tiwari *et al.*, 2016). Simple drying systems such as solar drying bridge the gap of addressing the issue of the perishability of food commodities and the availability of energy resources. It provides relatively low running cost making it suitable to be applied in the rural areas in a developing country like Ghana.

In Ghana, open sun drying is widely practiced, the commodities are placed on the ground or on a mat under the sun (Illustration 1). Even though this method is simple and economical, it has several limitations with respect to control of the drying process and parameters; weather variations such as rain, wind, etc.; demand large drying area; insect infestation and introduction of foreign materials and dust thereby producing low quality products (Jain and Pathare, 2007).

University of Ghana http://ugspace.ug.edu.gh

(a) (b)

(C)

Illustration 1: Open sun drying of pepper (a and b) and cassava (c)

According to Singh *et al*., (2018), many drying equipment and techniques developed are energy intensive and indirectly increase the cost of product. Following the recent development in solar drying equipment, it has provided an alternative option to dry products of good quality while using minimal energy costs. Singh *et al*., (2018), reported many modifications in the implementation of the active and passive method of drying to advance the greenhouse solar dryer's performance including;

i. PV integrated greenhouse solar dryer
ii. Use of opaque Northern wall to insulate and prevent heat loss.

University of Ghana http://ugspace.ug.edu.gh

iii. Use of thermal storage materials i.e. rock-bed, sand, black painted concrete floor and PVC sheet, to allow continuous drying in greenhouse dryers when there is no sun.

iv. The use of reflecting and inclined North wall to trap utmost solar radiations.

v. Use of solar air heater in greenhouse dryers to attain faster drying.

Obimpeh, (2018), designed and constructed a passive mode greenhouse type solar dryer and used it to dry cassava chips and cocoa beans. She reported relatively good drying rates but observed that there was increase in humidity and the partially dried samples picked up moisture overnight and this is partly because solar drying design has relied on natural conditions to effect drying with no control systems for managing humidity in the dryer.

1.2 Objectives

The key objective of this research was to design and construct a Photovoltaic (PV)-assisted greenhouse solar dryer with humidity and temperature sensor control system and evaluate dryer performance.

1.3 Specific Aims

The specific aims were;

1. To design, build and test a control system for the PV-greenhouse solar dryer.
2. To design and construct a PV assisted greenhouse solar dryer with shelves to increase load capacity and introduce solar-powered fans to improve the flow of air during drying.
3. To study the temperature-humidity profile of the dryers over a period considering the prevailing weather conditions.
4. To compare the drying characteristics of the greenhouse solar dryer with existing dryer and open sun drying of red pepper and cassava and applying mathematical models for the drying curves.

University of Ghana http://ugspace.ug.edu.gh

5. Evaluate selected quality parameters on the dried products and link these to dryer performance and consumer acceptability.

University of Ghana http://ugspace.ug.edu.gh

CHAPTER TWO

2.0 LITERATURE REVIEW

2.1 Drying

Drying of food commodities as a form of preservation is one of the oldest techniques practiced around the world. Drying can simply be defined as a process of removing water from a product involving simultaneous heat and mass transfer with precise process control (Karthikeyan and Murugavelh, 2018). Drying of food products is done mainly to reduce spoilage by decreasing the moisture level, hence improving the storage life of the product. Also, by removing appropriate amounts of water, the shelf-life can be extended, reduction in overall weight and often its volume to lessen storage, packing and transportation costs (Mercer, 2018).

Solar drying is widely practiced in developing countries such as Ghana. It is an effective method of exploiting the solar energy and storing food products for an extended period without deteriorating.

Even though, open sun drying is much preferred in the rural areas, crops are easily contaminated with dirt, pest infestation and other foreign materials. Postharvest losses to birds, rodents and other animals are often experienced. Solar dryers provide economic advantages over the other dryers making it a better alternative especially for rural and off-grid communities.

2.1.1 Mechanism of drying

Food drying is a time dependent method that can be described as a kinetic process that deals with the movement of water molecules within the food material being dried. Drying involves four stages; warm-up period, constant rate period, falling rate period and complete removal of moisture.

University of Ghana http://ugspace.ug.edu.gh

The first stage of drying, when a wet food material enters the dryer, there may be a relatively short period where heat is being absorbed and the product is brought to equilibrium temperature it assumes with the drying medium. During the warm-up period, there may be a slight moisture loss. In many cases, drying begins immediately and there is no obvious warm-up period, especially for materials under room temperature, warm-up period may not be observed (Mercer, 2018).

During the constant rate period, there is enough heat to vaporize water found at the surface of the material. Due to the saturation of moisture at the surface, moisture is evaporated at a uniform and constant rate. And this will remain present as long as there is enough flow of moisture from the interior of the wet material to replace moisture lost at the surface due to evaporation. This period depends on the air temperature, humidity, area of exposed surface and speed of moisture to the surface (Karthikeyan and Murugavelh, 2018; Mercer, 2018).

A falling rate period occurs when evaporation of the surface moisture progress to a point where internal moisture cannot reach the surface quickly enough to replenish the surface moisture pool. As such, moisture begins to diffuse through the pores in the material from its inner regions where it is evaporated at the surface by hot air in the dryer while drying rate gradually decreases.

During this stage of drying, moisture removal is diffusion-controlled, and the drying rate is reliant on the physical nature of the material, temperature and its moisture content (Karthikeyan and Murugavelh, 2018; Mercer, 2018).

As time progresses, the moisture inside the material reduces until ultimately approach a complete removal of moisture. The Figure 3 below shows the drying curve based on moisture content against time. A similar plot of the weight of the material versus time can be used since the change in weight is as a result of water lose during drying (Mercer, 2018).

University of Ghana http://ugspace.ug.edu.gh

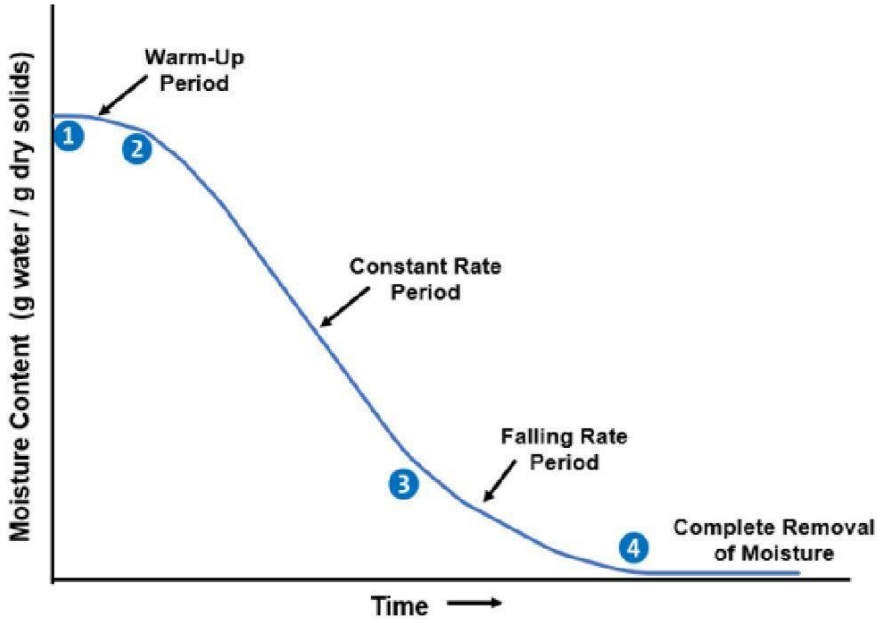

Figure 1: Representative drying curve showing periods of drying (Source: Mercer, 2018)

2.1.2 Drying Rate

Drying rate is achieved by the temperature and initial moisture content of the product as well as the temperature, relative humidity and velocity of the drying air (Belessiotis and Delyannis, 2011). It is determined from the time when the dryer is charged with fresh samples till dried to the required moisture level. A graphical presentation as seen in Figure 1 above, of the moisture content against the time indicates the drying rate, a similar plot of the weight of the material against time, since the change in weight is due solely to the removal of water during drying, could be plotted as drying rate curve (Mercer, 2014).

The drying rate of the different commodities is calculated as equation (1) (Wang *et al*., 2018);

$$DR = \frac{M_{t1} - M_{t2}}{t_2 - t_1} \quad (g/h) \qquad \text{Eq. (1)}$$

where, M_{t1} and M_{t2} are the moisture contents at time t_1 and t_2, respectively; t_1 and t_2 are the drying times in hours.

University of Ghana http://ugspace.ug.edu.gh

The rate of water removal from a product and ultimately the quality of the product after drying is greatly affected or influenced by two factors (Mercer, 2018);

a) Product-related attributes

b) Dryer-related attributes

Product-related attributes that can affect the drying rate include; the product composition and structure of material; surface characteristics; the particle size; moisture content and specific heat of the material (Mercer, 2018).

Dryer-related attributes is also a contributing factor to the rate of drying, these include; the type of dryer, the air temperature and relative humidity (Mercer, 2018).

2.1.2.1 Humidity

Humidity is expressed as the amount of water vapour or moisture in the atmosphere. It plays a key role in drying processes and influence the drying rate of materials. Humidity can be categorized into absolute humidity or relative humidity. Relative humidity (rh) is the percentage of saturated water vapour or humidity at a specified temperature while Absolute humidity (AH) measures the actual mass of moisture in air irrespective of temperature (g/kg, g/m^3 or kg/kg) (Kemp, 2007).

Drying rate generally increase with increasing temperatures and decreasing humidity. Rate of drying are usually higher at higher temperature and lower at higher relative humidity (Sigge, *et al*., 1998). Also, Observations from work done by Obimpeh, (2018), showed that at higher humidity especially during the night or during relatively low temperatures tend to slow the drying rate due to food materials picking up moisture in the drying chamber.

2.1.3 Water activity, (α_w)

Another important attribute for food preservation is water activity, an index that influences microbial growth, occurrence of enzymatic and non-enzymatic browning, etc. (Belessiotis and

University of Ghana http://ugspace.ug.edu.gh

Dalyannis, 2011). Every agricultural food has a water activity level below which microorganisms cannot survive (Belessiotis and Dalyannis, 2011). The majority of bacteria survive in the region of $\alpha_w = 0.85$ mold, yeast about $\alpha_w = 0.61$ and fungi at $\alpha_w < 0.70$, etc.

Keeping the water activity at a lower limit by drying helps to prevent food spoilage and hence improving the shelf life stability.

2.2 Open sun drying

Solar radiation hitting the surface of a food material during drying is either absorbed or reflected. The temperature of the food material is increased due to the absorbed radiation and moisture travels to the surface by convection. Water vapour diffusion begins and mass of material finally decreases in the form of evaporated moisture from the surface of the material. The rate of dehydration depends on the rate of the diffusion process (Tiwari *et al*., 2016).

In Ghana, open sun drying is widely used to preserve food commodities such as pepper, cassava, salted dried tilapia (*Koobi*) and cocoa.

2.2.1 Drying of Red Pepper

The cayenne chilli pepper (*Capsicum annuum* L.) is a vital spice used in culinary and industrial purposes providing strong colour and flavour. It could be eaten fresh, dried and in the form of powder. However, it is highly perishable due to its high moisture content. In Ghana, red pepper is dried under the sun by spreading on mats, sheets or on the bare floor usually by the road sides (Figure 1). This demands long drying hours, a large area and the product is prone to contamination with foreign materials, hence substantial losses and poor-quality dried product occur. During drying, these products may undergo physical and chemical changes which influence their storage properties and quality attributes. (Yang *et al.*, 2018).

University of Ghana http://ugspace.ug.edu.gh

2.2.2 Drying of Cassava (*Kokonte*)

Cassava (*Manihot esculenta Crantz*) is a highly valued staple food in Ghana along with rice and maize. In West Africa, cassava is used both in animal feed and human food (Koua *et al.*, 2009) and the tubers are handled in several forms for consumption. Cassava like any other fresh agricultural produce is highly perishable and hence value-addition is paramount to increase shelf life and reduce postharvest losses. Drying allows safe storage of cassava pieces over a long period by decreasing the biological deterioration rate of raw cassava. Cassava drying in Ghana is mostly done under the open sun. Prior to drying, the cassava is peeled, washed and cut into halves or big chunks.

The method of drying cassava affects the final quality of the cassava flour and the drying rate is influenced by the geometry and the weather conditions. According to Dziedzoave *et al.* (2003), the rate of drying of the cassava pieces has an influence on the final colour and particle size distribution. Longer drying rates gives room for microbial (specifically molds) contamination which in tend can affect the color quality of the dried product.

2.3 Solar Dryer

To address the numerous drawbacks of open sun drying, solar dryers have been developed (Everitt and Stanley,1976). Several researches have been done to improve solar drying technology by employing auxiliary source of heating, forced and natural circulation to achieve the desirable drying characteristics (Kumar *et al.*, 2016). During solar drying, moisture is evaporated from the products by solar heated air temperature of 50 to 60°C in the drying chamber because of solar radiation trapped inside the dryer.

Solar drying has proven to enhance the product quality considerably, minimize crop losses and shorten drying time for a given commodity as likened to the traditional methods of drying (Kumar

University of Ghana http://ugspace.ug.edu.gh

et al., 2016; Tiwari *et al.*, 2016). Solar dryers also have the advantage of optimizing energy and time while occupying less space for producing better quality dried products with almost zero energy cost.

According to Hage *et al*., (2018), solar dryers are categorized based on the mode of heat transfer, air flow and structure of dryer. Figure 2 shows the classification of solar dryers.

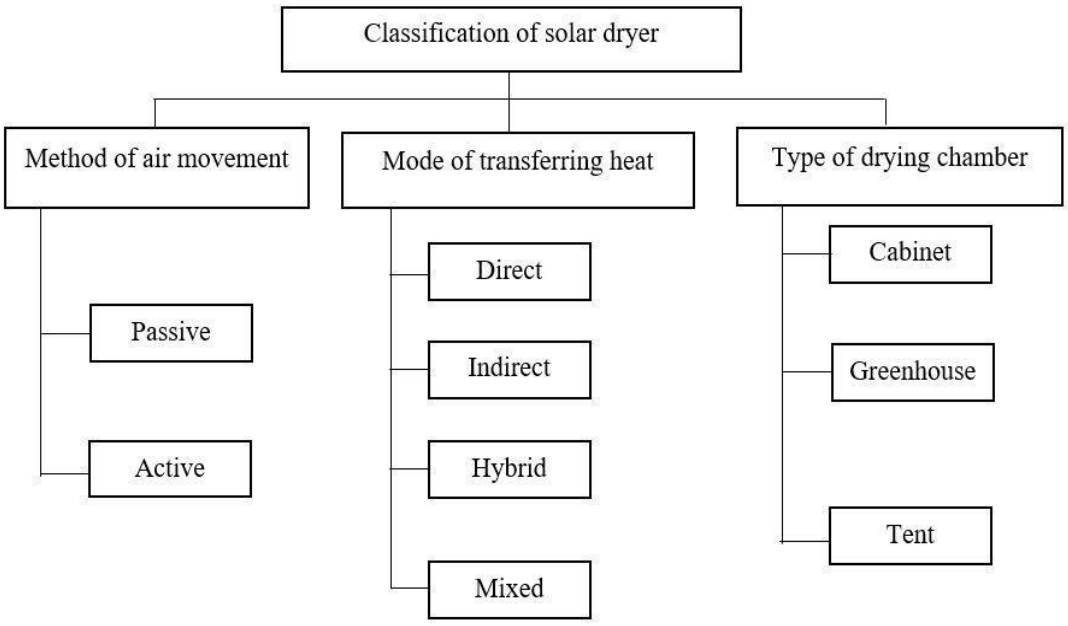

Figure 2: Classification of solar dryers (source: (Hage *et al*., 2018))

2.3.1 Greenhouse Solar Dryer

Greenhouse dryers are used in several applications. The greenhouse solar dryer works under the principle of greenhouse effect, it permits short wavelength solar radiations from the sun while trapping the long wavelength solar radiations inside the drying chamber (Singh *et al*., 2018). This type of dryer principally functions either in active mode (forced convection) or passive mode (natural convection). The passive mode greenhouse solar dryer uses a ventilator or chimney to provide natural movement of air entering inside the dryer. While in the active mode greenhouse

University of Ghana http://ugspace.ug.edu.gh

solar dryer, exhaust fan is used for extracting humid air outside the dryer (Singh *et al.*, 2018).

According to Singh *et al.*, (2018), modifications in greenhouse solar dryers have been classified on the basis of airflow, dryer structure, covering material, north wall and the dryer floor to improve performance and efficiency.

Figure 3 below shows in detail the various design options and specifications that can be applied in the modification of a greenhouse solar dryer.

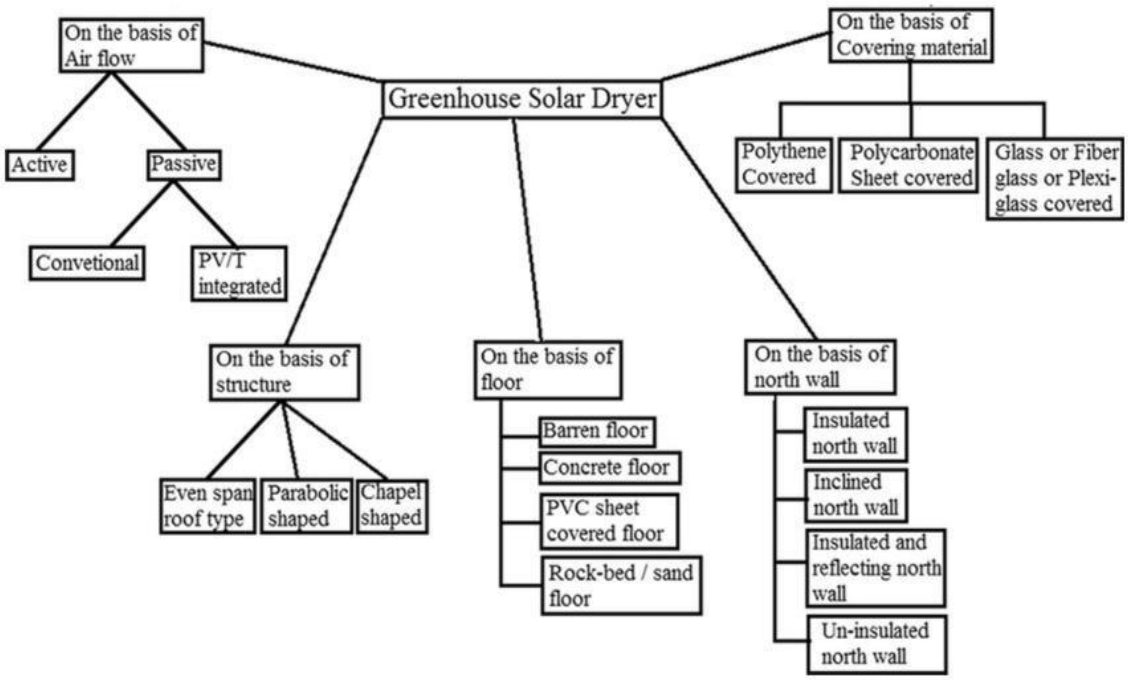

Figure 3; Classification of greenhouse solar dryer
(Source: Singh *et al.*, 2018)

The installed exhaust fan in a forced mode greenhouse aid in ventilating extra moisture from the drying chamber especially during low temperatures and can also sustain the desired atmosphere for drying (Chauhan *et al.*, 2018; Singh *et al.*, 2018) and can be recommended for high moisture content products. High quality dried products can be achieved with controlled temperature and humidity conditions.

University of Ghana http://ugspace.ug.edu.gh

2.4 Thin layer solar drying

To help predict the drying performance of several agricultural products, researchers have developed several theoretical and empirical equations for thin layer drying. For thin layer drying, the assumption that the ratio of air volume to crop volume is infinitely large, hence drying rate depends on the characteristics of the material to be dried, sample size, drying temperature and the moisture content (Tiwari *et al.*, 2016). These models have been used to evaluate drying times of many agricultural products and to generalize drying curves. The measured moisture content of the material at any time after undergoing drying conditions is used to develop the thin layer drying models (Akpinar, 2006).

Thin layer drying equations require moisture ratio (*MR*) variation versus time (*t).* To achieve the best model, regression analysis is done with the selected models to ascertain the constant values. Validation of the various models is analyzed with various statistical methods. The value of the correlation coefficient (R^2) is one of the main criteria for selection. Other statistical parameters include root mean square error (RMSE) and chi-square (χ^2) test, to select best of fit. These parameters are calculated from equations 2, 3 and 4 below (Erbay and Icier, 2010; Fadhel *et al.*, 2014; Karthikeyan and Murugavelh, 2018);

$$R^2 = \frac{\sum_{i=1}^{n}(MR_i - MR_{pre,i}).\ \sum_{i=1}^{n}(MR_i - MR_{exp,i})}{\sqrt{[\sum_{i=1}^{n}(MR_i - MR_{pre,i})^2].[\sum_{i=1}^{n}(MR_i - MR_{exp,i})^2]}} \qquad Eq.(2)$$

$$\chi^2 = \frac{\sum_{i=1}^{N}(MR_{exp.i} - MR_{pre.i})^2}{N-n} \qquad \text{Eq.(3)}$$

$$RMSE = [\frac{1}{N}\sum_{i=1}^{N}(MR_{exp.i} - MR_{pre.i})^2]^{\frac{1}{2}} \qquad \text{Eq.(4)}$$

University of Ghana http://ugspace.ug.edu.gh

Where; $MR_{exp.i}$ is the ith experimentally observed moisture ratio; $MR_{pre.i}$ is the ith predicted moisture ratio; *n* is the number constants; *N* is the number of observations.

According to Erbay and Icier, 2010, the model is said to be good fit if R^2 value is high, χ^2 and RMSE values are low.

2.4.1 Mathematical models

Some of the mathematical models used to describe the drying kinetics and calculate moisture ratio (MR) under thin layer drying are listed in Table 1 below. The moisture ratio in dry basis (d.b.) is expressed with equation 5 as (Zhang *et al*., 2019):

$$MR = \frac{M_t - M_e}{M_o - M_e} \qquad \text{Eq.(5)}$$

Where M_t is the moisture content at any time *t*, M_o is the initial moisture content, M_e is the equilibrium moisture content which approximately equals to zero.

The drying rate (DR) of the samples is calculated using equation 6 (Wang *et al.*, 2018; Zhang *et al.*, 2019):

$$DR = \frac{M_{t1} - M_{t2}}{t_1 - t_2} \qquad \text{Eq. (6)}$$

where, t_1 and t_2 represent drying time, M_{t1} and M_{t2} are the moisture contents (d.b.) at time t_1 and t_2, respectively.

University of Ghana http://ugspace.ug.edu.gh

Table 1: Mathematical models for describing the drying kinetics

Model no.	Model Name	Model
1	Newton	MR= exp (-kt)
2	Henderson and Pabis	MR = a exp (–kt)
3	Page	MR = exp(–kt^n)
4	Modified Page	MR= exp(-(kt)^n)
5	Two term	MR = a exp(-k_0t) + b exp(-k_1t)
6	Wang and Singh	MR = 1 + at + bt^2
7	Approximation of diffusion	MR=a exp(-kt) + (1-a) exp(-kbt)
8	Logarithmic	MR= a exp(-kt) + c
9	Two-term exponential	MR= a exp(-kt) + (1- a) exp (-kat)
10	Midilli and Kucuk	MR = a exp(-kt^n) + bt
11	Verma et. al	MR= a exp(-kt) + (1-a)exp(-gt)
12	Modified Henderson and Pabis	MR=aexp(-kx) + bexp(-gx) + cexp(-hx)

Source: (Karthikeyan and Murugavelh, 2018; Tiwari *et al*., 2016)

2.4.2 Determination of the moisture effective diffusivity coefficients

The term moisture effective diffusivity describes the rate of moisture movement irrespective of the mechanism involved. The moisture transport processes are modeled mathematically using Fick's second law to ascertain the moisture effective diffusivity (D_{eff}) of several foods undergoing drying equation 7 (Wang *et al*., 2018):

$$\frac{\partial M}{\partial t} = D_{eff}\nabla^2 M \qquad \text{Eq.(7)}$$

University of Ghana http://ugspace.ug.edu.gh

With the assumption of disregarding constant temperature, shrinkage, diffusion coefficients and uniform initial moisture distribution, equation 7 is solved using the analytical solution given in Equation 8 (Chong *et al.*, 2008):

$$MR = \frac{M_t - M_e}{M_o - M_e} = \frac{8}{\pi^2} \sum_{n=0}^{\infty} \frac{1}{(2n+1)^2} exp\left(-\frac{(2n+1)^2 \pi^2 D_{eff} t}{4L^2}\right) \quad \text{Eq.(8)}$$

Equation 8 is made simpler by taking the first term of series solution:

$$MR = \frac{8}{\pi^2} exp\left(-\frac{\pi^2 D_{eff} t}{4L^2}\right) \quad \text{Eq.(9)}$$

Taking logs gives the following equation:

$$ln(MR) = ln\left(\frac{8}{\pi^2}\right) - \left(\frac{\pi^2 D_{eff}}{4L^2}\right) t \quad \text{Eq.(10)}$$

The effective diffusivity is determined by taking the slope of equation when natural *In(MR)* versus drying time (*t)* is plotted, a straight line with the slope k_0 is obtained:

$$k_0 = -D_{eff}\left(\frac{\pi^2}{4L^2}\right) \quad \text{Eq.(11)}$$

where, D_{eff} is the moisture effective diffusivity (m^2/s) and L is the half thickness of the sample.

2.5 Process control system

The drying rate or the rate at which moisture evaporates depends on many factors including temperature, airflow rate and relative humidity. Precise control of humidity is critical for maintaining product quality. While the temperature of air is increased the relative humidity is decreased hence increasing the rate of drying or otherwise. The drying rate of products in solar dryers is mostly slower at night when the temperature is minimum, and humidity is maximum. This makes it paramount to control the humidity mostly at night. To keep the humidity in the

University of Ghana http://ugspace.ug.edu.gh

drying chamber at an acceptable level to help reduce the drying rate of the food samples, extractor or exhaust fans are introduced into the solar dryer design to extract excess moisture out of the dryer based on a programmed embedded device that interact with environmental variables such as temperature and humidity. This can be constructed using the microcontroller Arduino and sensors, which can read the temperature and humidity inside the solar dryer and display the information on a serial monitor or a liquid crystal display (LCD) and also send output data via a short message service (SMS) and communicate via general packet radio service (GPRS).With the required programming software, a microcontroller board such as an Arduino can serve as a platform to create and develop interacting objects that can sense the environment and control it. Work has been done by Dangi, (2017), using Arduino based microcontroller and sensors to monitor environmental parameters such as humidity and temperature in and outside buildings.

University of Ghana http://ugspace.ug.edu.gh

CHAPTER THREE

3.0 MATERIALS AND METHODS

The research was conducted in three sections.

a. Development and testing of the control system and its accompanying multifunction workstation.
b. The design and construction of the PV-greenhouse solar dryer.
c. Thin layer modeling of the drying of a) pepper and b) cassava slices and chunks and post drying evaluation.

3.1 MATERIALS

3.1.1 Multi-Function Control System

a. Energy Generation

The various components used to generate power to the entire system were three (03) solar panels (All Tech, Model:AT-SP30, South Korea), a solar charge controller (All Tech, Model: BSC-10A, South Korea), a power inverter (All Tech, Model: AT-500A 12V, South Korea), a 12V battery (Delkor, Model: HICA80, South Korea) and two 12V battery (Sunfit, Model: 6GFM100, Korea). A detail description of the components is listed below.

i. Solar Panel

Three 30W solar panels of dimension 55 x 43x 0.25 cm each were connected in parallel to supply the same voltage across. When the battery was connected, the maximum output voltage received was 17.7V and an open circuit voltage of 21.85V when no load (battery or fan) was connected. The Table 2 shows the detail specifications of the solar panel.

University of Ghana http://ugspace.ug.edu.gh

Table 2: Specifications of solar panel

Parameter	Specification
Peak power (Pmax)	30 W
Production tolerance	±3%
Maximum power current (Im)	1.69 A
Maximum power voltage (Vm)	17.7 V
Short circuit current	1.84 A
Open circuit voltge	21.85 V
Maximum system voltage	1000 VDC
Dimensions	550 x 430 x 25 mm
Weight	2.8kg
AM	1.5
Energy	1000 W/m^2
Tc	25°C

ii. Solar Charge Controller

The BSC-10A 12V/24V type solar controller uses the Pulse Width Modulation (PWM) charging method of photovoltaic power generation. This allows slowly a low quantity of power sent to the battery as it becomes fully charged. It has a timer function that can be set up to 15 hours in two modes of daily or 365 days. The LCD screen shows the voltage of the battery, the time and load connected. The controller has three terminals for the solar module, battery and load. Table 3 shows detail specification of the solar charge controller.

University of Ghana http://ugspace.ug.edu.gh

Table 3: Specification of solar charge controller.

Parameter	**Specification**	
Rated cable charging current	10A	
Rated load current	10A	
System voltage	12V	24V
Overload, short circuit protection	Yes	
No load current	≤20mA	
Charging circuit voltage drop	Not more than 0.26V	
Discharging circuit voltage drop	Not more than 0.15V	
DC charge voltage	14.4V	28.8V
Float charging	13.7V	27.4V
Output voltage	10.5V	21V
Temperature compensation	-5mV/°C/2V	

iii. DC to AC Power Inverter

The power inverter was used to change the direct current (DC) power from the battery into alternating current (AC) power. A power inverter (model; AT-500A 12V, Korea) was used as a source of power to the Arduino UNO and the GSM module. A detail specification is shown in Table 4.

University of Ghana http://ugspace.ug.edu.gh

Table 4: Specification of the Power Inverter

Parameter	Description
Output power continuous rated output capacity	500W
Standby current No-load power consumption	<400 mA
Dc Input Voltage DC Input Voltage	10.5 to 15V
AC Output Voltage AC Output Voltage	220Vac
Over Load Shut-Down Overload Shutdown	500W ± 10% (Fuse)

iv. Battery

A 12-volt Delkor HICA80 and two 12-volt Sunfit 6GFM100 batteries were used . The batteries were charged by the energy supply through the charge controller from the solar panels. A detail specification is shown in Table 5 and Table 6.

University of Ghana http://ugspace.ug.edu.gh

Table 5: Specification of Delkor HICA80 battery

Parameter	Specification
Model	HICA80
Voltage	12V
AH(20HR)	80Ah
Polarity	L(-,+)
Length	277 mm
Width	174 mm
Height	174 mm
Power	80 watts

Table 6: Specification of Sunfit 6GFM100 battery

Parameter	Specification
Model	6GFM100
Voltage	12V
AH	100Ah
Power	1200 watts

b. Control System

The control system component consisted of an Arduino UNO Rev3, DHT22-sensor, solderless breadboard, liquid crystal display (LCD) screen, LED red, jumper cables, GSM communication module, 10k, 220 Ω and 1k resistors and two 5V one channel relays. A detail description of the components is listed below.

University of Ghana http://ugspace.ug.edu.gh

i. Arduino UNO Rev3

This was an open source single-board microcontroller based on ATmega328P for building digital objects and interactive devices (Dangi, 2017). It had 14 digital input/output pins (of which 6 could be used as PWM outputs), 6 analog inputs, a 16 MHz quartz crystal, a USB connection, a power jack, an ICSP header and a reset button. Detail technical specification is listed in Table 7.

Table 7: Technical specification of Arduino UNO Rev3

Parameter	**Specification**
Microcontroller	ATmega328P
Operating Voltage	5V
Input Voltage (recommended)	7-12V
Input Voltage (limit)	6-20V
Digital I/O Pins	14 (of which 6 provide PWM output)
PWM Digital I/O Pins	6
Analog Input Pins	6
DC Current per I/O Pin	20 mA
DC Current for 3.3V Pin	50 mA
Flash Memory	32 KB (ATmega328P) of which 0.5 KB used by bootloader
SRAM	2 KB (ATmega328P)
EEPROM	1 KB (ATmega328P)
Clock Speed	16 MHz
LED_BUILTIN	13
Length	68.6 mm
Width	53.4 mm
Weight	25 g

University of Ghana http://ugspace.ug.edu.gh

ii. DHT22 Sensor

DHT22 is a temperature and humidity sensor that is temperature compensated and calibrated with extreme precision and the calibration-coefficient saved in a One-Time-Programmable (OTP) Memory. During detection, it references this coefficient from memory. The relatively small size, low power consumption and long-distance range of the DHT22-sensor makes them suitable for harsh environmental conditions. The sensor DHT22 performance range and accuracy are shown in the Table 8 below.

Table 8: Specification of DHT22-sensor

Parameter	**Specification**
Temperature	-40 to 80°C
Humidity	0 to 100 % RH
Accuracy	
Temperature	<±0.5°C
Humidity	±2% (Max ±5%)
Operating voltage	3.3V to 6V DC

iii. Resistors

Resistors were used to regulate the flow of electrical current in the electronic circuit. A two 10k Ω, 1k Ω and 220 Ω resistors were used for the connection.

iv. Relay

Two 5V one channel relays were used to control much higher voltage and current than the Arduino. The output terminals of the relay consist of one common terminal (COMM), one normally closed

University of Ghana http://ugspace.ug.edu.gh

terminal (NC) and one normally open terminal (NO). The relays are used to switch on/off the fans. Table 9 shows the detail specification of the relay.

Table 9: Specification of relay.

Parameter	**Specification**
Control voltage	5V DC
VCC	5V power supply
GND	Ground
IN	Input signal
NO	Normally open
NC	Normally closed
COMM	Normally common

v. GSM Communication Module

Global System for Mobile (GSM) communication module allowed connection to the internet over general packet radio service (GPRS) network and send/receive SMS. GSM SIM900 was used to control the fans remotely through sending an SMS to turn on or off based on a specified absolute humidity threshold value. The GSM further allowed logging of periodic sensor data (temperature, humidity, voltage and solar radiation values) by sending SMS to an allocated phone number and server. It also had the capacity to send notifications via SMS to the cellphone when the sensor reading fails. Table 10 shows the features of the GSM SIM900.

University of Ghana http://ugspace.ug.edu.gh

Table 10: Key features of SIM900

Feature	Implementation
Power supply	3.4V – 4.5V
Frequency bands	SIM900 quad-band: GSM 850, EGSM 900, DCS 1800, PCS 900
GSM class	Small MS
Transmitting power	Class 4 (2W) at GSM 850 and EGSM 900 Class 1 (1W) at DCS 1800 and PCS 1900
GPRS connectivity	GPRS multi-slot class 10
Temperature range	-30°C to +80°C
Timer function	Programmable via AT command
Real time clock	Implemented

c. Air Flow Control System

Two sensor-controlled extractor fans were installed at the top front view of the greenhouse-dryer to draw out excess moisture from the drying chamber. These were 50 watts, 12V of 12.6inches diameter with a 12inches blade fan.

d. Multifunction Workstation

The multifunction workstation performed two functions; energy generation and the control of temperature and humidity. A workstation was fabricated from aluminum sheet to house the two units providing these functions. The structure of total dimension of 1.22m x 0.61m x 0.89m comes with a handle and mounted on four wheels to allow easy movement.

University of Ghana http://ugspace.ug.edu.gh

3.1.2 PV-Greenhouse Solar Dryer, Drying Rack and Trays

Considerations given in the selection of materials for constructing the solar dryer were; ability to trap solar radiation for drying purposes and local availability of the materials. The greenhouse dryer was constructed using wood (0.0508m x 0.1016m x 4.2672m; 0.0508m x 0.0762m x 4.2672m; 0.0254m x 0.3048m x 4.2672m and polycarbonate sheet. Drying trays were constructed hand-woven cane sieves fixed to 0.58m x 0.55m wooden frames. The racks were constructed with wood (0.0508m x 0.0508m).

3.1.3 Food Samples for Dehydration

a. Red Pepper

Fresh red peppers (*Capsicum annuum* L.) were purchased from a local market (Agbogbloshie, Accra, Ghana). Prior to drying, the peppers were sorted, pedicles were removed and washed. The surface water was quickly wiped with tissue paper.

b. Cassava Samples

Cassava samples (*Manihot esculenta*) were purchased from a local market (Madina, Accra, Ghana). Prior to drying, samples were weighed, sorted, manually peeled and washed. For the first batch, a total weight of 20.7kg of cassava was peeled and 11.88kg of peeled cassava was used in the drying process. For the second batch of drying, a total weight of 38.24kg of cassava was peeled and 22kg of peeled cassava was used in the drying process.

3.2 METHODS

3.2.1 Multi-Function Control System

a. Energy Generation

The energy generation component was designed to supply power to a) charge the battery, b) the fans installed on the solar dryer, c) the control system and d) provide AC electrical power for other

University of Ghana http://ugspace.ug.edu.gh

devices. This was to allow continuous operation of the systems. It was envisaged that the use of solar panels to generate and store power in the batteries will be very useful for operation in rural areas where grid power supply may not be available. Three solar panels, each with a 30-watts capacity were connected in parallel. The positive and negative terminals were then connected to the solar charge controller at a polarity of L (+,-). The battery was then connected to the solar charge controller. The charge controller charged the battery with energy received from the solar panels and kept the voltage at 12V. The charge controller protected the battery from overcharging and also protected the panels from current back flow from the battery. The power inverter was connected to the battery, to convert the direct current (DC) to alternating current (AC) (Figure 4). A plug wall multi-socket was connected to the power inverter to supply power to AC electrical devices.

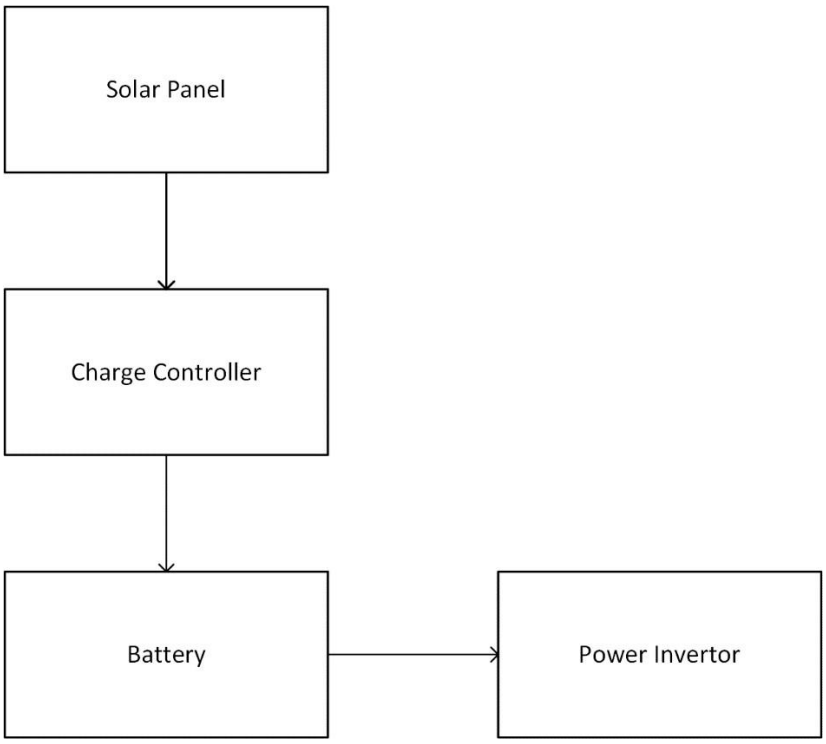

Figure 4: Block diagram of the energy generation function

University of Ghana http://ugspace.ug.edu.gh

b. Control System

The control system was designed and built to monitor and help control the humidity in the PV-greenhouse solar dryer;

a) The microcontroller was programmed with the aid of a temperature and humidity sensor to read the temperature and relative humidity inside the dryer
b) The microcontroller was programmed to turn on and off the extractor fans at a set absolute humidity
c) The microcontroller was programmed with the voltage value based on the sun's intensity received from the solar panels, measure the solar radiation
d) The microcontroller was programmed to send output data through GSM communication module to a phone and a server.

The following connections were made for the system to function properly;

1. Arduino to DHT22- sensor
2. Arduino to LCD
3. Arduino to relays
4. Arduino connection to GSM communication module
5. Arduino connection for measuring solar radiation

DHT22-sensor to Arduino UNO Rev3

Pin 1 (positive) of the DHT22-sensor was connected to the power source of the Arduino (5V or VCC terminal on the Arduino). Pin 4 (negative) of the DHT22-sensor was connected to the Ground (GND) terminal on the Arduino. Pin 2 (out) of the DHT22-sensor was connected to digital pin 2 on the Arduino. A Light emitting diode (LED red) was connected to signal on or off when the

University of Ghana http://ugspace.ug.edu.gh

humidity value goes above or below the specified threshold value. A 220 Ω resistor was connected across the anode of the LED and digital pin 9 of the Arduino, whilst the cathode of the LED was connected to ground. Power was supplied to the Arduino by either connecting the positive and negative terminals of a 9V battery to the Vin and GND respectively of the Arduino or powered by the power inverter using a USB cable. The wiring diagram of the connection can be seen in Figure 5.

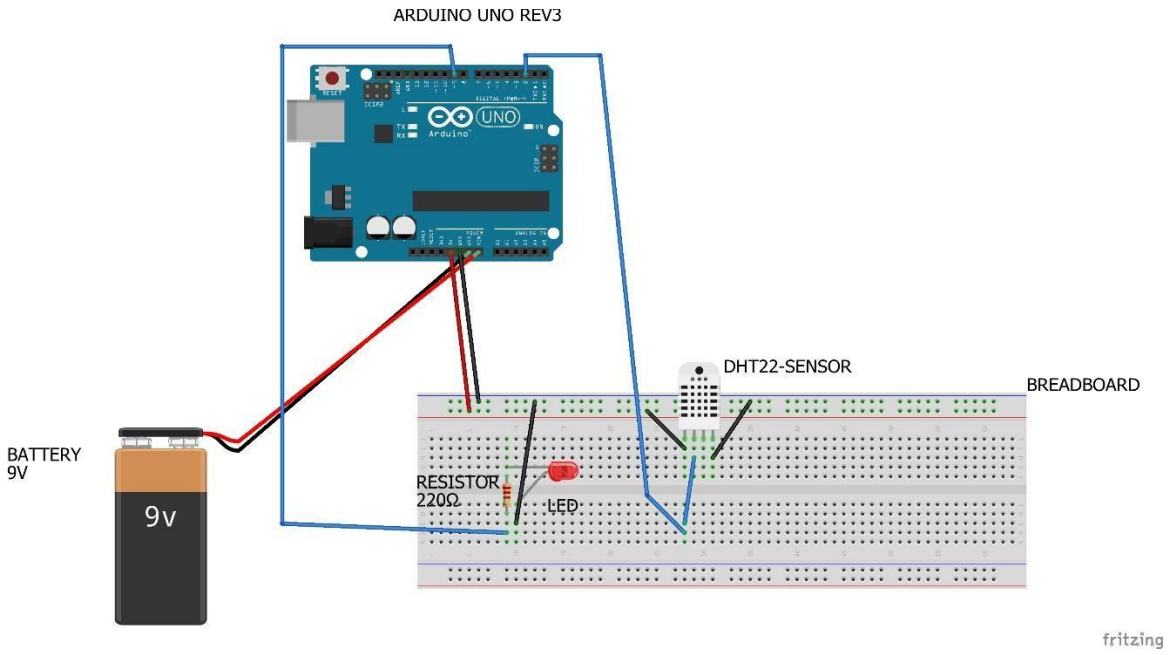

Figure 5: Wiring diagram of DHT22-sensor to Arduino

LCD screen to Arduino UNO Rev3

The liquid crystal display (LCD) screen was connected to the Arduino UNO to enable display of near real time sensor values from the DHT22-sensor. The pins RS, RW, E, D4, D5, D6 and D7 of the LCD were already connected to pins 4, 5, 6, 9, 10, 11 and 12 of the I2C bus respectively. Pins GND, VCC, SDA and SCL of the I2C bus were connected to Analog pins GND, VCC, A4 and A5 on the Arduino. The wiring diagram of the connection can be seen in Figure 6.

University of Ghana http://ugspace.ug.edu.gh

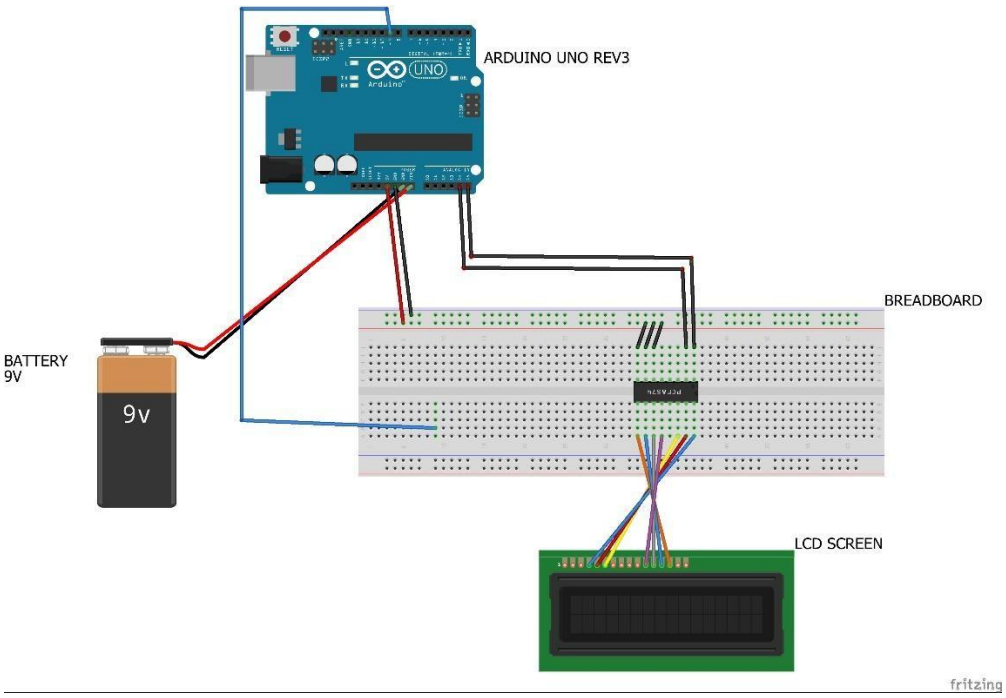

Figure 6: Wiring diagram of LCD screen to Arduino

Relays to Arduino UNO Rev3

Two 5V one channel relays were employed in the circuitry to control the two 12V fans. The VCC and GND terminals of the relays were connected to the VCC (5V) and GND pins of the Arduino respectively. The signal pins of the relays were connected to digital pins 7 and 8 of the Arduino. Making the relay connected to digital pin 7 the primary fan and digital pin 8 the secondary fan. The positive terminals of the fans were connected to positive terminal of the battery, the negative terminals of the fans to the normally open (NO) of the relays and the negative terminal of the battery to the common GND (COMM) pin of the relays. The wiring diagram of the connection can be seen in Figure 7.

University of Ghana http://ugspace.ug.edu.gh

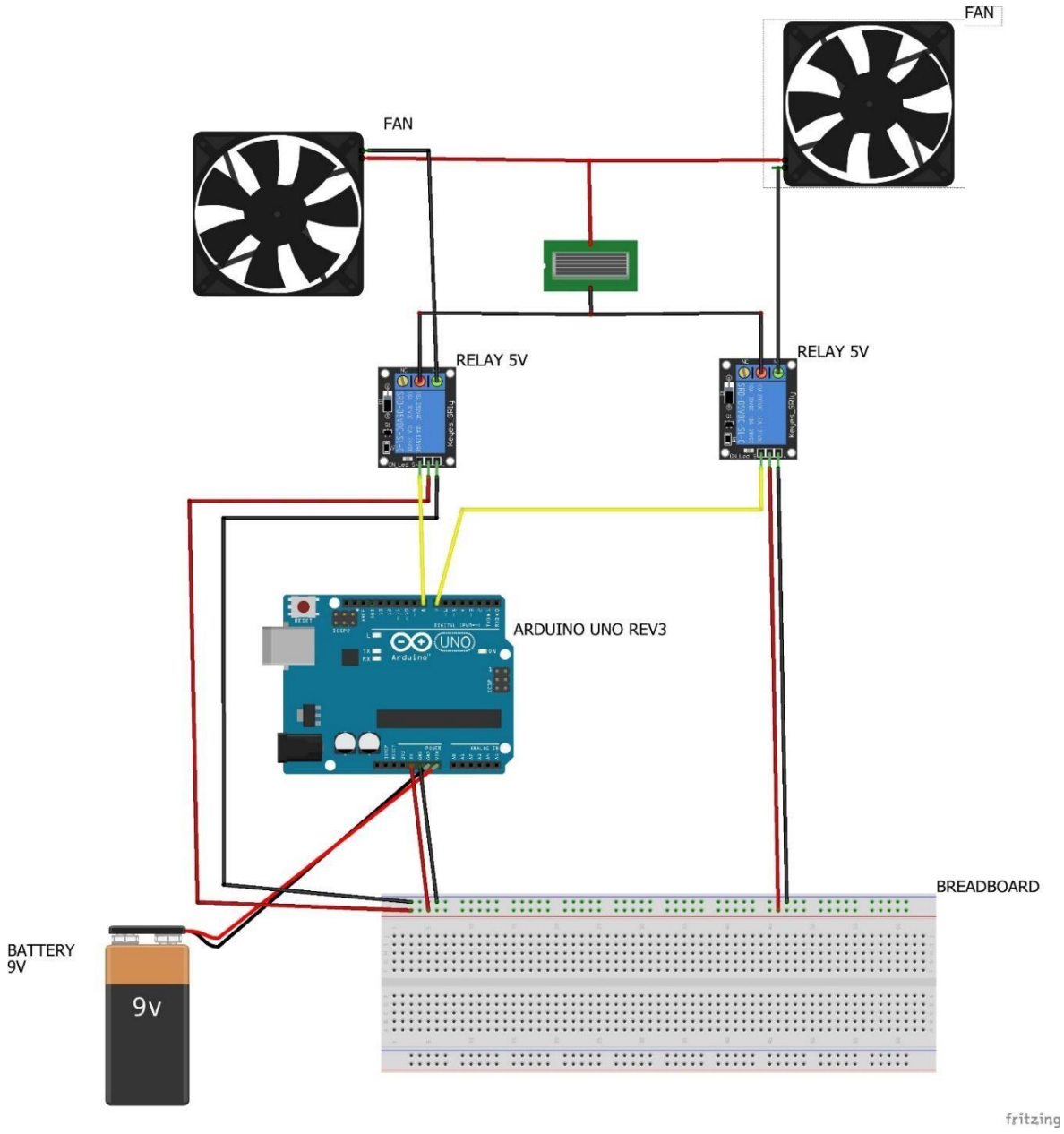

Figure 7: Wiring diagram of the relays to the Arduino and fans

GSM communication module to Arduino connection

Pins TXD and RXD of the GSM module were connected to digital pins 4 and 5 respectively of the Arduino. Pin GND of the GSM module was connected to GND of the Arduino. The wiring diagram of the connection can be seen in Figure 8.

University of Ghana http://ugspace.ug.edu.gh

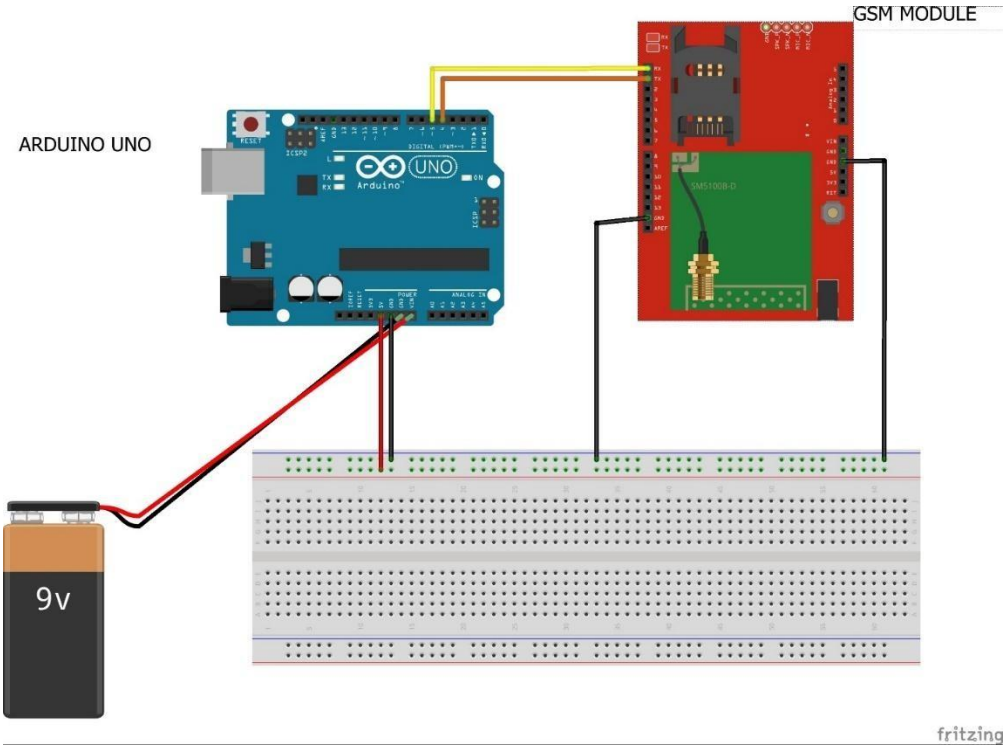

Figure 8: Wiring diagram of the Arduino to GSM communication module.

Arduino connection for solar radiation measurement

Solar irradiance is the power per unit area received from the sun in the form of electromagnetic radiation in the wavelength range of the measuring instrument. The instrument to measure solar radiation is a Pyranometer but due to the inaccessibility of this instrument, the Arduino was programmed to estimate the amount of solar radiation incident on the solar panels.

The principle for this was based on the fact that solar cells generate energy by converting solar energy from the sun into electrical energy. Sunlight is collected directly by the photovoltaic (PV). The higher the energy (radiation and light energy) from the sun, the higher the voltage produced. Hence the higher the light intensity the higher the voltage across the terminals of the solar panel (Jumaat and Othman, 2018). This was used to estimate the solar radiation. Based on the light intensity incident on the solar panel the voltage was recorded and used in the calculation of power.

University of Ghana http://ugspace.ug.edu.gh

The solar radiation was estimated by calculating the power from the solar cell and dividing by its area. The area of the solar panel was measured as 0.7095m^2. The formula for the power used in the program code was;

$$P = \frac{V^2}{R} \text{ watts} \qquad \text{Eq. (12)}$$

The maximum Arduino Analog Reference voltage required was 5V. To avoid the risk of damaging the analog pins, the voltage was measured using a voltage divider, as the voltage produced by the solar panels were higher than the Arduino could handle (Jumaat and Othman, 2018). For a higher degree of freedom or a wider range of values for the voltage likely to be received from the solar panel and considering the combinations of resistors available to produce a maximum input voltage of 5V to the analog pin A0 of the Arduino, a 0 to 55 V range was chosen.

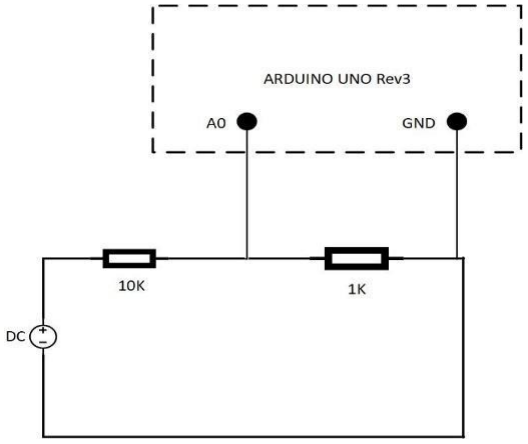

Figure 9: Block diagram for the Arduino to voltage divider

The 10k and 1k resistors connection are shown in Figure 5. A 1k resistor was connected across the terminals A0 and GND of the Arduino. One 10k resistor was also connected across pin A0 of the Arduino and the positive terminal of the independent voltage source (solar panel). The negative terminal of the voltage source was connected to common GND. All connections were made possible using the jumper cables. The wiring diagram of the connection can be seen in Figure 10.

University of Ghana http://ugspace.ug.edu.gh

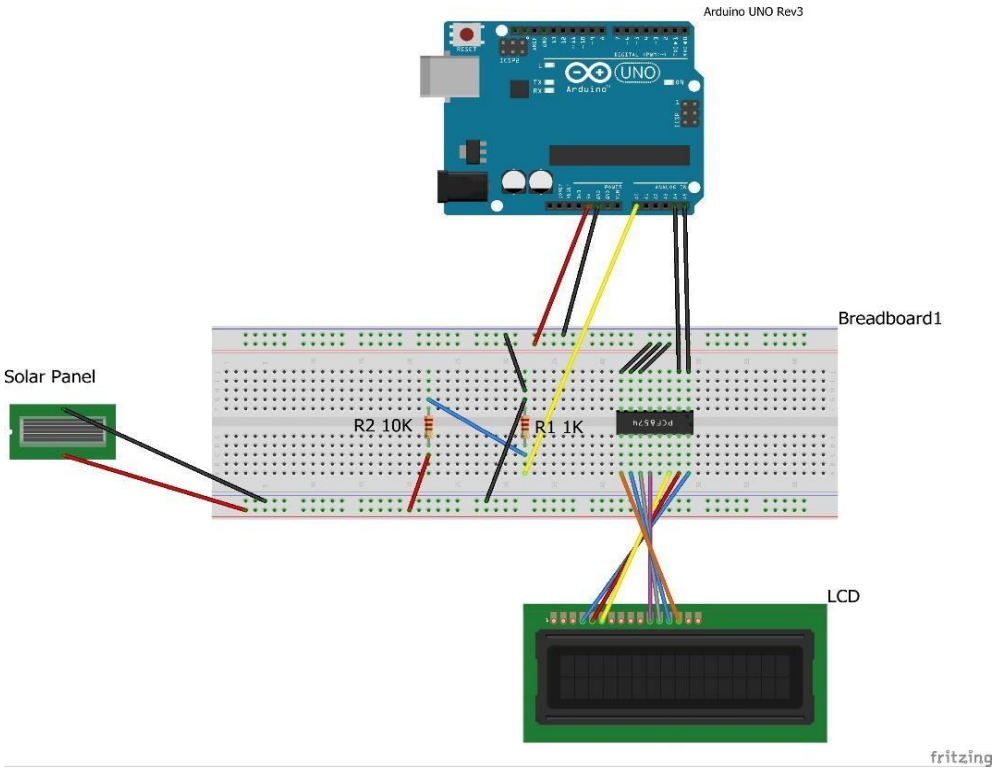

Figure 10: The wiring diagram for the connection for solar radiation measurement

The integrated complete wiring diagram and circuit diagram of the control system function can be seen in Figures 11 and 12 respectively.

University of Ghana http://ugspace.ug.edu.gh

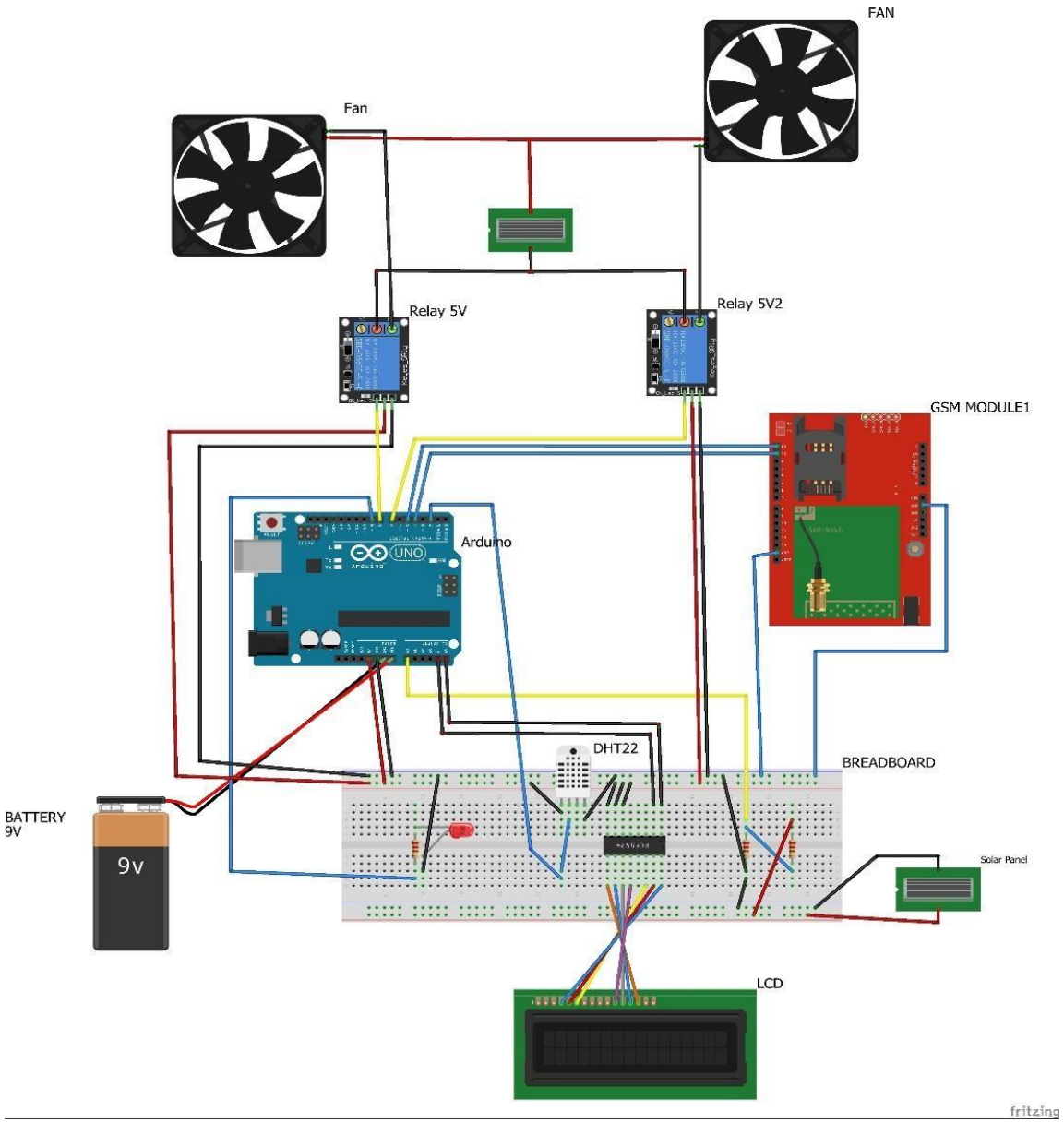

Figure 11: Complete wiring diagram of the control system function using Fritz software.

University of Ghana http://ugspace.ug.edu.gh

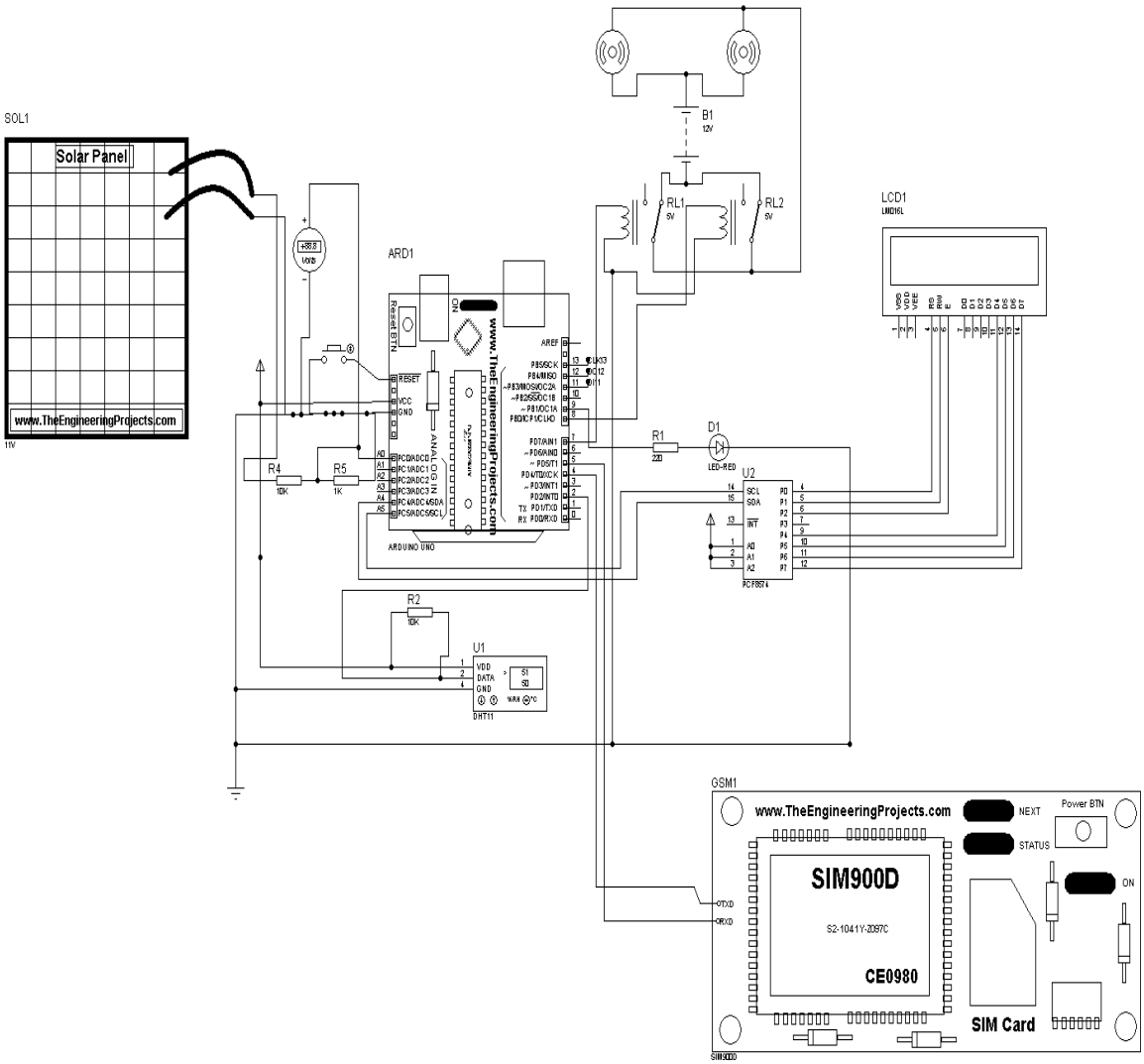

Figure 12: Circuit diagram of the control system function using Proteus 8 Professional.

University of Ghana http://ugspace.ug.edu.gh

c. Program Code

A program code was written in Arduino 1.8.8 IDE software and uploaded to the board (Arduino). The IDE which also has a cross-compilation capabilities coverts the Arduino code into machine language, then transfers it to the Arduino's Flash Memory. To help reduce the overall RAM usage and avoid memory stability issues, the F() macro was extensively used to store strings in the flash memory rather than the RAM. This helped reduce the overall RAM usage by 25-35%. The code uploaded to the board formed the underlying logic for the entire control system including instructions to read and map temperature and humidity values from raw analog values to human readable form, displaying characters on the LCD, turning the motors on or off and performing GSM operations such as sending SMS and sending data via the internet to a remote server. Since the sensor could only read temperature and relative humidity, the formula to read the absolute humidity was included in the program code. Equation 13 shows the conversion of the temperature and relative humidity to absolute humidity. The necessary code for sending signals from the sensor to the Arduino Uno to turn on the fan on or off is given in Appendix 1.

From the ideal gas equation;

$$PV = nRT \qquad \text{Eq. (13)}$$

$$Relative\ humidity, rh = \frac{P}{P_{sat}} \times 100\% \qquad \text{Eq.(14)}$$

$$Absolute\ humidity, AH = \frac{6.112 \times e^{\left(\frac{17.67 \times T}{T+243.5}\right)} \times rh \times 2.1674}{(273.15+T)}\ (\text{grams/m}^3) \qquad \text{Eq. (15)}$$

d. Circuit Simulation

Figure 13 shows the complete simulation circuit for the control system function developed using Proteus 8 Professional. This simulation circuit consist of: a) the temperature and humidity sensor, b) extractor fans, c) LCD screen display, d) LED light indicator, e) GSM module and the voltage

University of Ghana http://ugspace.ug.edu.gh

divider. The main controller used was the Arduino UNO and its power supply from the power inverter.

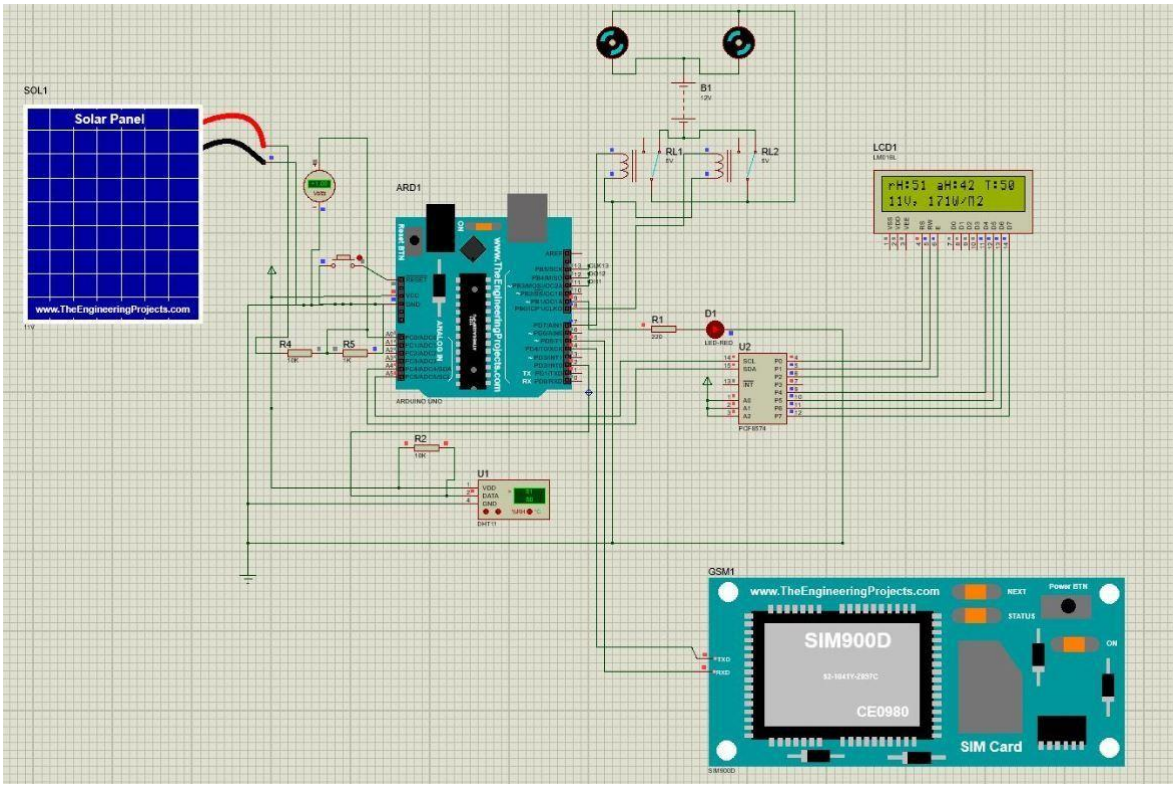

Figure 13: The Simulation Circuit

e. Multifunction Workstation

The workstation was fabricated to house the solar panels and the control systems. The three solar panels linked in parallel were mounted on the roof at an angle of 15°. The two fans and temperature and humidity sensor connectors were extended from the workstation to the greenhouse solar dryer.

University of Ghana http://ugspace.ug.edu.gh

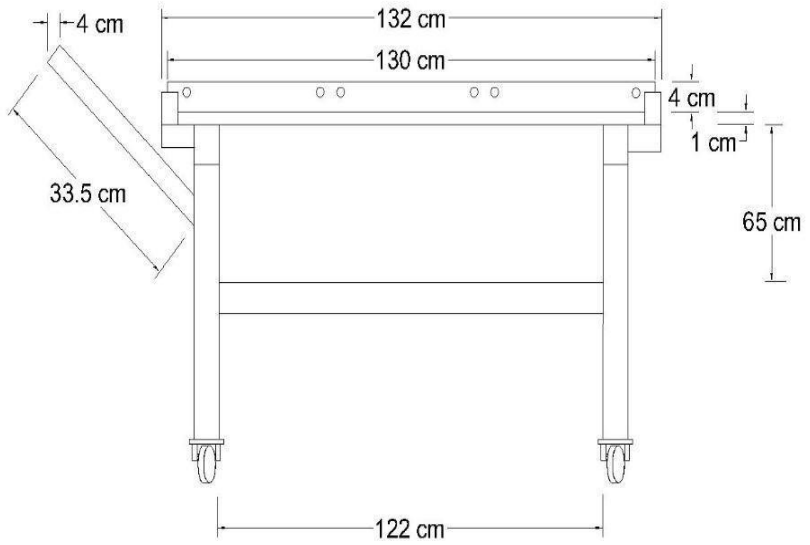

Illustration 2: Isometric drawing of the multifunction workstation (Front view).

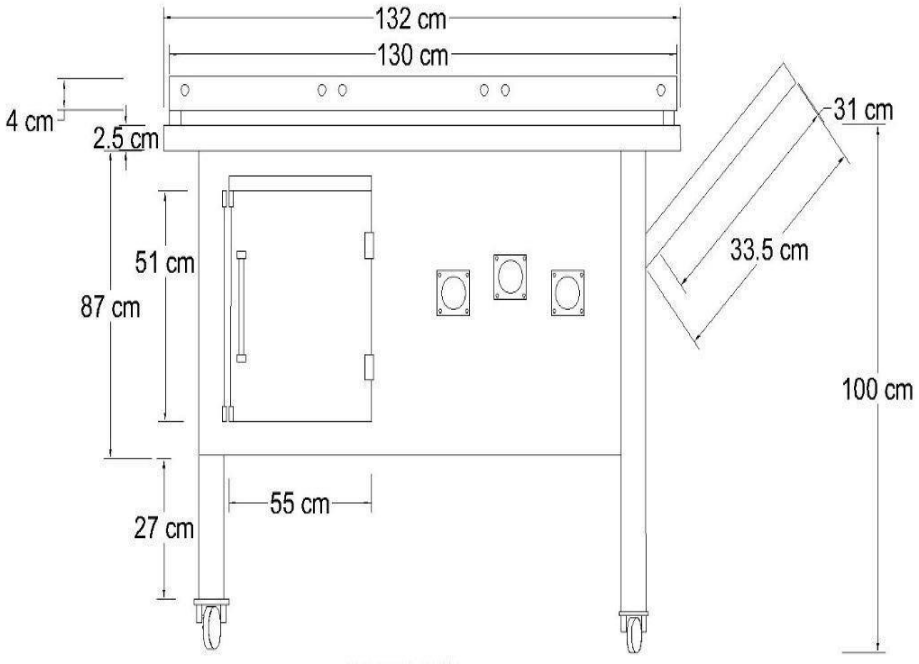

Illustration 3: Isometric drawing of the multifunction workstation (Back view)

University of Ghana http://ugspace.ug.edu.gh

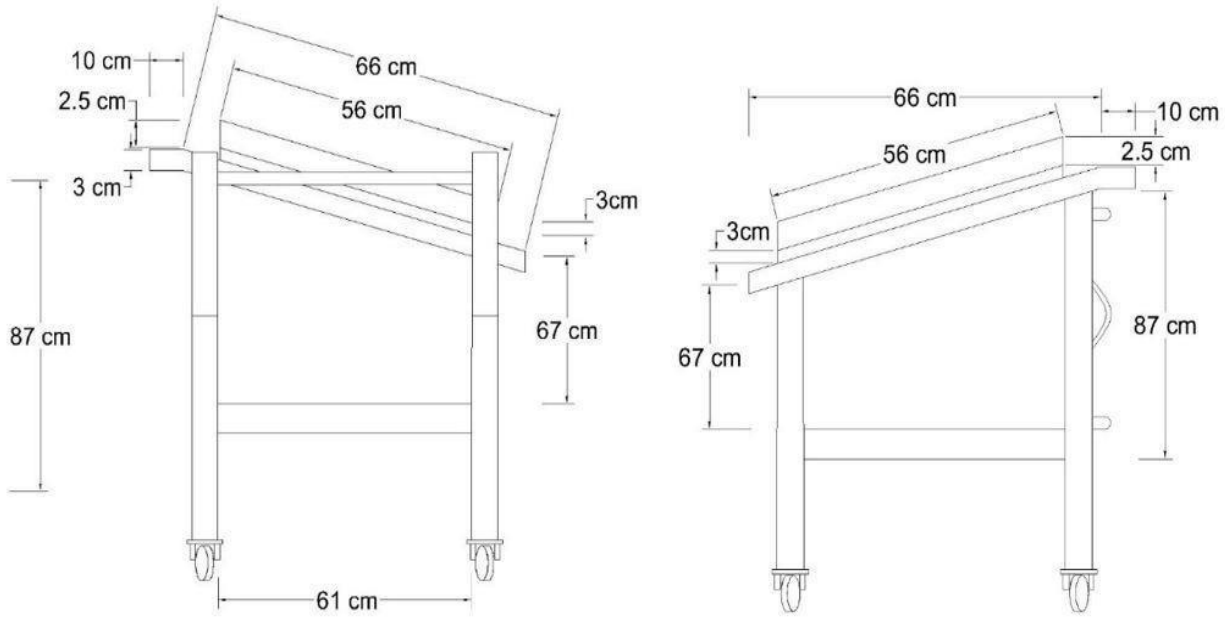

Illustration 4: Isometric drawing of the multifunction workstation (Left and Right views)

3.2.2 PV-Greenhouse Solar Dryer Drying rack and Trays

The design concept was an improvement of an existing greenhouse type solar dryer constructed as part of research by Obimpeh, (2018), the critical differences were the introduction of two extractor fans, a multifunction control system for humidity and temperature, introduction of racks to increase product load capacity and hand-made woven sieves. The constructed PV-greenhouse solar dryer and existing greenhouse type solar dryer can be seen in Illustrations 5 and 7 respectively.

University of Ghana http://ugspace.ug.edu.gh

Illustration 5: The front view of the PV-Greenhouse solar dryer

Illustration 6: The side view of the Greenhouse solar dryer

University of Ghana http://ugspace.ug.edu.gh

Illustration 7: Existing greenhouse type solar dryer
(Source: Obimpeh, 2018)

The design of the greenhouse solar dryer was based on the forced convection mode working principle. In this case, fans were introduced to assist in removing humid air from inside the dryer. Design consideration for the greenhouse solar dryer based on the classification of greenhouse solar dryers can be seen in Figure 14 below. The total surface area of the dryer was 62.76m^2 and total volume of 21.2m^3. The dryer consisting of a chapel structure made from polycarbonate sheets had two 12V DC fans operated by three 30-watts solar panels connected in parallel on the multifunction workstation. Two racks of total area of 1.21m^2 and total volume of 2.03m^3 each were placed inside the dryer. Each rack had four shelves to increase the load capacity of the dryer. Locally hand-woven sieves of area 0.319m^2 each with an average standard sieve size of 3 (3mesh; ASTM- inch 0.265) were used for holding the samples during drying. This was to reduce heat possible heat transmission from a metal sample tray to the samples during drying. The dryer was designed with four windows with netting screen to prevent entry of insects and foreign matter. The DHT22-

University of Ghana http://ugspace.ug.edu.gh

sensor was positioned inside the dryer from the top center, to read the temperature and relative humidity inside the dryer.

The empty solar dryer was monitored for a period of 11 days from 6 a.m. to 6 p.m. without the multifunction workstation. The dryer was monitored with all four windows closed, two windows opened, and all four windows opened during which temperature and relative humidity were measured and recorded. A data logger (Lascar electronics, Easylog EL-USB-2, UK) was used in measuring the temperature, relative humidity and dew point.

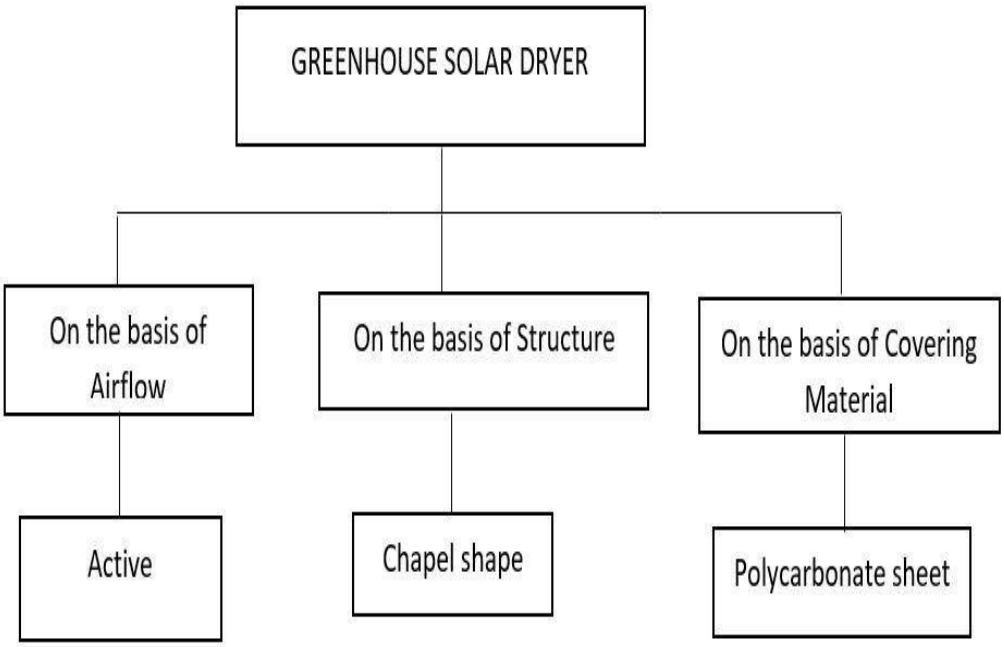

Figure 14: Modification based on the classification of greenhouse solar dryer (Source: Singh *et al.*, 2018)

University of Ghana http://ugspace.ug.edu.gh

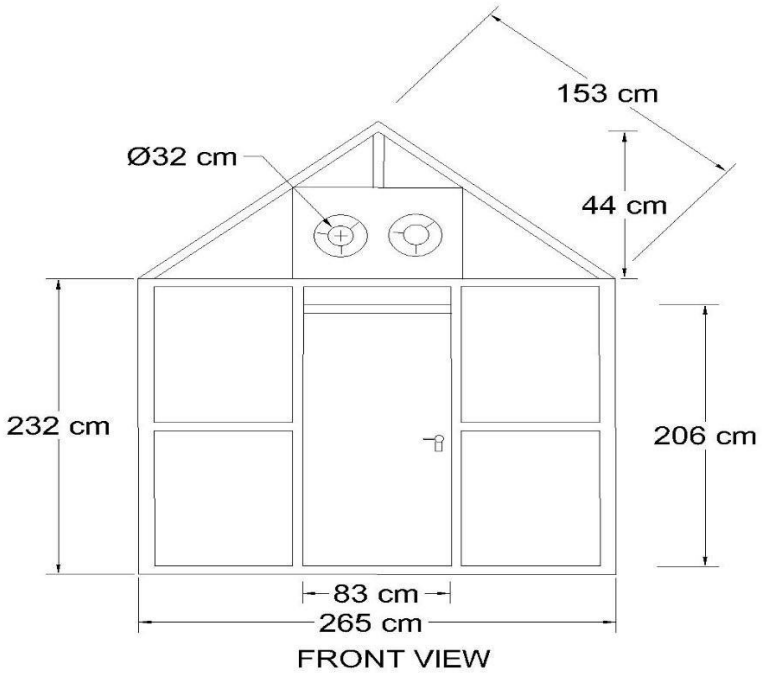

Illustration 8: Isometric drawings of the PV-Greenhouse Solar Dryer (Front view)

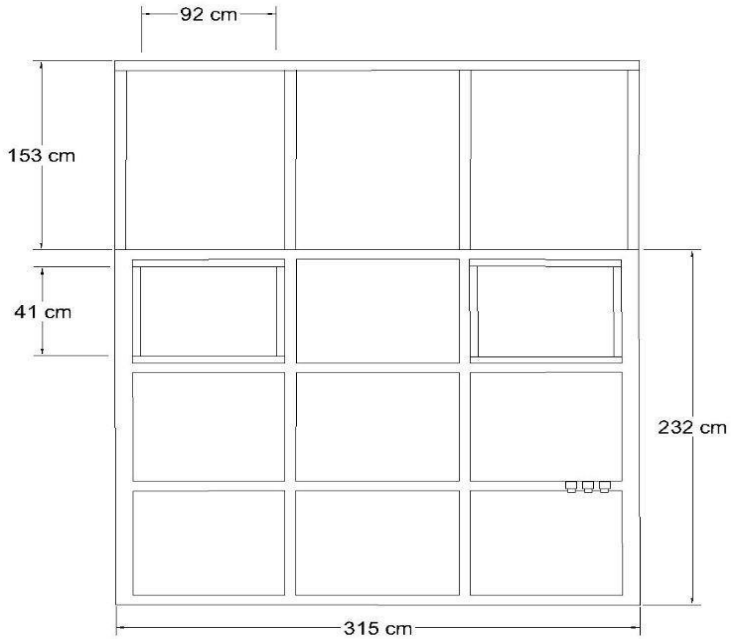

Illustration 9: Isometric drawings of the PV-Greenhouse Solar Dryer (Side view)

University of Ghana http://ugspace.ug.edu.gh

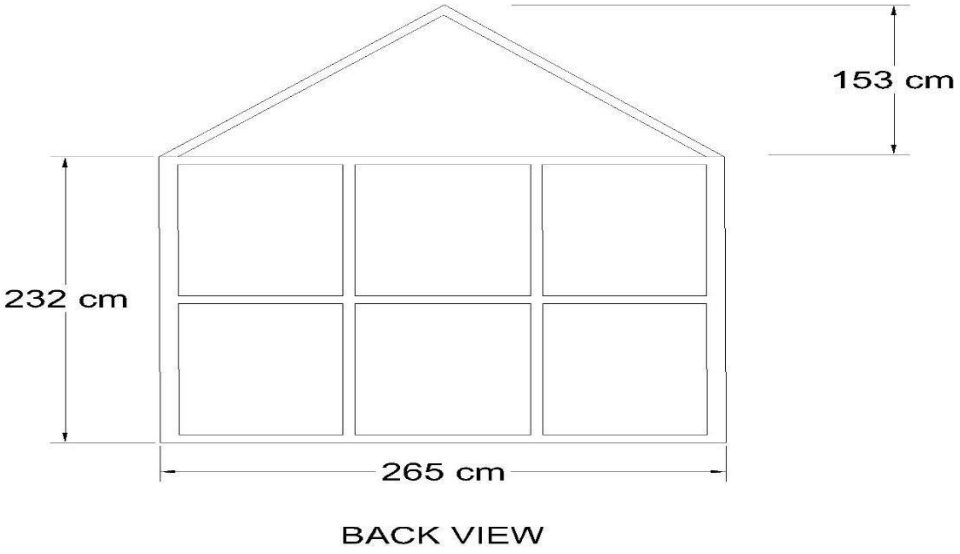

Illustration 10: Isometric drawings of the PV-Greenhouse Solar Dryer (Back view)

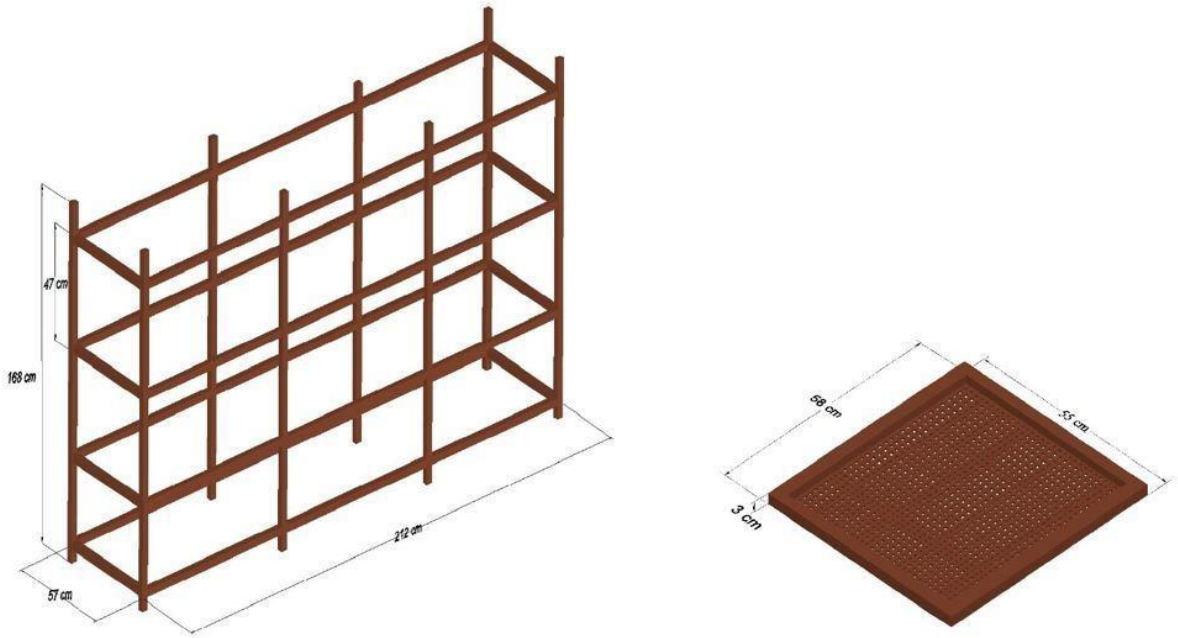

Illustration 11: Three-dimensional view of the rack (left) and sieve (right)

University of Ghana http://ugspace.ug.edu.gh

a. Design Calculations of the Greenhouse Solar Dryer

Total volume covered by the greenhouse solar dryer, V_T

The total volume was calculated from the volume covered by the rectangular section and the triangular prism section of the dryer.

$$V = volume\ of\ triangular\ prism\ section, v_T + volume\ of\ rectangular\ base, v_R$$

Volume of triangular prism section, $v_T = \frac{1}{2}(l \times b \times h)$ Eq.(16)

$$v_T = \frac{1}{2}(315 \times 265 \times 44)$$

$$v_T = 1836450\ cm^3$$

Volume of rectangular base, $v_R = L \times b \times h$ Eq.(17)

$$v_R = 315 \times 265 \times 232$$

$$v_R = 19366200\ cm^3$$

$$\therefore V = v_T + v_R$$

$$V = 1836450 + 19366200$$

$$V = 21202650\ cm^3 \approx \mathbf{21.20\ m^3}$$

Total Surface Area, A_s

The total surface area of the dryer consisted of the area of the triangular prism roof and the rectangular cuboid base. The calculation of the total surface area can be seen below;

A_S = Area of triangular prism, A_P + Area of rectangular cuboid base, A_R

$$Area\ of\ triangular\ prism, A_P = bh + l(w_1 + w_2 + b)$$ Eq. (18)

University of Ghana http://ugspace.ug.edu.gh

$A_P = (265 \times 44) + 315 \times (153 + 153 + 265)$

$A_P = \mathbf{191525\ cm^2}$

$Area\ of\ rectangular\ cuboid\ base, A_R = 2(wl + lh + hw)$ Eq.(19)

$A_R = 2[(265 \times 315) + (315 \times 232) + (232 \times 265)]$

$A_R = \mathbf{436070\ cm^2}$

$\therefore A_S = A_P + A_R$

$A_S = 191525 + 436070$

$A_S = 627595 cm^2 \approx \mathbf{62.75 m^2}$

3.2.4 Drying Experiment of Red Pepper

The drying process were performed in the PV integrated greenhouse solar dryer (PVGSD), greenhouse-type solar dryer (GSD) and under open sun (OSD). The initial moisture content of the pepper samples was measured as 77% ±1% (w.b.) using the AOAC Method 930.15 (AOAC, 2005) for moisture determination. Lots of red pepper of 2.504kg, 2.001kg and 1.001kg were dried in the PVGSD, GSD and OSD respectively. The samples were spread on the hand-woven sieves and periodically taken out for weight loss measurement using an electronic balance (Axis, model BTA2100D; an accuracy of 0.01g) at 2hours intervals. In the PV-greenhouse solar dryer (PVGSD), samples where positioned on two compartments labelled A1 and A2 for shelf A from top to bottom and B1, B2 and B3 for shelf B from top to bottom to assess the effect of shelf position on drying rate of samples. Continuous drying was carried out until a constant drying weight of the products were achieved. Monitoring of the drying experiment started from 6 a.m. in the morning and ended at 8 p.m. each day. Temperature and humidity variations for all the drying methods were monitored with readings recorded at 10 minutes intervals. The dried samples were cooled to room temperature

University of Ghana http://ugspace.ug.edu.gh

and packed in air-tight polyethylene bags. The moisture ratio (MR) and drying rate (DR) of pepper were calculated from Equations 5 and 6. All measurements were performed in triplicate.

Illustration 12: Drying of red pepper samples under GSD (a), OSD (b) and PVGSD (c)

University of Ghana http://ugspace.ug.edu.gh

3.2.5 Drying Experiment of Cassava samples

a. Cassava drying to test the ability of the workstation to reduce humidity at night (with 80watts battery)

The PV-greenhouse solar dryer (PVGSD), the greenhouse type solar dryer (GS) and under open sun drying (OSD) were used. A total of 8.04 kg cassava slices of average thickness 0.7cm and length 4.5cm and 3.84 kg cassava chunks of average thickness of 1.6 cm and length of 4.8 cm were dried under the three drying methods. All cutting was done manually using a kitchen knife. The initial moisture content of the cassava samples was measured as 64%±0.58 (w.b.) using the AOAC Method 930.15 (AOAC, 2005). The cassava samples were spread evenly on the hand-woven sieves and taken out for weight loss measurement using an electronic balance (Axis, model BTA2100D; an accuracy of 0.01g) at 2hours intervals.

In the PV-greenhouse solar dryer (PVGSD), samples where positioned each on the four shelves with 47cm spacing on one rack labelled B with the shelf level labelled B1, B2, B3 and B4 from top to bottom. Power supply was generated using the Delkor HICA80 battery.

For the greenhouse type solar dryer (GSD), samples were placed on a flat wooden mat. While samples for open sun drying (OSD) were placed on an elevated bench under the open sun, at 8pm samples were brought into the laboratory to protect it from rain and dew. Continuous drying was carried out until a constant drying weight of the products were reached. Monitoring of the drying experiment started from 6 a.m. in the morning and ended at 8 p.m. each day. Temperature and humidity variations for all the drying methods were monitored with readings recorded at 10 minutes intervals. The dried samples were cooled to room temperature, weighed and packed in air-tight polyethylene bags.

University of Ghana http://ugspace.ug.edu.gh

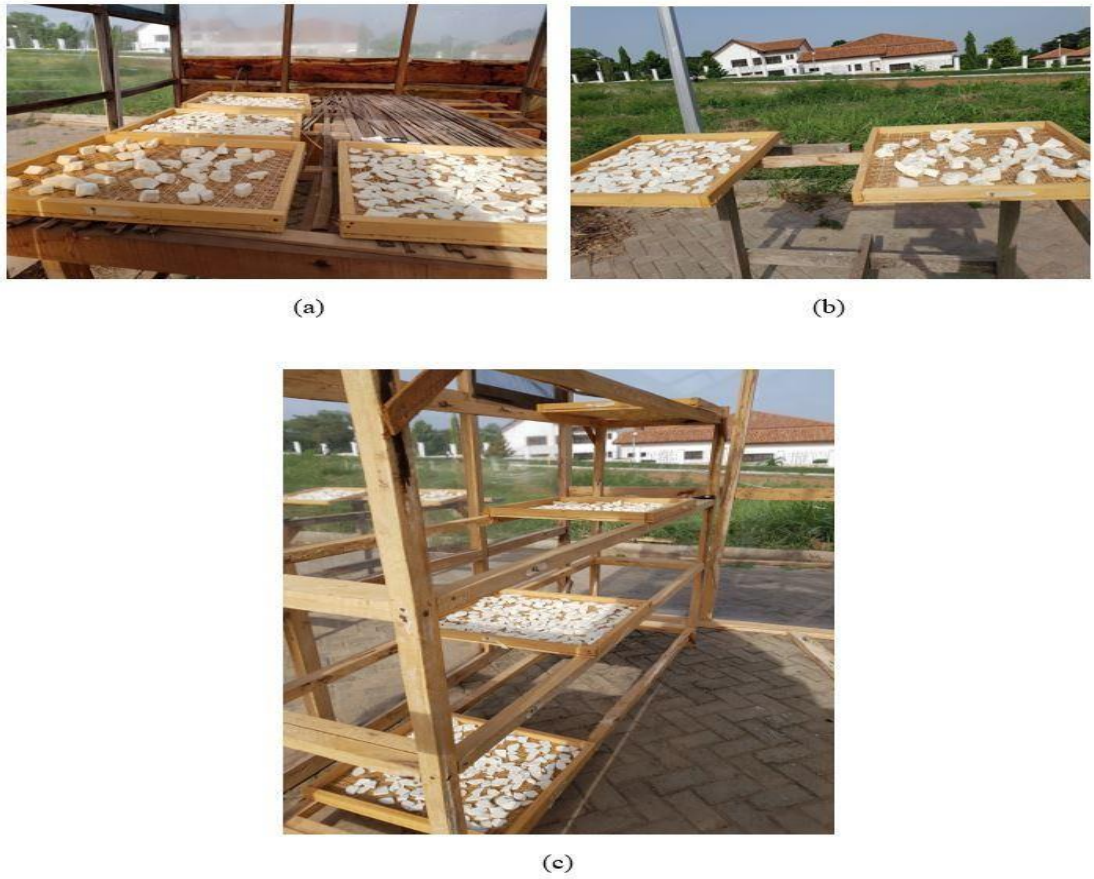

Illustration 13: Drying of cassava slices and chunks under GSD (a), OSD (b) and PVGSD (c)

b. Cassava drying to test the ability of the workstation to reduce humidity at night (with 1200watts battery)

In an earlier experiment, the battery installed in the workstation attached to the PVGSD could not have enough power to run the two fans continuously during the night due to a higher power rating of the fans (100 watts) as to 80watts of the battery. The fans could not function overnight. The experiment was repeated with a stronger power (two batteries each with a capacity of 1200 watts). The system was able to run the fans throughout the night.

The PV-greenhouse solar dryer (PVGSD), the greenhouse type solar dryer (GS) and under open sun drying (OSD) were used. A total of 16.42 kg cassava slices of average thickness 0.5cm and

University of Ghana http://ugspace.ug.edu.gh

length 3.5cm and 5.58 kg cassava chunks of average thickness of 2.3 cm and length of 4.5 cm were dried under the three drying methods. All cutting was done manually using a kitchen knife. The initial moisture content of the cassava samples was measured as 65%±0.72 (w.b.) using the AOAC Method 930.15 (AOAC, 2005). The cassava samples were spread evenly in a single layer on the hand-woven sieves and samples periodically taken out for moisture content measurement using a hot air oven (Binder hot air oven, Model: FD 56, Germany) at 2 hours intervals.

In the PV-greenhouse solar dryer (PVGSD), samples where positioned each on the four shelves with 47cm spacing on the two racks labelled A and B with samples on the shelf level labelled B1, B2, B3, B4, A1 and A2 from top to bottom. Power supply to the two fans and the control system components was generated using the two Sunfit 6GFM100 battery.

For the greenhouse type solar dryer (GSD), samples were placed on a flat wooden mat. While samples for open sun drying (OSD) were placed on an elevated bench under the open sun, at 6pm samples were brought into the laboratory to protect it from rain and dew. The drying process was continued until the products reached a moisture content of about 10% (w.b). Monitoring of the drying experiment started from 6 a.m. in the morning and ended at 6 p.m. each day. Temperature and humidity variations for all the drying methods were monitored with readings recorded at 10 minutes intervals. The dried samples were cooled to room temperature, weighed and packed in air-tight polyethylene bags.

3.2.6 Laboratory Analysis

All laboratory analyses were performed in triplicate

a. Moisture determination

Moisture content was determined as percent wet basis (w.b.%) by measuring 3 g of the fresh and dried red pepper and cassava samples and dried at 105°C for 18 hours in a hot air oven (Binder hot

University of Ghana http://ugspace.ug.edu.gh

air oven, Model: FD 56, Germany) to a constant weight. Samples were removed, cooled and weighed. The moisture content was calculated and expressed as a percentage of the mass of sample taken (AOAC 2005). Moisture content as wet basis was expressed as (Wang *et al*., 2018);

$$Moisture\ content, M.C\ \%\ (w.b) = \frac{W_w - W_d}{W_w} \times 100\% \qquad \text{Eq. (20)}$$

b. Color analysis

The Surface colour of fresh and processed samples were measured using a colorimeter (Minolta Chroma CR-410, Konica Minolta Co., Osaka, Japan) according to Wang *et al*., (2017). The CIE Lab color parameters, L^* (whiteness or brightness) with a range from 0 (black) to 100 (white), a^* (redness or greenness) with a range from -60 (green) to +60 (red), and b^* (yellowness or blueness) with a range from -60 (blue) to +60 (yellow) coordinates were used to describe quantitatively the colour change during the drying period. Calibration of the colorimeter was done with the white standard plate before use. Measurements were made at random points of the samples and in triplicates to get the average values. The differences of L^*, a^* and b^* were used to calculate the change in different color parameters, L^*_0, a^*_0 and b^*_0 as the initial color of the samples. The total color change (ΔE), browning index (BI) and huge angle (H^O) was determined by using the Equations (21)-(24) ((Wang *et al*., 2018):

$$\Delta E = \sqrt{(L^* - L^*_O)^2 + (a^* - a^*_o)^2 + (b^* - b^*_o)^2} \qquad \text{Eq.(21)}$$

$$BI = 100 \times \left(\frac{X - 0.31}{0.17}\right) \qquad \text{Eq.(22)}$$

where;

$$X = \frac{(a^* + 1.75L^*)}{(6.645L^* + a^* - 3.012b^*)} \qquad \text{Eq.(23)}$$

$$\mathrm{H}^0 = \tan^{-1}\left(\frac{\mathrm{b}^*}{\mathrm{a}^*}\right) \qquad \text{Eq.(24)}$$

University of Ghana http://ugspace.ug.edu.gh

c. Water activity

The water activity before, during and after drying period was determined using a water activity meter (Rotronic HP23-AW-A, Switzerland: accuracy of 23±5°C). The sample was placed inside the sample plastic container and together into the sample holder. The measurement probe was then placed on top of the sample holder which is connected to the handheld instrument that displays the water activity and the temperature.

3.2.7 Size Reduction

The dried samples from all the drying methods were milled into fine powder using a grinder (Mulry function disintegrator WF-20). The dried cassava slices and chunks were milled into flour using a high-speed disintegrator IC-10B for 1min at a blade speed of 25000 rpm. The resultant product was packed into an air tight plastic container and stored in the laboratory at room temperature.

3.2.8 Particle Size Distribution

Cassava flour (100g) was used for the analysis. Sieves with screen size of ASTM 500, 300, 212, 150, 106, 75, 53 and 45 were arranged in descending order of sieve size (Sonaye and Baxi, 2012). The stack of sieves was placed in a vibratory sieve shaker (AS 200-digit cA, Retsch GmbH, Germany) for 20 minutes at an amplitude of 2mm. The empty weight of each sieve was measured before sieve analysis and after which the mass of sample retained on each sieve was measured.

The percentage retained on each sieve was calculated by dividing the weight of the sample of each sieve by the total weight. The cumulative percent of aggregate retained in each sieve is calculated by adding up the total amount of retained aggregate in each sieve and the amount in the previous sieves. The two parameters are calculated using Equation (25) and (26) below (Sonaye and Baxi, 2012);

University of Ghana http://ugspace.ug.edu.gh

$$\%\ Retained = \frac{W_{sieve}}{W_{total}} \times 100\% \qquad \text{Eq. (25)}$$

$$\%Cumulative\ passing = 100\% - \%Cumulative\ retained \qquad \text{Eq. (26)}$$

3.3 Statistical data analysis

The laboratory analyses were performed in triplicates and data presented as the mean of three determinations ± standard deviation. The data were analyzed by Analysis of Variance (ANOVA) using Minitab statistics software (Version 18.1, Minitab, Inc., Pennsylvania, USA). A statistical significance for differences was tested at 5% probability level ($p < 0.05$). The statistical analysis of drying experiments for model fitting was performed with MATLAB software (MATLAB R2018b, Version 9.5.0, MathWorks, USA).

University of Ghana http://ugspace.ug.edu.gh

CHAPTER FOUR

4.0 RESULTS AND DISSCUSSIONS

4.1 Multi-Function Control System

4.1.1 Control system function – Simulation output

The outcome from the simulation is shown in Figure 15, which shows the results of the relative humidity, absolute humidity, temperature, voltage and solar radiation during the simulation. It varies depending on the DHT22-sensor and voltage of the solar panel setting during the simulation. Real time data of the parameters measured were sent via SMS to the designated cell number (Illustration 14) and retrieved as a comma-separated values (CSV) file format. From the virtual terminal display results shown that the circuit function as expected and can be continued to build the prototype for the control system.

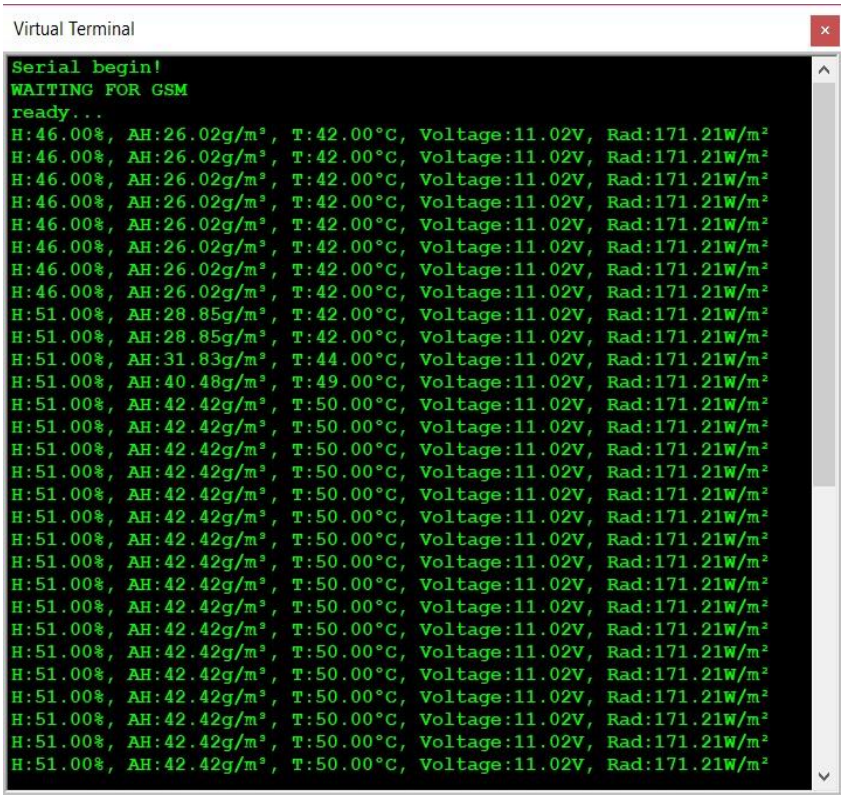

Figure 15: The simulation virtual terminal output

University of Ghana http://ugspace.ug.edu.gh

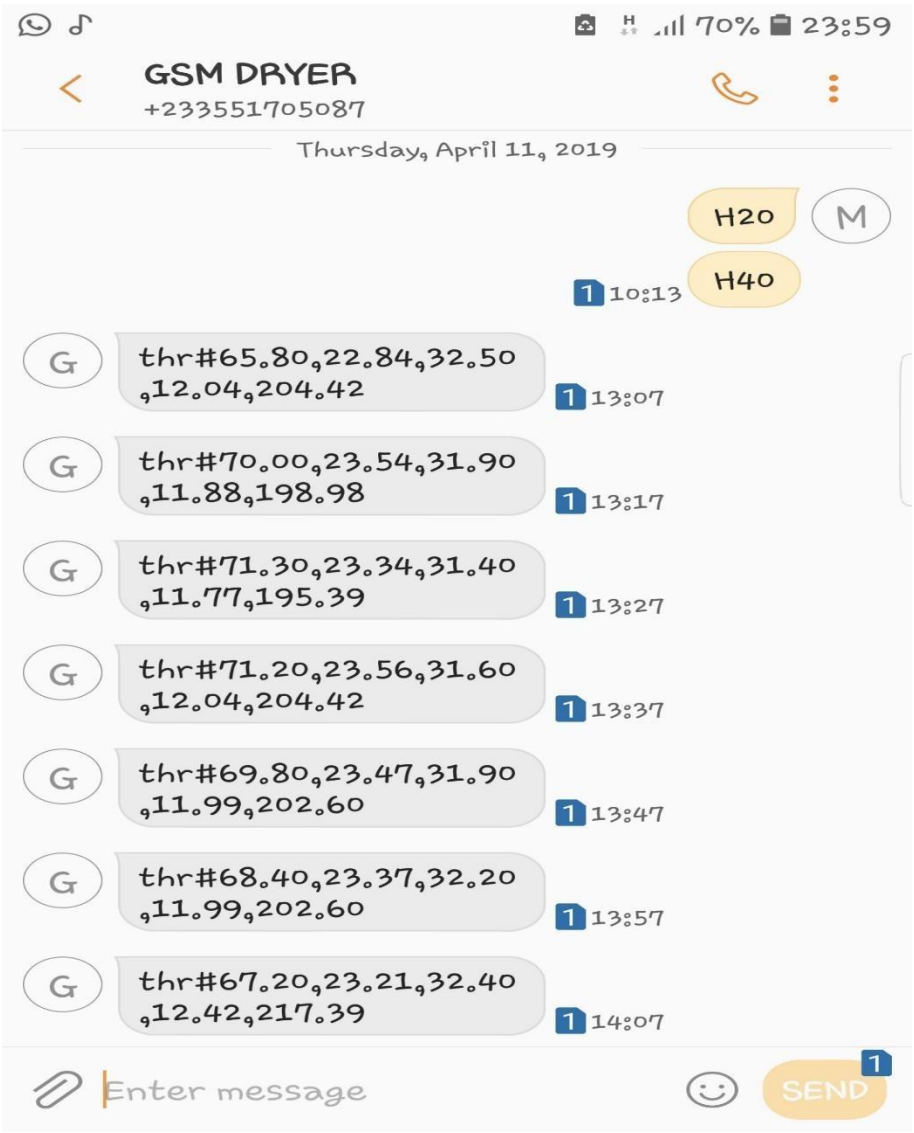

Illustration 14: Measured parameters sent via SMS

University of Ghana http://ugspace.ug.edu.gh

4.1.2 Development of Control system function – Prototype stage

Illustration 15 shows the image of the prototype developed to test the working principle before translating that into the actual development of the control system with the PV greenhouse solar dryer.

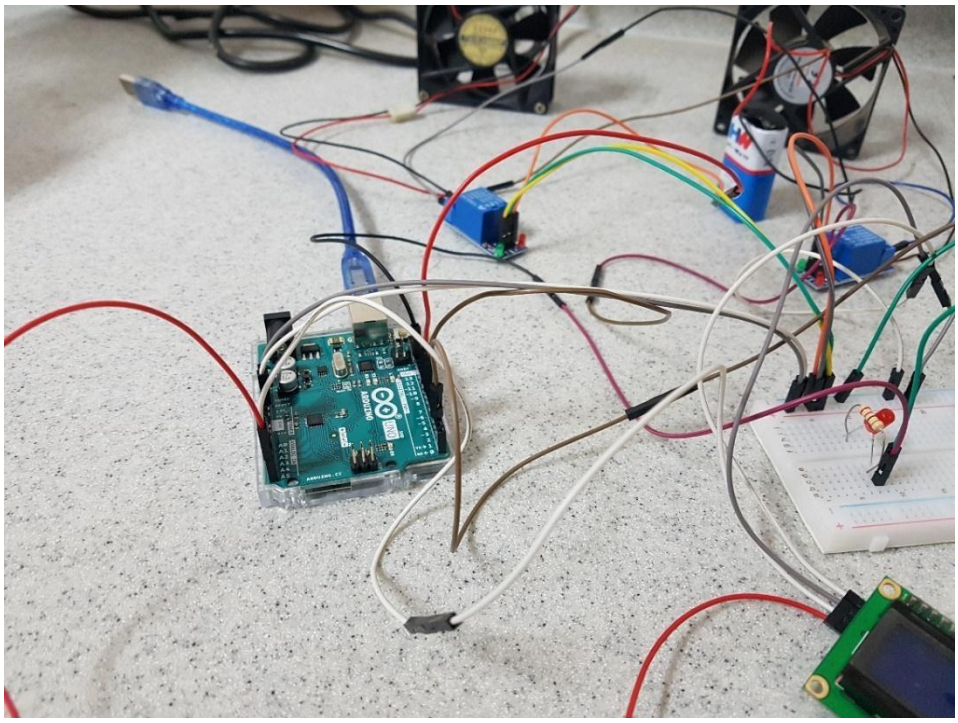

Illustration 15: Prototype of the control system component

4.1.3 Development of Control system function – Actual design

Illustration 16 shows the complete development of the control system function consisting of the Arduino UNO, GSM module, relays, jumper cables, breadboard, etc. The components were cased to protect them from dust and unauthorized tempering.

University of Ghana http://ugspace.ug.edu.gh

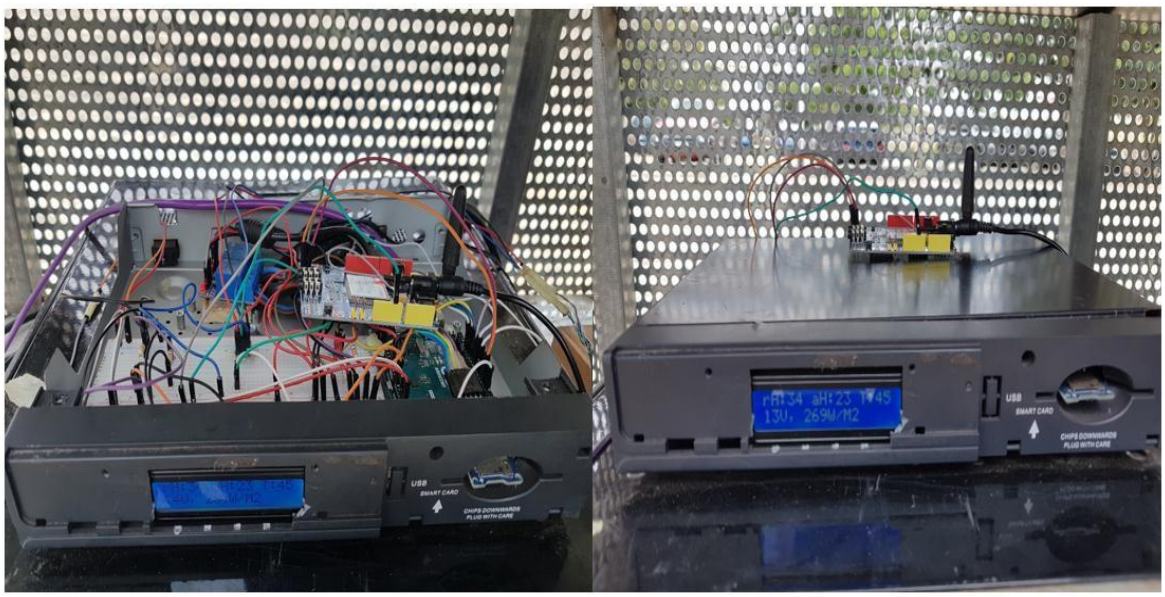

Illustration 16: Shows the control system component opened (left) and cased (right) inside the workstation

4.2 Design characteristics and construction of the multifunction workstation

The multifunction workstation was designed to have a floor area 8.35m^2. It housed and protected the charge controller, power inverter, battery and the system control components. The workstation had a handle on the right side and four wheels to allow the movement of the workstation to and from the solar dryer. It also provided a link to the dryer, the fans and the DHT22-sensor. Illustrations 17 and 18 shows the constructed workstation and the cased components. It was found out that the workstation performed the expected tasks and aided in monitoring and recording the data during the drying.

University of Ghana http://ugspace.ug.edu.gh

Illustration 17: Front view (left) and back view (right) of the multifunction workstation

Illustration 18: Inside the multifunction workstation

University of Ghana http://ugspace.ug.edu.gh

4.3 Design, construction and evaluation of performance of the PV-greenhouse solar dryer.

4.3.1 Design and construction of the dryer

The chapel shaped greenhouse solar dryer operated under active mode with two 12V DC extractor fans fitted at the top front view of the dryer. The dryer with a total surface area of 62.7595m^2 and a total volume of 21.20m^3 was enveloped with polycarbonate sheets. The dryer also had two racks for positioning the samples being dried. A DHT22-sensor was positioned at the center of the drying chamber to read the temperature and relative humidity. The Illustration 19 below shows the constructed PV greenhouse solar dryer with the multifunction workstation.

Illustration 19: Complete experimental set-up of the PV-greenhouse solar dryer and the multifunction workstation

University of Ghana http://ugspace.ug.edu.gh

4.3.2 Temperature and relative humidity profile of the empty PV greenhouse solar dryer and open sun drying

The temperature and relative humidity profile measured in the drying chamber as compared to open sun or ambient environment for 11 days are summarized in Appendix 2 and Figures 16 to 21. Variations in the temperature and relative humidity measured for the period were observed. The peak temperatures for most days were found between 12:00 to 14:00 hours GMT. From the values measured, the temperatures were rather higher for the PV-greenhouse solar dryer (PVGSD) with the highest temperature of 69°C and lowest at 29.5°C as compared to ambient air temperature (OSD) with the highest temperature of 41.5°C and lowest at 26.4°C. This indicate that the greenhouse solar dryer potentially created a higher temperature environment for drying and will have a faster drying rate than the open sun drying.

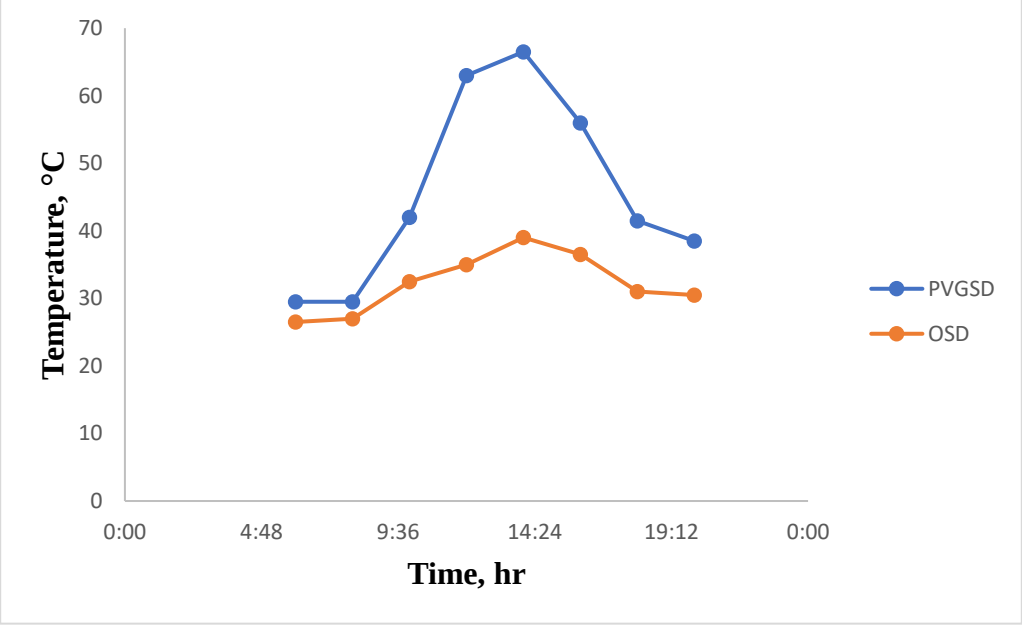

Figure 16: Day 1 Changes in temperature of empty PVGSD and OSD

University of Ghana http://ugspace.ug.edu.gh

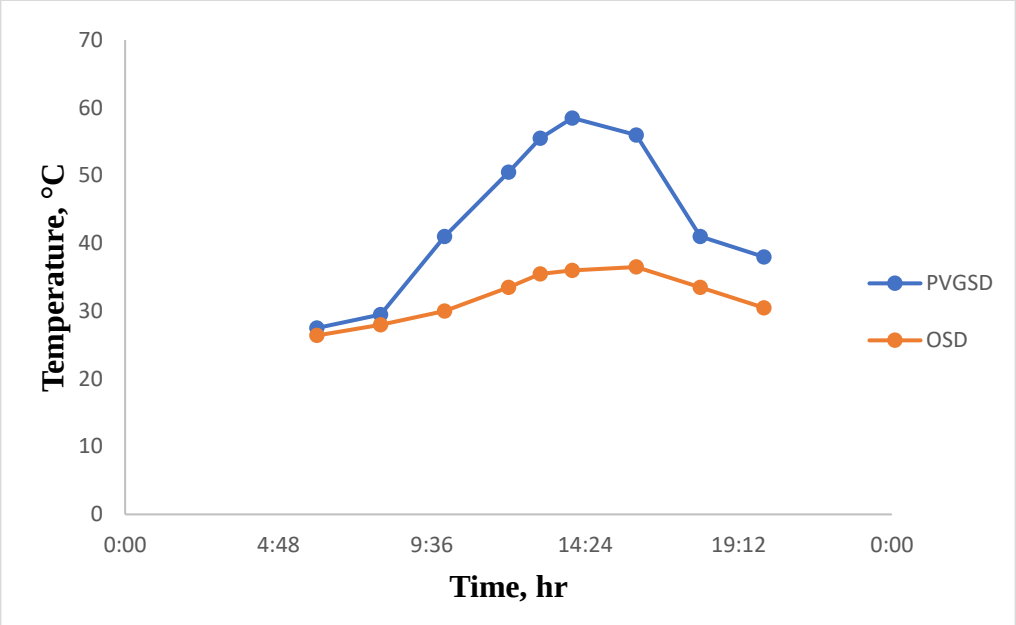

Figure 17: Day 6 Changes in temperature of empty PVGSD and OSD

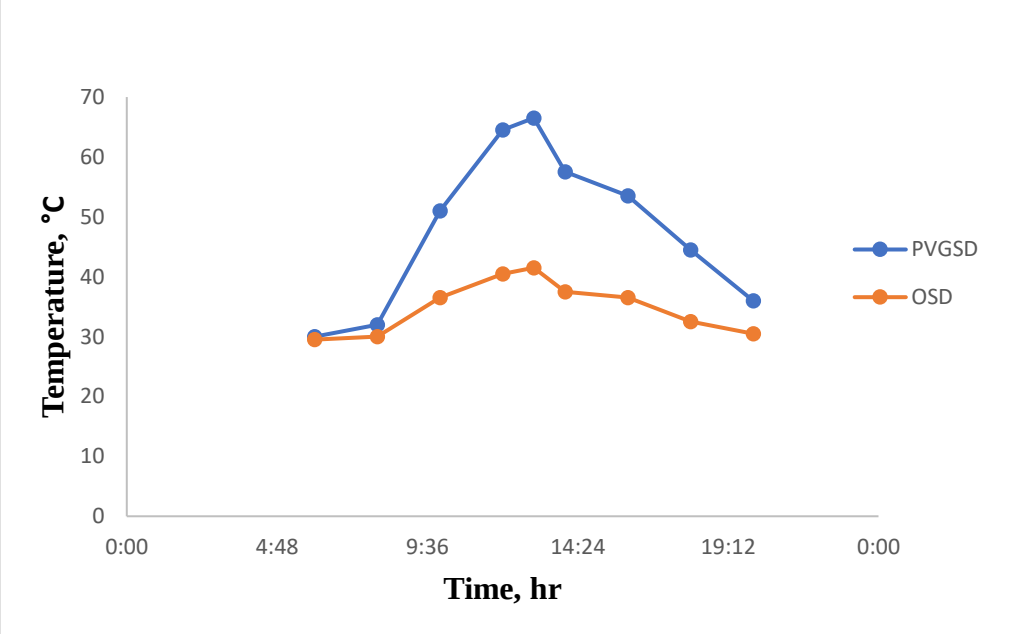

Figure 18: Day 11 Changes in temperature of empty PVGSD and OSD

For both drying process, relative humidity varied with time, generally, it was higher during the night but dropped significantly during the day time when temperatures were high. The relative humidity of the open sun drying (OSD) was comparatively higher to PVGSD throughout recording

University of Ghana http://ugspace.ug.edu.gh

a value of 83.1% compared to 75.5% at night in the PVGSD, while the PVGSD recorded a relatively lower relative humidity of 17.5% as compared to 42% under OSD during the day.

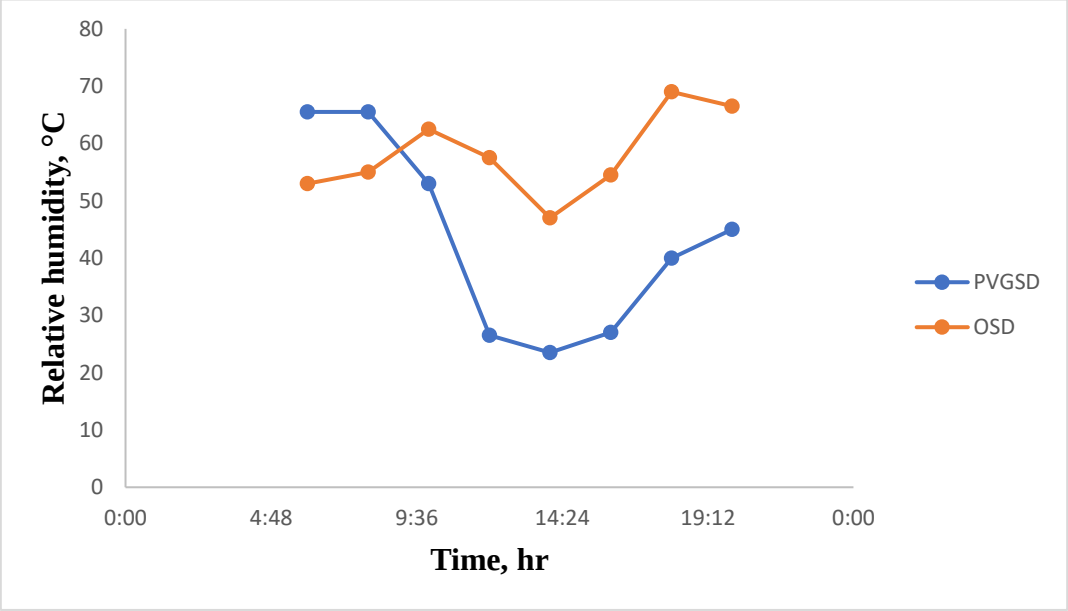

Figure 19: Day 1 Changes in relative humidity in the empty PVGSD and OSD

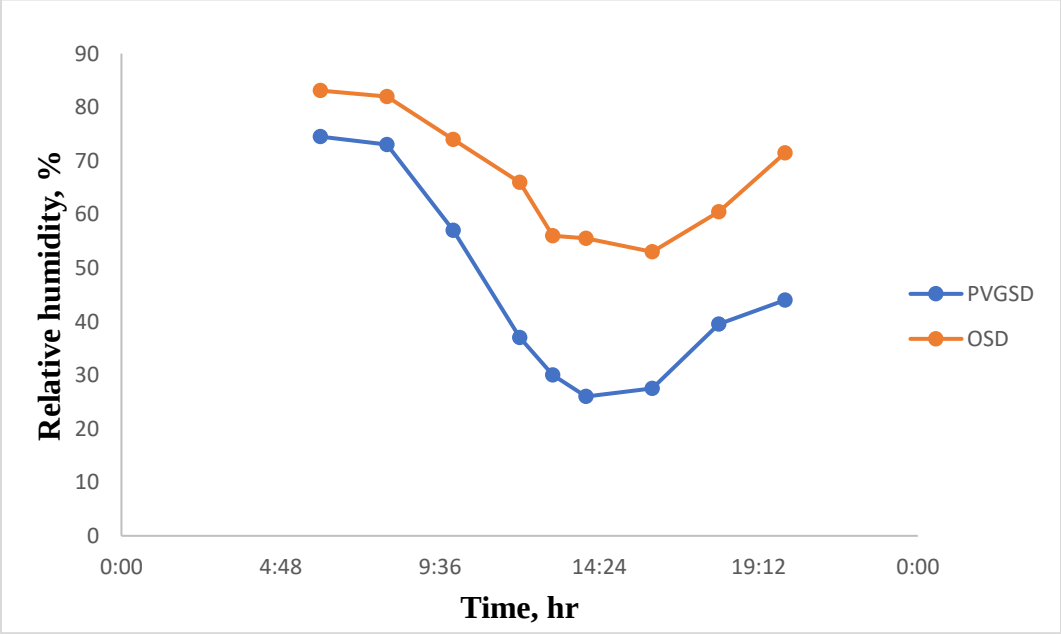

Figure 20: Day 6 Changes in relative humidity in the empty PVGSD and OSD

University of Ghana http://ugspace.ug.edu.gh

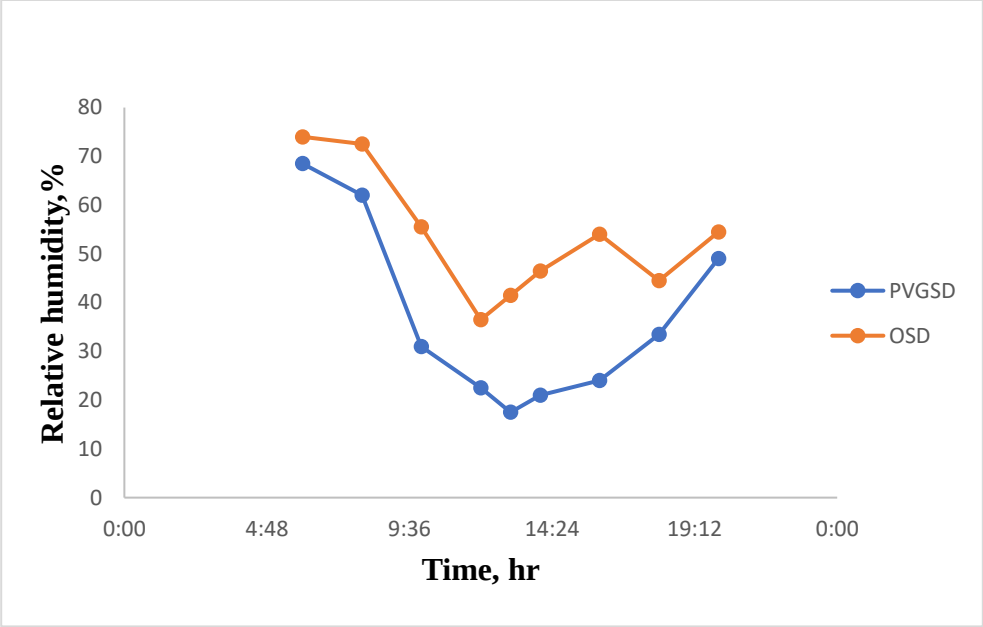

Figure 21: Day 11 Changes in relative humidity in the empty PVGSD and OSD

4.4 Drying of Red Pepper and Cassava samples in the PV-Greenhouse Solar Dryer (PVGSD), Greenhouse Type Solar Dryer (GSD) and Open Sun (OSD)

4.4.1 Climate variation

4.4.1.1 Drying of Red Pepper

The temperature and humidity recorded during the drying of the red pepper are shown in Figure (22) – (24). The Figures 22 and 23 show the changes in solar radiation, ambient and solar dryers' temperatures. The ambient air temperature and relative humidity were found to range from 27°C to 46°C and 34% to 85%, respectively. The same parameters in the PVGSD varied from 27°C to 72°C with an average of 44°C and a relative humidity range of 15% to 84% with an average of 48.3%. The original GSD showed a similar pattern as the PVGSD, i.e. temperature varied from 27°C to 71°C with an average of 41°C and a relative humidity range of 15% to 84%. The intensity of solar radiation was varied between 11.9W/m^2 and 978.17W/m^2 with an average of 364.22 W/m^2.

University of Ghana http://ugspace.ug.edu.gh

It was observed that during the day, from sunrise to sunset, the solar radiation, ambient temperature as well as temperatures in the PVGSD and GSD was maximum from 12pm to 3pm and minimum at night after 6pm. The relative humidity was observed to record the lowest when the solar radiation and temperatures were high. However, the relative humidity was considerably lower in the PVGSD than the GSD, this can be attributed to the fans introduced in the PVGSD.

The correlation coefficient (r) between ambient temperature and solar radiation was calculated as 0.705896 ≈ 0.706. This shows a strong positive relationship between the two parameters, as solar radiation increases ambient temperature also increases. In general, the solar radiation and ambient air temperature affect the two solar dryers' performance. However, the PVGSD obtained the highest temperature and lowest relative humidity throughout the experimental drying of red pepper. The data for temperatures, relative humidity and solar radiation is shown in Appendix 3.

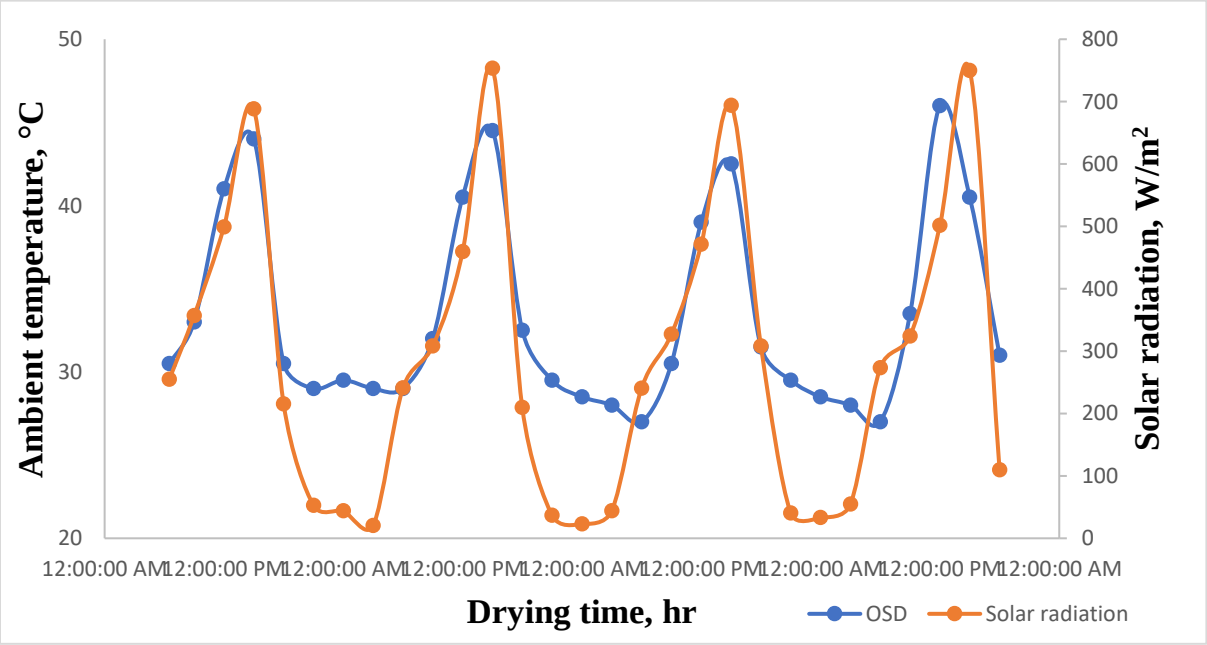

Figure 22: Changes in ambient temperature and solar radiation during drying of red pepper

University of Ghana http://ugspace.ug.edu.gh

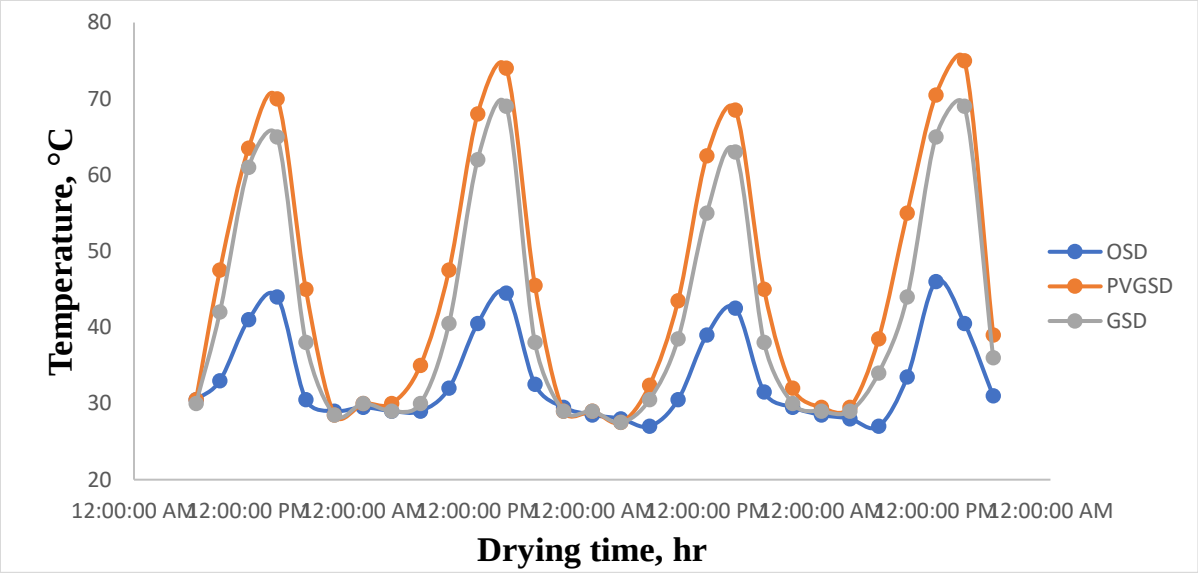

Figure 23: Comparison of the temperatures of PVGSD, GSD and OSD during drying of red pepper.

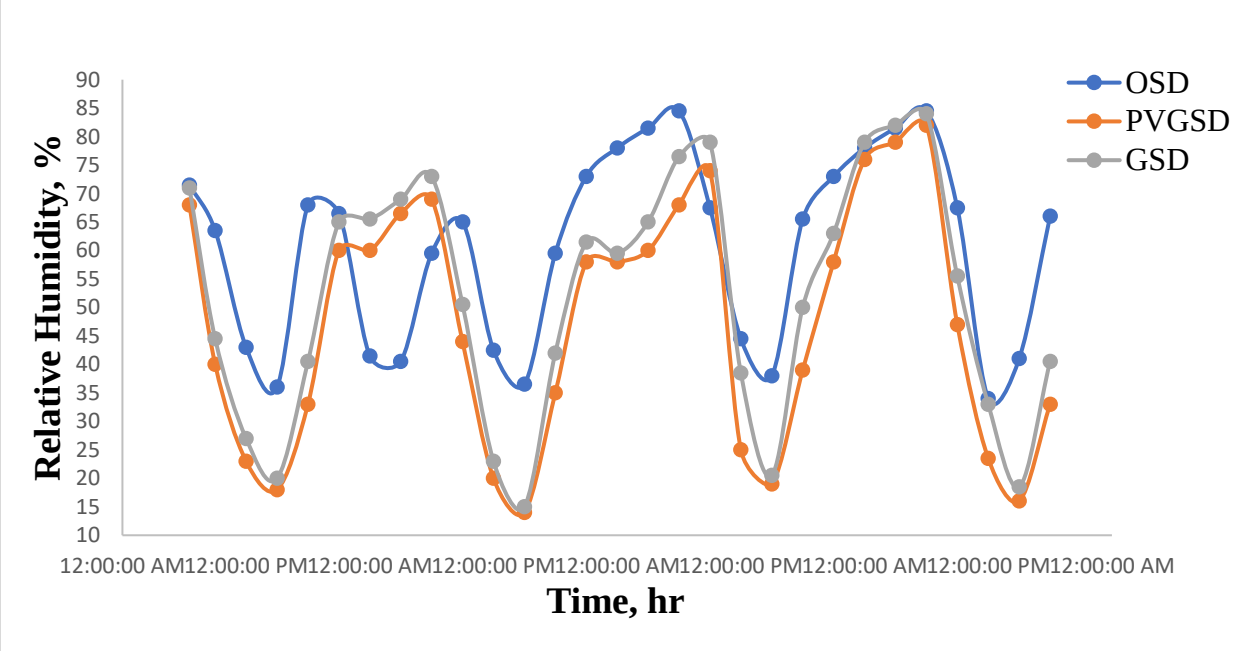

Figure 24: Comparison of the relative humidity of PVGSD, GSD and OSD during drying of red pepper.

Analysis of variance performed on the temperature and relative humidity data delineating drying method and drying time revealed that both the temperature and relative humidity measured was

University of Ghana http://ugspace.ug.edu.gh

significantly influenced by the drying methods (PVGSD, GSD and OSD) and the time of drying. This indicated that the temperature and relative humidity attained during the experimental drying of red pepper was dependent on the dryer type and drying time. The ANOVA Tables for temperature and relative humidity can be seen in Tables 11 and 12 respectively.

Table 11: Analysis of Variance (ANOVA) of Temperature variations of Red Pepper during drying.

Source	SS	DF	MS	F-Value	P-value	F crit.
Drying time	13150.36	28	469.6557	12.88706	0.000	1.677507
Drying method	1350.511	2	675.2553	18.52858	0.000	3.161861
Error	2040.863	56	36.44398			
Total	16541.73	86				

Table 12: Analysis of Variance (ANOVA) of Humidity variations of Red Pepper

Source	SS	DF	MS	F-Value	P-value	F crit.
Drying time	29794.32	28	1064.083	15.27909	2.27E-17	1.677507
Drying method	2612.489	2	1306.244	18.75627	5.82E-07	3.161861
Error	3900.011	56	69.64306			
Total	36306.82	86				

4.4.1.2 Drying of Cassava

a. Cassava drying to test the ability of the workstation to reduce humidity at night (with 80 watts)

The Figures 25, 26 and 27 below show the variations of solar radiation, ambient and solar dryers' temperatures and relative humidity throughout the drying experiments of cassava samples. For all the drying methods, it was observed the temperature reading from 8 p.m. to 5 a.m. was about the same and highest from 12 p.m. to 3 p.m. The OSD temperature and relative humidity were found

University of Ghana http://ugspace.ug.edu.gh

to vary from 27°C to 42°C and 34% to 85% respectively. The PVGSD drying temperature ranged from 28°C to 75°C and a relative humidity range of 14.5% to 71.5%. The GSD drying temperature varied from 28°C to 70°C and a relative humidity range of 17.5% to 82.5%. It appears that the temperatures attained in the PVGSD and GSD were similar, the main differences being in the range of relative humidity. The intensity of solar radiation was varied between 10.19W/m^2 and 806.76W/m^2. The PVGSD obtained the highest temperature and lowest relative humidity throughout the drying of cassava samples.

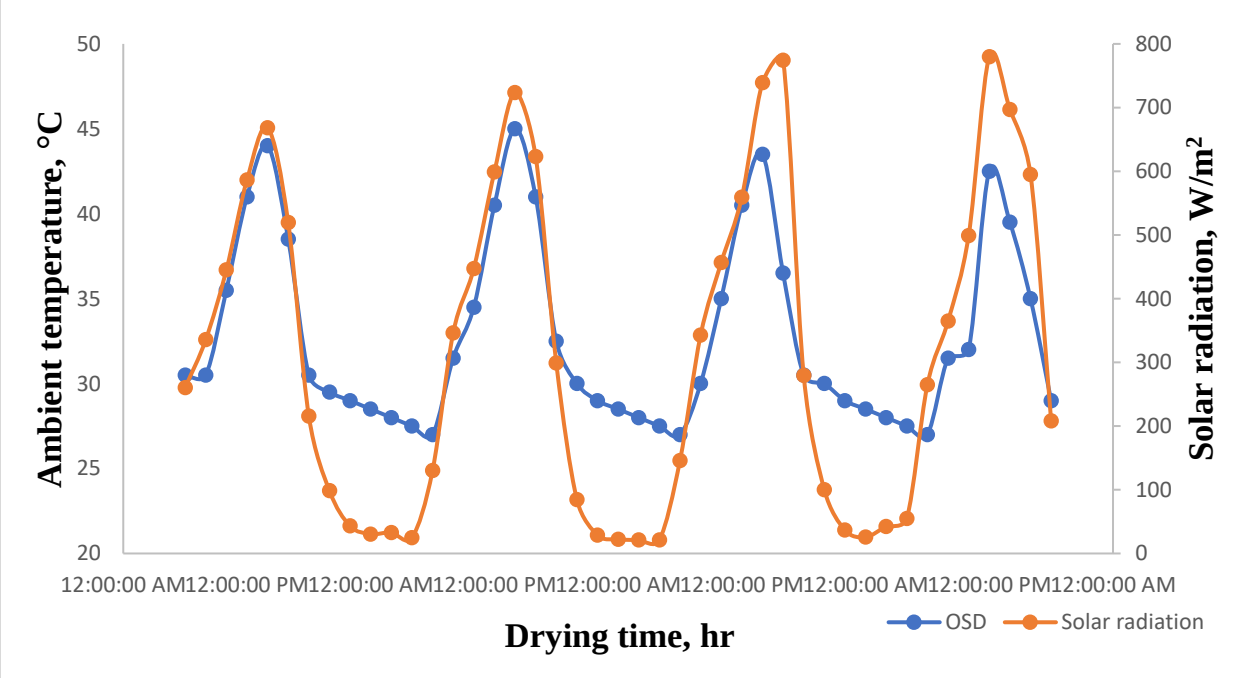

Figure 25: Changes in ambient temperature and solar radiation during drying of cassava

University of Ghana http://ugspace.ug.edu.gh

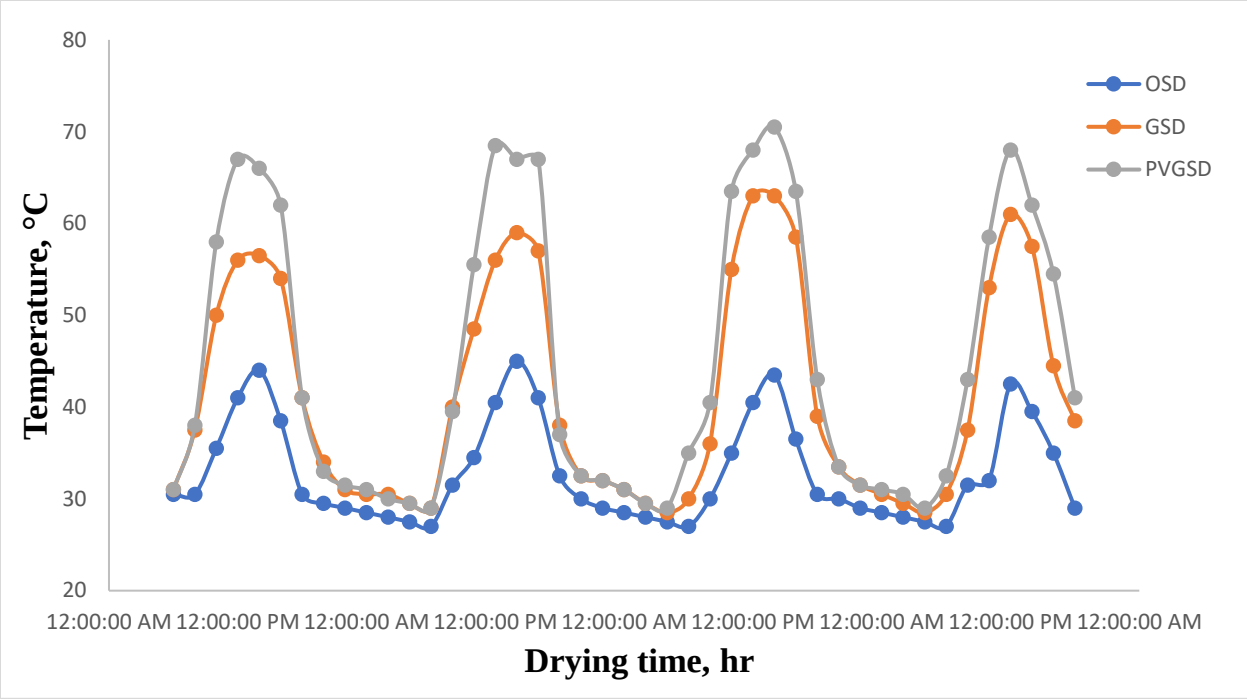

Figure 26: Comparison of the temperatures of PVGSD, GSD and OSD during drying of cassava samples.

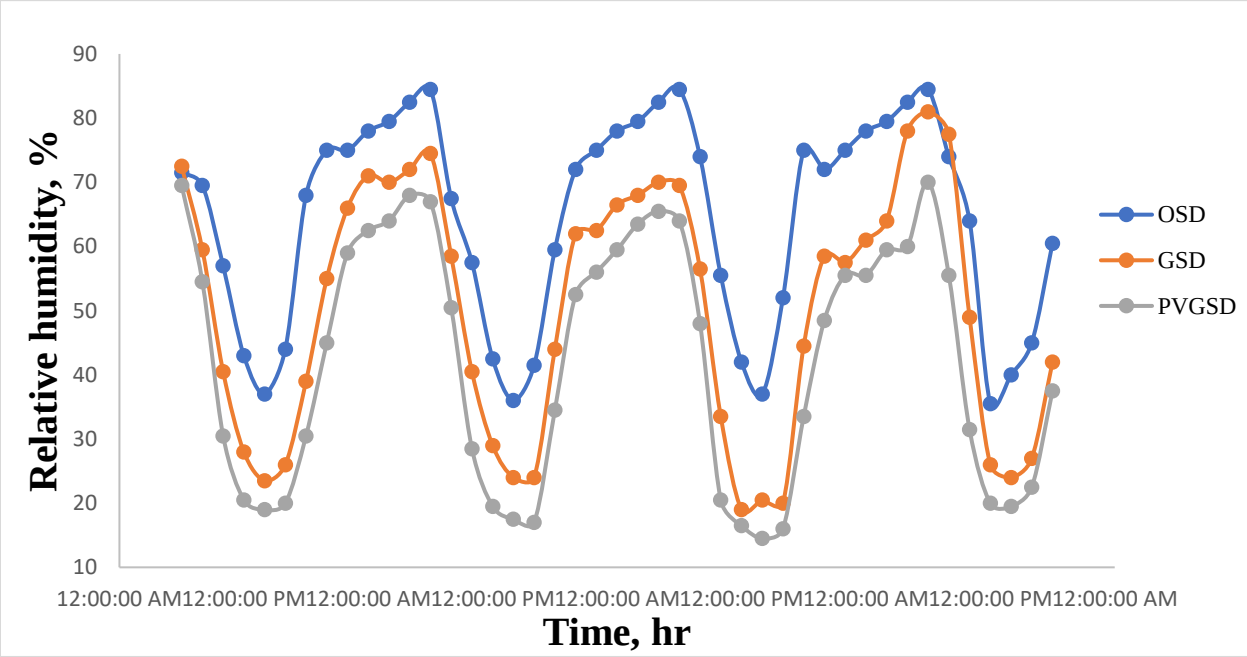

Figure 27: Comparison of the relative humidity of PVGSD, GSD and OSD during drying of cassava samples.

University of Ghana http://ugspace.ug.edu.gh

Analysis of variance performed on the temperature and relative humidity data showed both the temperature and relative humidity measured was greatly influenced by the drying methods (PVGSD, GSD and OSD) and the time of drying, this indicates that the temperature and relative humidity attained during the experimental drying of cassava samples are dependent on the dryer type and drying time. The ANOVA Tables for temperature and relative humidity can be seen in Tables 13 and 14 respectively.

Table 13: Analysis of Variance of (ANOVA) Temperature variations of Cassava samples during drying.

Source	SS	DF	MS	F-Value	P-value	F crit.
Drying time	14735.4	42	350.8427	12.28146	0.000	1.529201
Drying method	3382.05	2	1691.025	59.19535	0.000	3.105157
Error	2399.616	84	28.56686			
Total	20517.06	128				

Table 14: Analysis of Variance (ANOVA) of Humidity variations of Cassava samples during drying.

Source	SS	DF	MS	F-Value	P-value	F crit.
Drying time	41370.39	42	985.0092	49.68525	0.000	1.529201
Drying method	10651.7	2	5325.851	268.6434	0.000	3.105157
Error	1665.298	84	19.82498			
Total	53687.39	128				

b. Cassava drying to test the ability of the workstation to reduce humidity at night (with 1200 watts)

The Figures 28 and 29 below show the variations of ambient and solar dryers' temperatures and relative humidity during the drying experiments of cassava samples. For all the drying methods,

University of Ghana http://ugspace.ug.edu.gh

highest temperatures were recorded from 12 p.m. to 3 p.m. The OSD temperature and relative humidity were found to range from 24°C to 43°C and 41.5% to 89% respectively. The PVGSD drying temperature varied from 25°C to 67°C and the relative humidity range from 25.5% to 73.%. The GSD drying temperature varied from 23°C to 62.5°C and a relative humidity range of 27.5% to 90.5%. It appears that the temperatures achieved in the PVGSD and GSD were similar, the main differences being in the range of relative humidity. The PVGSD obtained the highest temperature and lowest relative humidity throughout the drying of cassava samples.

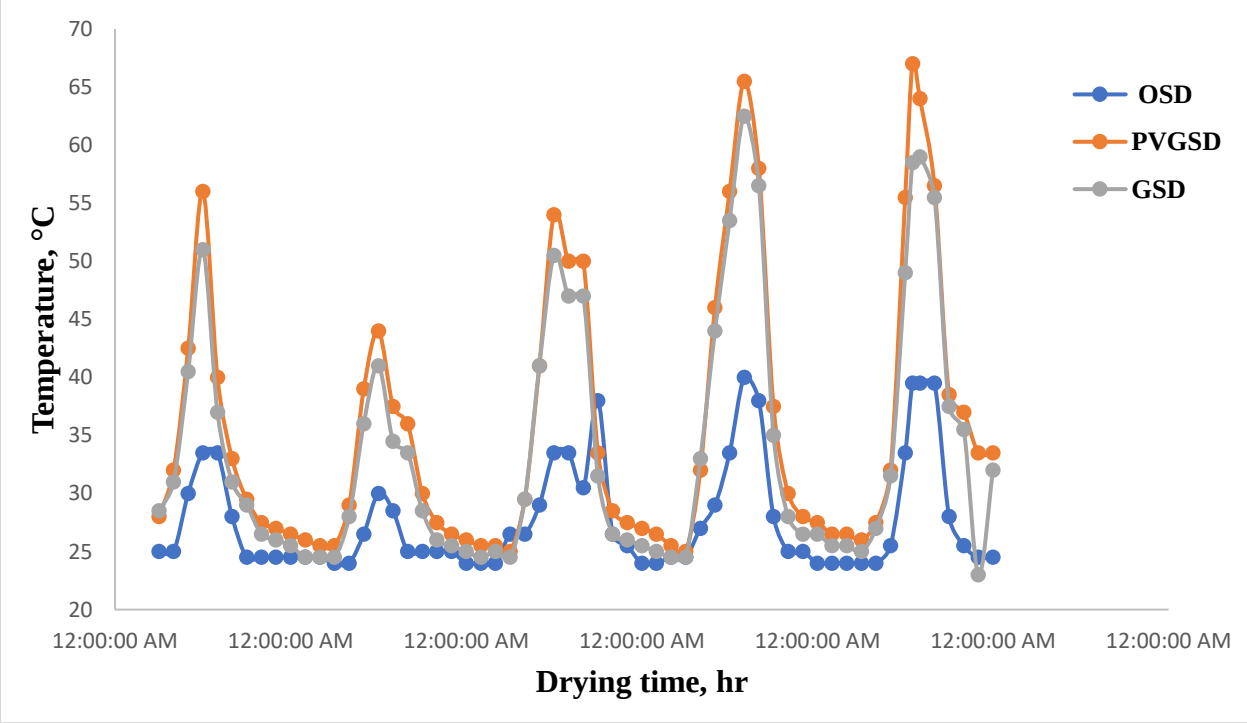

Figure 28: Comparison of the temperatures of PVGSD, GSD and OSD during drying of cassava samples

University of Ghana http://ugspace.ug.edu.gh

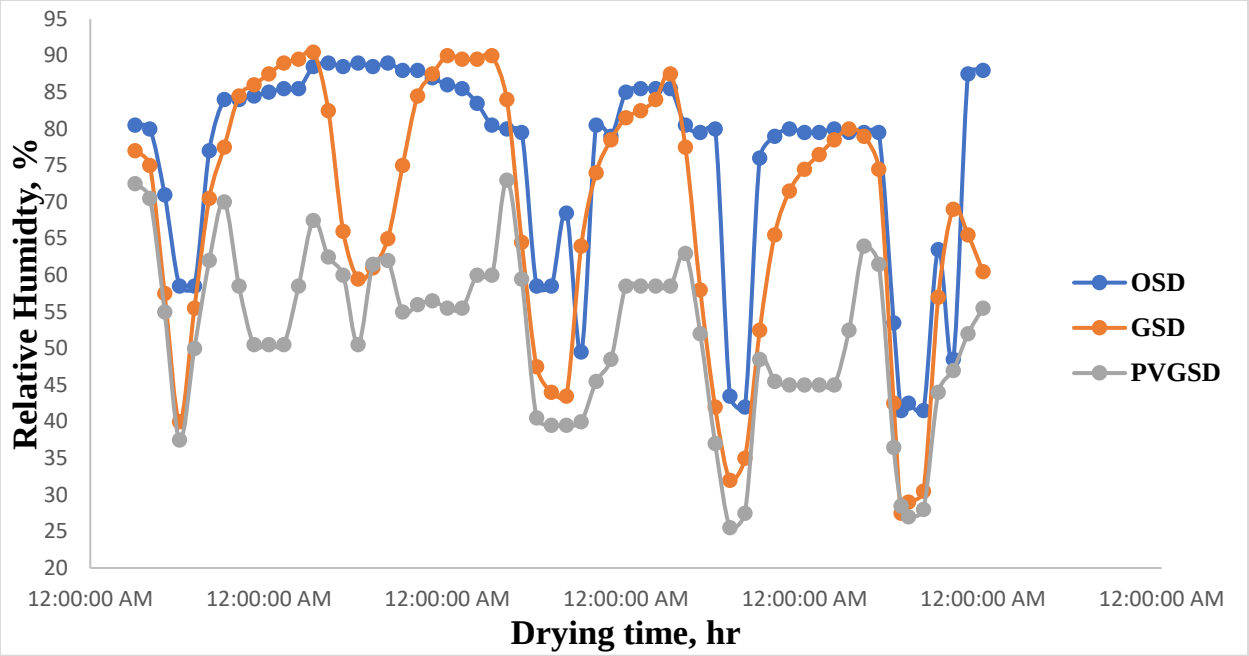

Figure 29: Comparison of the relative humidity of PVGSD, GSD and OSD during drying of cassava samples.

Analysis of variance performed on the temperature and relative humidity data showed both the temperature and relative humidity measured were greatly influenced by the drying methods (PVGSD, GSD and OSD) and the time of drying, this indicates that the temperature and relative humidity attained during the experimental drying of cassava samples are dependent on the dryer type and drying time. The ANOVA Tables for temperature and relative humidity can be seen in Tables 15 and 16 respectively.

Table 15: Analysis of Variance of (ANOVA) Temperature variations of Cassava samples during drying.

Source	SS	DF	MS	F	P-value	F crit.
Drying time	14306.08	58	246.6566	13.26853	0.000	1.437545
Drying method	2077.774	2	1038.887	55.88541	0.000	3.074447
Error	2156.393	116	18.58959			
Total	18540.25	176				

University of Ghana http://ugspace.ug.edu.gh

Table 16: Analysis of Variance (ANOVA) of Humidity variations of Cassava samples during drying.

Source	SS	DF	MS	F	P-value	F crit.
Drying time	32152.18	58	554.3478	9.322524	0.000	1.437545
Drying method	17994.93	2	8997.463	151.3113	0.000	3.074447
Error	6897.74	116	59.46328			
Total	57044.84	176				

It was also observed that for the rainy periods during drying, due to high relative humidity and low temperatures in the solar dryers, the GSD accumulated moisture which was evidence on the surfaces of the polycarbonate sheets while such occurrence was not observed in the PVGSD due to the ability of the fans to extract excess moisture from the drying chamber. These observations are seen in Illustrations 20 and 21.

Illustration 20: Accumulation of moisture on the surface of the polycarbonate sheet inside the GSD

University of Ghana http://ugspace.ug.edu.gh

Illustration 21: No accumulation of moisture on the surface of the polycarbonate sheet inside the PVGSD

4.5.2 Drying Kinetics

4.5.2.1 Moisture Content of Dried Red Pepper

Untreated red peppers dried under the three drying systems, exhibited varying rate of moisture removal (Figure 30). The moisture content reduced continuously with drying time for all the systems. The data is summarized in Appendix 4. The PVGSD observed a faster moisture removal than the OSD and also a slight difference from the GSD possibly due to higher temperatures trapped inside the PVGSD with associated lower humidity. The moisture content of red pepper in the PVGSD, GSD and OSD was reduced from an initial value of 77%± 1% (w.b) or 3.35 g water/g dry matter to a final moisture content of 7.6%±0.141(w.b) in 72 hours for PVGSD and 9.9%±0.129(w.b) for the GSD in 72 hours and 8.4%±0.158(w.b) in the OSD in 152 hours. This

University of Ghana http://ugspace.ug.edu.gh

indicated that the solar dryers are able to dry the peppers faster than Open Sun Drying. The drying time virtually reduced by 50%.

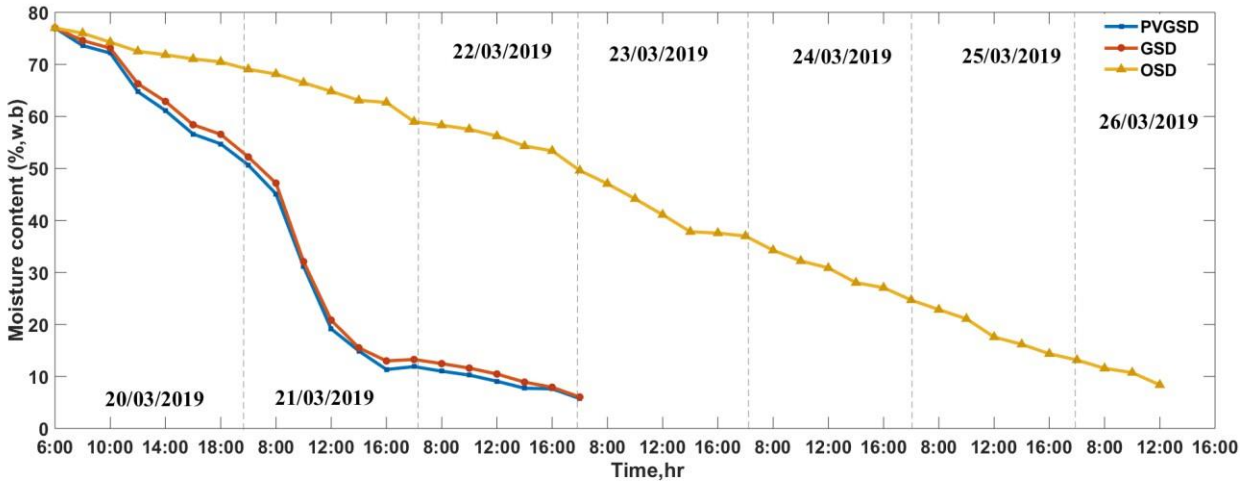

Figure 30: Moisture content variation with time for red pepper

Analysis of variance considering the influence of drying method and time on the moisture content of red pepper indicated that moisture removal was significantly affected by both the drying method and the time of drying (Table 17). Time of drying is a factor in that, highest temperatures for all the drying systems were recorded during 12:00 p.m. to 15:00 p.m. GMT which is critical for moisture evaporation from a food material, while as lowest temperatures was recorded during 18:00 p.m. to 5:00 a.m. GMT. The drying methods used are different in relations to design considerations (design concepts, material selection, temperature and humidity variations, etc.) and as such expected to demonstrate three different modes of moisture removal from the red pepper samples. The two fans were turned on mostly at night (6 p.m.) when relative humidity was high, however this was only sustained on an average of 7hrs/day on full battery power (Delkor HICA80 battery).

University of Ghana http://ugspace.ug.edu.gh

Table 17: ANOVA of Moisture Content changes for Red Pepper

Source of Variation	SS	DF	MS	F-Value	P-value	F crit
Drying time	47966.12	19	2524.533	5165.124	0.000	1.7625
Drying method	23190.83	2	11595.41	23723.9	0.000	3.1504
Interaction	9550.596	38	251.3315	514.2173	0.000	1.6032
Error	29.32591	60	0.488765			
Total	80736.87	119				

4.5.2.2 Drying Rate of Dried Red Pepper

Different food materials show different drying rate curves due to difference in structural compositions. The drying rates versus time for the three drying methods is represented in Figure 31. It was observed that the drying rate of red pepper was faster in the two solar dryers than the open sun drying with a drying rate of 0.097g/g.h in the PVGSD as compared to GSD with 0.094g/g.h and OSD with 0.047g/g.h, and it decreased continuously with the drying time. From drying rate data summarized in Appendix 5, the PVGSD demonstrated a higher drying rate as compared to the other two. The data illustrated in Figure 31 show that the drying rate of red pepper at the start of experimental drying increased and subsequently decreased. The observation made could be attributed to lower evaporation rate in red pepper. All the drying operations was observed in the falling rate period, the constant rate drying period however was not seen. In the falling rate period, the material surface was not saturated with water and drying rate is controlled by diffusion of moisture from within the solid to the surface.

University of Ghana http://ugspace.ug.edu.gh

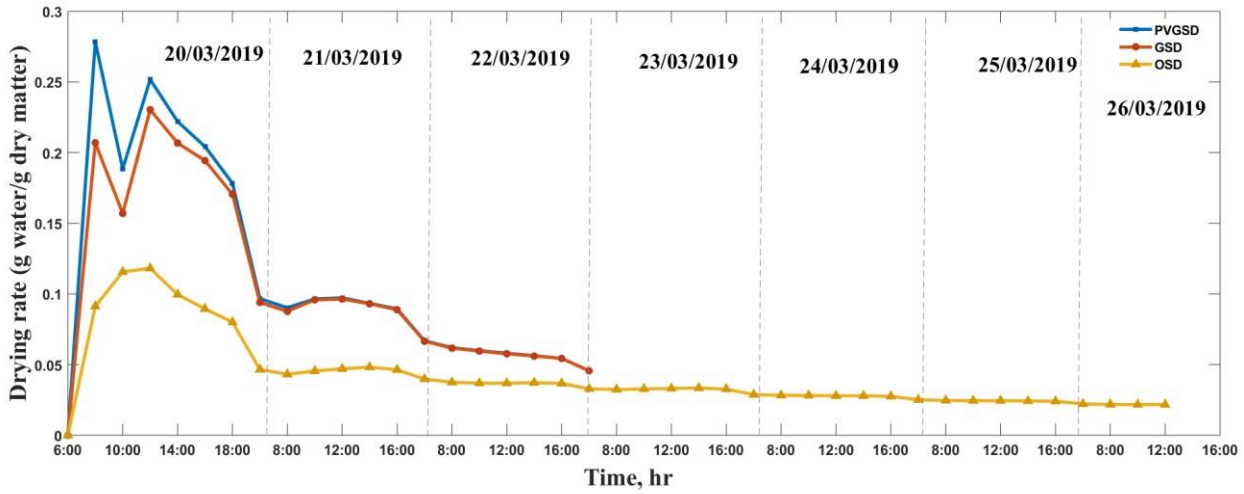

Figure 31: Changes in drying rate with time for red pepper in PVGSD, GSD and OSD.

Analysis of variance considering the effect of drying method and time on the drying rate of red pepper indicated that drying rate was significantly affected ($p<0.05$) by both the drying method and the time of drying as seen in Table 18.

Table 18: ANOVA of Drying rates changes for Red Pepper

Source	SS	DF	MS	F	P-value	F crit.
Drying time	0.350761	19	0.018461	413.8687	0.000	1.762547
Drying method	0.073309	2	0.036654	821.7324	0.000	3.150411
Interaction	0.047628	38	0.001253	28.09846	0.000	1.603237
Error	0.002676	60	4.46E-05			
Total	0.474374	119				

4.5.2.3 Effect of shelf position on the Moisture Content and Drying Rate of Red Pepper

To further appreciate the influence of shelf position on the rate of moisture removal and drying rate in the PVGSD samples of red pepper were spread on the trays and positioned on the two racks labelled A and B. From top to bottom samples were labelled T1-A1, T2-B1, T4-A2, T5-B2 and T3-B3. The variations in moisture content and drying rate of red pepper samples at the different

University of Ghana http://ugspace.ug.edu.gh

positions on the shelves in the dryer are shown in Figure 32 and 33 respectively. Moisture content was noticed to decreased continuously with time from an initial moisture content of 77% (w.b) to 10.2% in 52 hours for T1-A1, 10.16% in 52 hours for B1-T2, 10.49% in 56 hours for T4-A2, 10.08% in 56 hours for T5-B2 and 10.01% in 72 hours for B3-T3. This show that irrespective of the rack position samples on the top shelf (T1-A1 and T2-B1) tend to dry faster as compared to samples on the bottom shelf (T3-B3).

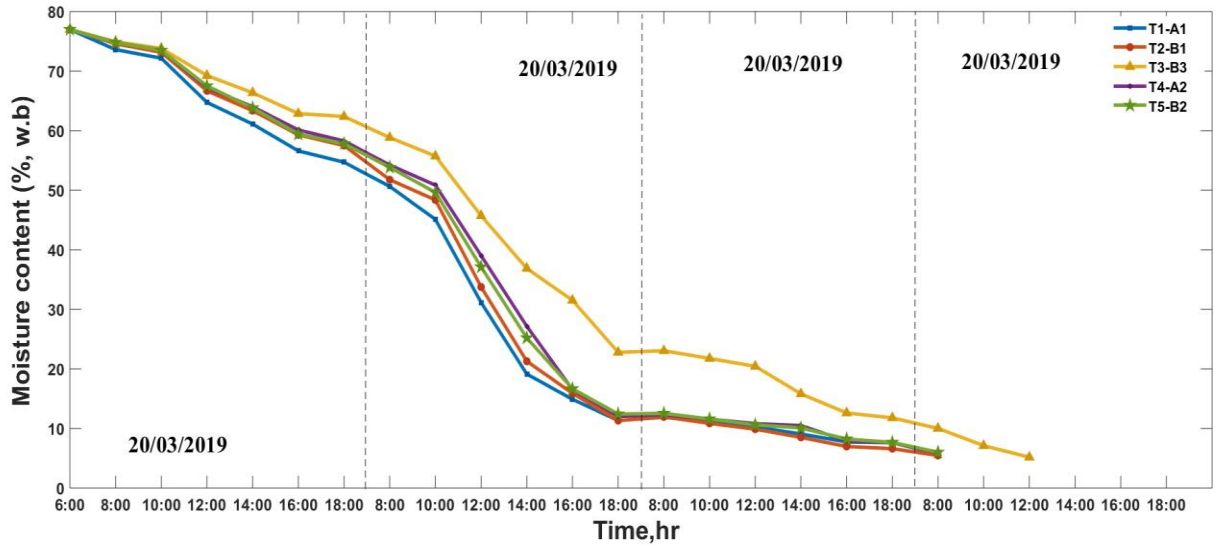

Figure 32: Changes in moisture content with time of red pepper at various shelf position inside the PVGSD.

University of Ghana http://ugspace.ug.edu.gh

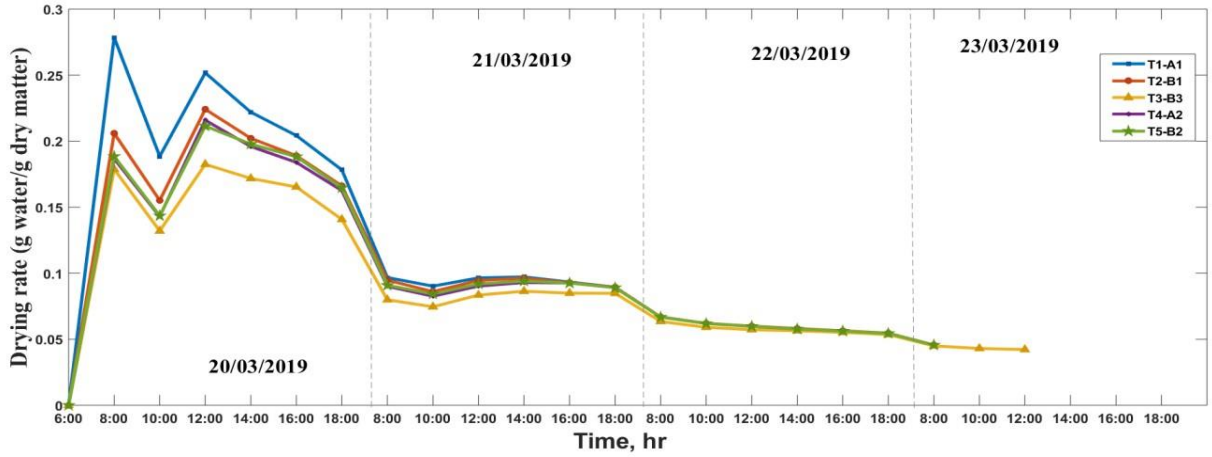

Figure 33: Changes in drying rate with time of red pepper at various shelf position inside the PVGSD.

Analysis of variance considering the effect of tray position and drying time on the moisture content and drying rate of red pepper indicated that moisture removal was significantly affected by both the tray position and the time of drying (Table 19 and 20). In drying practice therefore, it may be prudent to interchange the position of the drying trays through a determined sequence to maximize drying efficiency.

Table 19: Analysis of Variance (ANOVA) of Moisture Content changes at different shelf position for Red Pepper

Source	SS	DF	MS	F-Value	P-value	F crit.
Drying time	66190.45	19	3483.708	711.5896	1.45E-77	1.725029
Tray position	761.4793	4	190.3698	38.88534	1.09E-17	2.492049
Error	372.071	76	4.89567			
Total	67324	99				

University of Ghana http://ugspace.ug.edu.gh

Table 20: Analysis of Variance (ANOVA) of Moisture Content changes at different shelf position for Red Pepper

Source	SS	DF	MS	F	P-value	F crit.
Drying time	0.362751	19	0.019092	152.3994	0.000	1.725029
Tray position	0.004892	4	0.001223	9.761812	0.000	2.492049
Error	0.009521	76	0.000125			
Total	0.377164	99				

4.5.2.4 Moisture Content of Dried Cassava Samples

a. Cassava drying to test the ability of the workstation to reduce humidity at night (with 80watts battery)

Cassava samples in the form of slices and chunks were dried in the three systems (PVGSD, GSD and OSD) and the change in moisture content versus time is represented in Figure 34 and 35. The data for the variation in moisture content with time is summarized in Appendix 6. The cassava pulp with an average initial moisture content of 64%±0.58(w.b) were dried to final moisture content for cassava slices of 9.21%, 9.62% and 10.05% respectively for PVGSD, GSD and OSD. Whilst the solar dryers attained a relatively low moisture in about 48 hours, the open sun drying took about 72 hours. The cassava chunks achieved a final moisture content of 8.43%, 9.43% and 10.09% for PVGSD, GSD and OSD respectively. Generally, the cassava slices demonstrated a faster moisture removal than the chunks (Appendix 6). The two fans were turned on mostly at night (6 p.m.) when relative humidity was high, however this was only sustained on an average of 7hrs/day on full battery power (Delkor HICA80 battery).

University of Ghana http://ugspace.ug.edu.gh

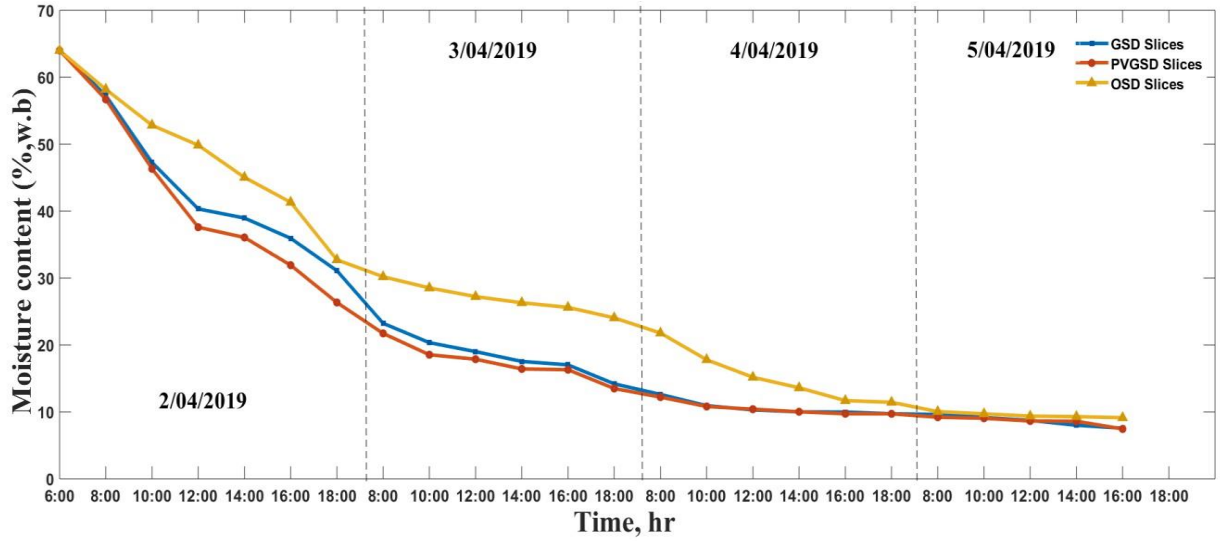

Figure 34: Changes in content with time of cassava slices in PVGSD GSD and OSD.

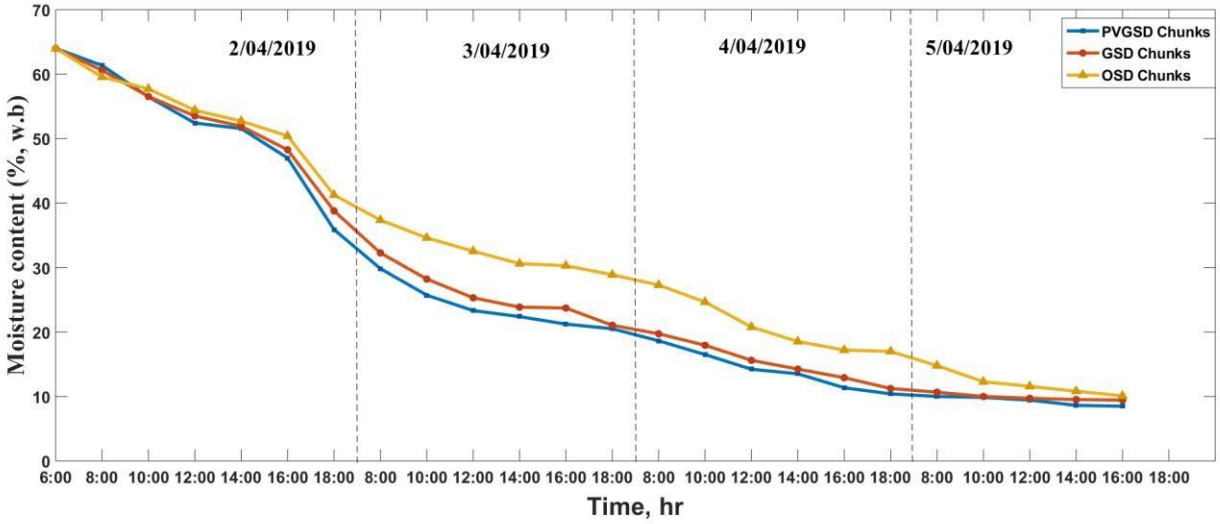

Figure 35: Changes in moisture content with time of cassava chunks in PVGSD GSD and OSD

Analysis of variance performed on the moisture content data delineating sample size, drying method and drying time showed that all factors significantly ($p<0.05$) affected the rate of moisture

University of Ghana http://ugspace.ug.edu.gh

loss during the drying experiment (Table 21). The size or shape of the sample is important in moisture removal since water travels from the center of the material along its radius to the surface (Mercer, 2018).

Table 21: ANOVA of Moisture Content changes for Cassava samples

Source	DF	SS	MS	F-Value	P-Value
Drying method	2	718.0	358.99	51.87	0.000
Sample size	1	1025.5	1025.51	148.16	0.000
Drying time	23	40368.0	1755.13	253.58	0.000
Interaction	2	31.9	15.97	2.31	0.104
Error	115	796.0	6.92		
Total	143	42939.4			

b. Cassava drying to test the ability of the workstation to reduce humidity at night (with 1200watts battery)

In an earlier experiment, the battery installed in the workstation attached to the PVGSD could not have enough power to run the two fans continuously during the night due to the fans having a higher power rating (100watts) than the battery (80watts). The fans could not function overnight. The experiment was repeated with a stronger battery power (two batteries each with a capacity of 1200watts). The system was able to run the fans throughout the night.

Cassava samples slices and chunks were dried using the three drying methods (PVGSD, GSD and OSD) and the change in moisture content with time are seen in Figure 36 and 37 respectively. The data for the variations in moisture content with time is summarized in Appendix 8. From Fig. 36 the PVGSD with the workstation and control system showed consistent reduction in the moisture content throughout the drying as compared to the GSD and the OSD where increases in moisture

University of Ghana http://ugspace.ug.edu.gh

and humidity were measured during the nights. This suggest that the fans were able to maintain a relatively lower humidity and the samples did not show any increase in moisture content. For the PVGSD, the two fans were operated in full capacity mostly at night (from 6 p.m.) when relative humidity was high, however power was sustained on an average of 13hrs/day on full battery power of 1200 watts. It was observed that for the PVGSD, moisture was extracted out instead of accumulating in the drying chamber during the night. During the period of this experiment it rained intermittently for the first three days. That is why the samples in the PVGSD took slightly longer time to dry.

The cassava had an initial moisture content of 65%±0.71(w.b) and was dried to final moisture content of 9.74% (d.b) in 84 hours, 9.89% (d.b) in 108 hours and 9.78% (d.b) in 124 hours respectively for PVGSD, GSD and OSD. The time gained in using a PVGSD was about 40 hours. The cassava chunks achieved a final moisture content of 10.13%, 10.09% and 10.11% for PVGSD, GSD and OSD respectively. Generally, the cassava slices demonstrated a faster moisture removal than the chunks (Appendix 8).

University of Ghana http://ugspace.ug.edu.gh

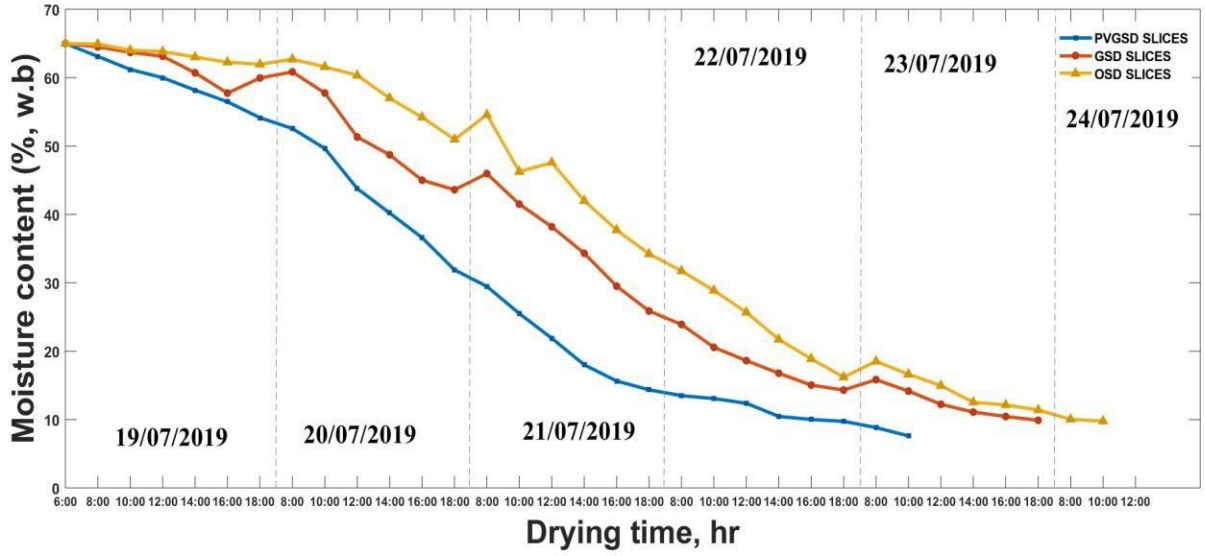

Figure 36: Changes in moisture content with time of cassava slices under PVGSD, GSD and OSD

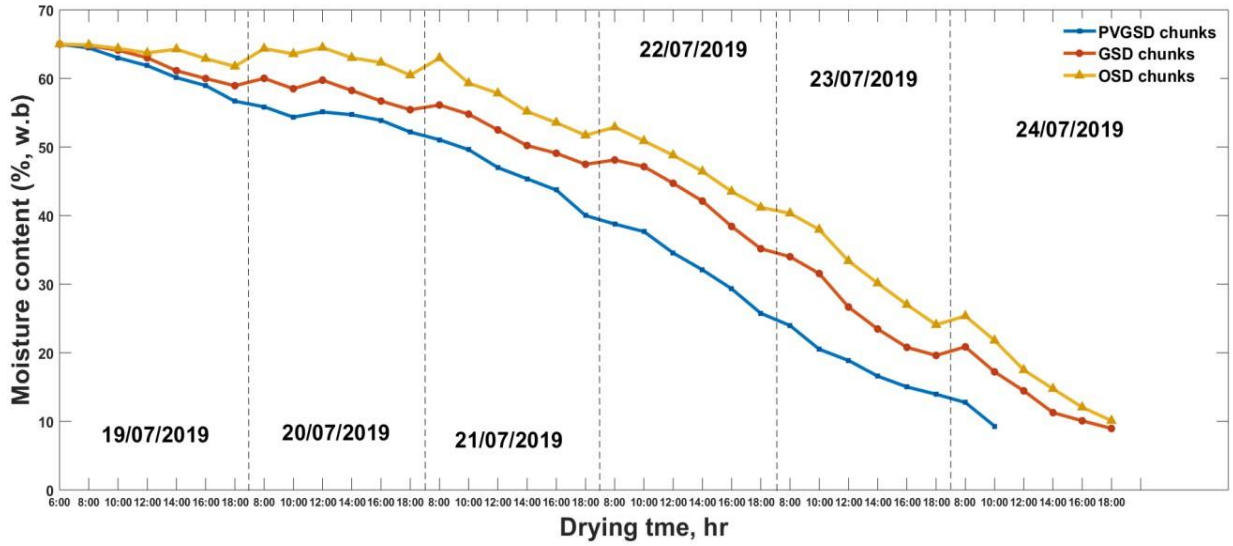

Figure 37: Changes in moisture content with time of cassava chunks under PVGSD, GSD and OSD

University of Ghana http://ugspace.ug.edu.gh

Analysis of variance performed on the moisture delineating sample size, drying method and drying time showed that all factors significantly affected ($p<0.05$) the rate of moisture loss during the drying experiment (Table 22). The size (slices/chunks) of the sample was important in moisture removal since water must move from the center of the material along its radius to reach the surface (Mercer, 2018).

Table 22: ANOVA for Moisture Content changes for Cassava samples

Source	DF	SS	MS	F-Value	P-Value
Drying method	2	3383	1691.56	49.38	0.000
Sample size	1	6280	6279.59	183.32	0.000
Drying time	26	32611	1254.27	36.62	0.000
Error	132	4522	34.26		
Total	161	46795			

4.5.2.5 Drying rate of Dried Cassava Samples

a. Cassava drying to test the ability of the workstation to reduce humidity at night (with 80watts battery)

The data for drying rate of cassava slices and chunks are summarized in Figures 38 and 39. It was observed that the drying rate fluctuates for all the drying methods. This was mainly due to the change in the solar radiation and the associated changes in the air temperature.

From the data summarized in Appendix 7, PVGSD recorded the highest drying rates of 0.114 g/g.hr and 0.060 g/g.hr for cassava slices and chunks respectively after 8 hours of drying.

University of Ghana http://ugspace.ug.edu.gh

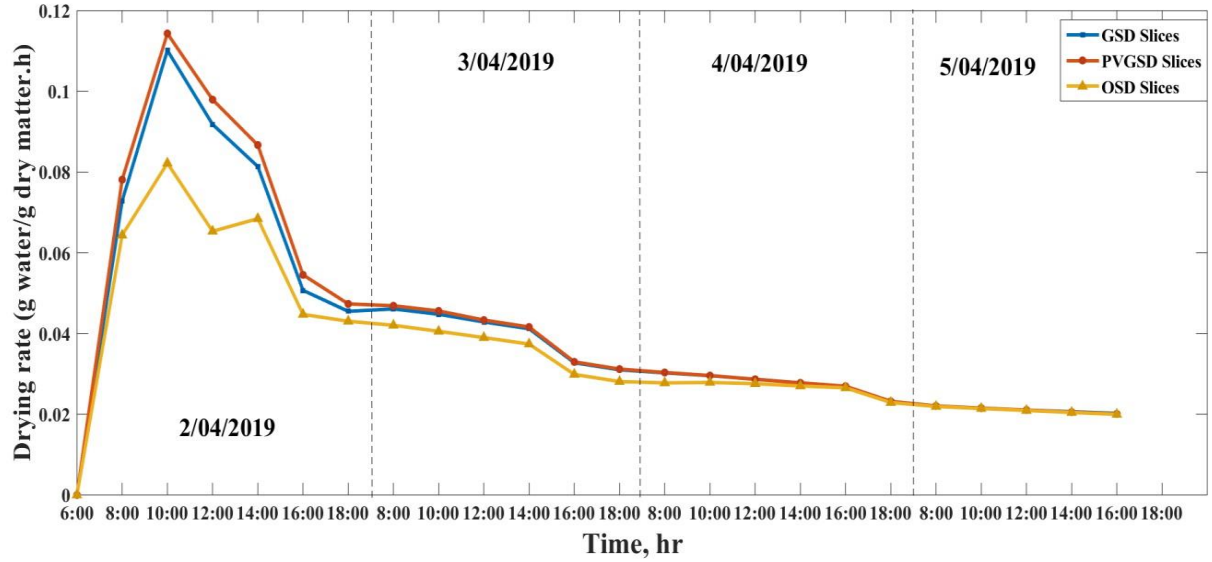

Figure 38: Variations in drying rate with time for cassava slices in PVGSD, GSD and OSD.

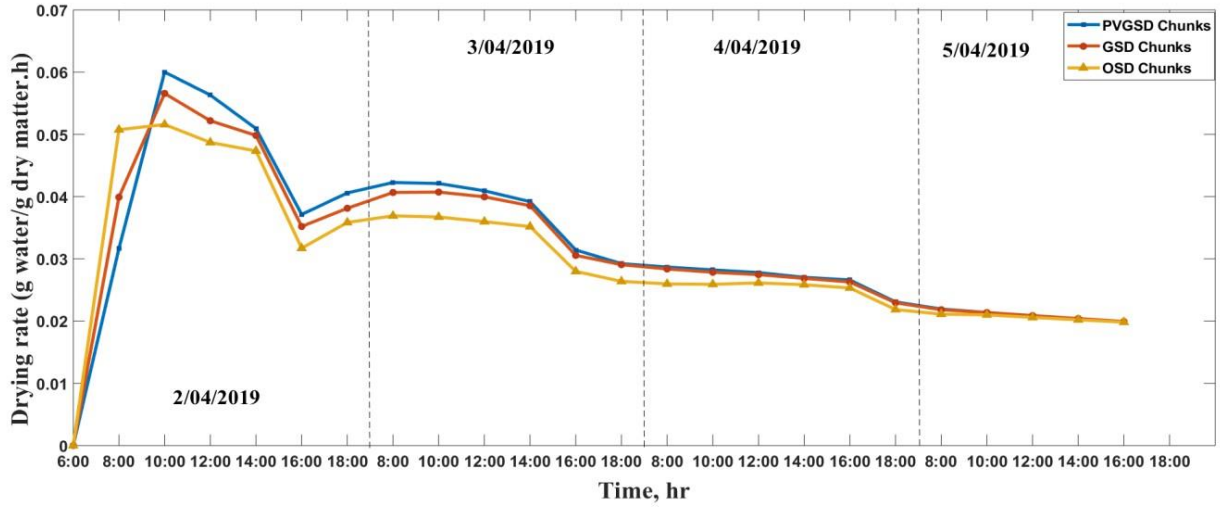

Figure 39: Variations in drying rate with time for cassava chunks in PVGSD, GSD and OSD.

Also, analysis of variance performed on the drying rate of cassava samples indicated that the drying method, drying time and sample size significantly affected the rate of drying cassava.

University of Ghana http://ugspace.ug.edu.gh

Table 23: Analysis of Variance (ANOVA) of drying rate changes for Cassava samples

Source	DF	SS	MS	F-Value	P-Value
Drying method	2	0.000409	0.000204	3.21	0.044
Sample size	1	0.002197	0.002197	34.51	0.000
Drying time	23	0.043971	0.001912	30.03	0.000
Interaction	2	0.000119	0.000060	0.94	0.395
Error	115	0.007322	0.000064		
Total	143	0.054018			

b. Cassava drying to test the ability of the workstation to reduce humidity at night (with 1200watts battery)

The data for drying rate of cassava slices and chunks are summarized in Figure 40 and 41. The drying rate was found to fluctuate for all the drying methods. This was as a result of the drying air temperature and relative humidity. From the data summarized in Appendix 9, PVGSD recorded the highest drying rates of 0.0732 g/g.hr and 0.0457 g/g.hr for cassava slices and chunks while GSD recorded at 0.0491g/g.hr and 0.0355g/g.hr for cassava slices and chunks respectively. The OSD drying rate for cassava slices and chunks was 0.02074g/g.hr and 0.01667g/g.hr respectively. This shows that PVGSD running under fan capacity has the potential of increasing drying rates hence reduce drying time.

University of Ghana http://ugspace.ug.edu.gh

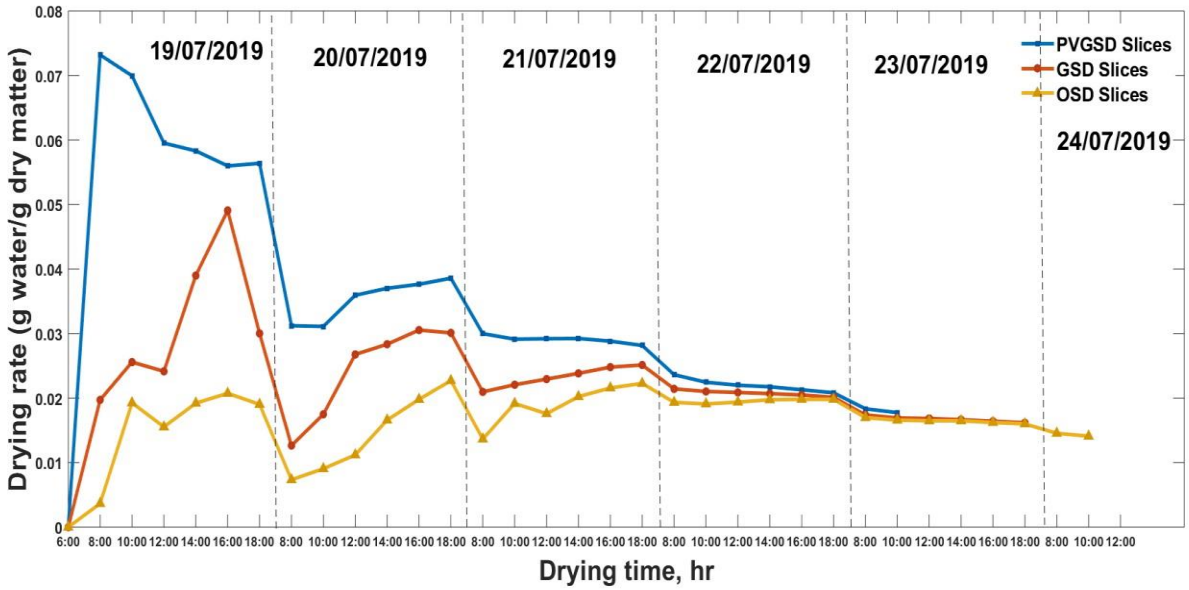

Figure 40: Variations in drying rate with time for cassava slices in PVGSD, GSD and OSD.

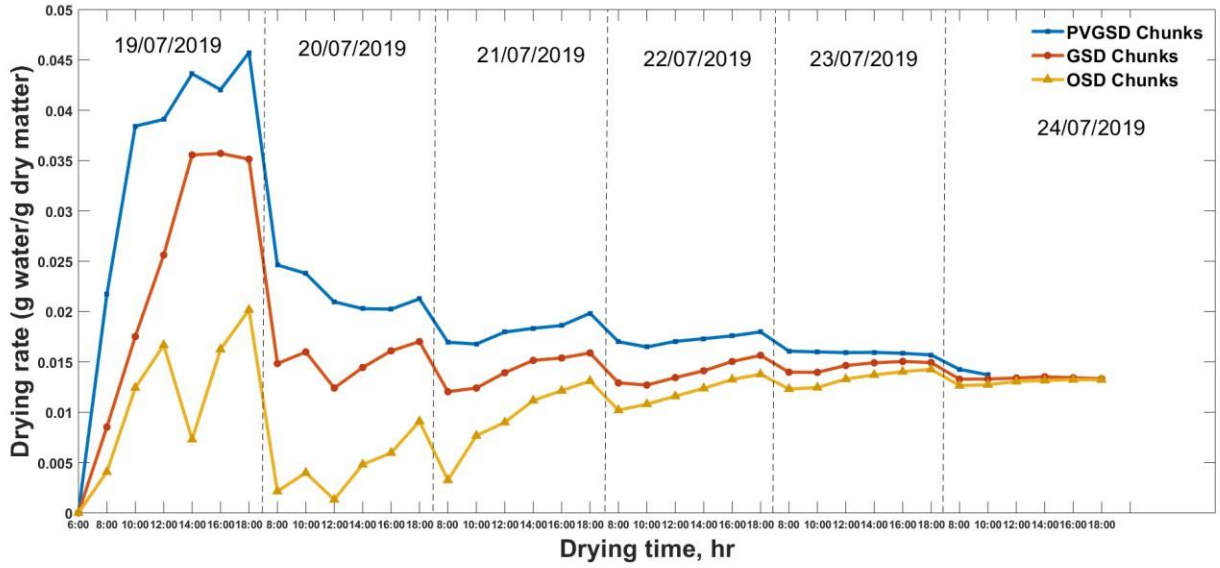

Figure 41: Variations in drying rate with time for cassava chunks in PVGSD, GSD and OSD.

University of Ghana http://ugspace.ug.edu.gh

4.6 Mathematical modelling for the drying process of red pepper and cassava root using the three drying methods, PVGSD, GSD and OSD.

Thin layer drying equations help evaluate the drying hours of many foods and as well generalize their drying behavior. The experimental moisture ratio (MR) against the time were modelled against twelve mathematical models as shown in Table 1 and were evaluated using MATLAB software for identifying the best fit on the basis of the corresponding coefficient of determination (R^2), root mean square error (RMSE) and reduced chi-square distribution (χ^2).

4.6.1 Mathematical modelling for red pepper

The outcome from the regression analysis and the values of the coefficients and constants for the three drying methods, PVGSD, GSD and OSD are shown respectively in Tables 24, 25 and 26. The suitability of the model's equations was assessed on the basis of the highest value of R^2 and lowest values of χ^2 and RMSE describing the best model to represent the drying process of the red pepper (Karthikeyan and Murugavelh, 2018).

The Midilli and Kucuk model yielded the higher value of R^2 = 0.98891 and lowest χ^2 = 0.00126 and RMSE = 0.03542 for PVGSD and R^2 = 0.98940, χ^2 = 0.00128 and RMSE = 0.03572 for GSD from the regression analysis performed on the *MR* data. While for OSD, the Logarithmic model yielded the highest value of R^2 = 0.99710, χ^2 = 0.00026 and RMSE = 0.01638. Thus, the Midilli and Kucuk model for PVGSD is expressed as:

$$MR = 0.98542\ exp\ (-2.0887t^{1.2011}) - 0.0023488t \qquad \text{Eq.(27)}$$

And Midilli and Kucuk model for GSD is expressed:

$$MR = 0.98947\ exp\ (-2.0694t^{1.3068}) + 0.0017757t \qquad \text{Eq.(28)}$$

University of Ghana http://ugspace.ug.edu.gh

Similarly, the Logarithmic model for OSD can be expressed by

$MR = 1.1317\ exp\ (-0.49834t) - 0.14417$ Eq.(29)

The experimental moisture ratio using the Midilli and Kucuk model and Logarithmic model for red pepper under PVGSD, GSD and OSD are presented in Figures 42 to 44 respectively. These models can be used to estimate the moisture ratio of red pepper under the three drying methods.

University of Ghana http://ugspace.ug.edu.gh

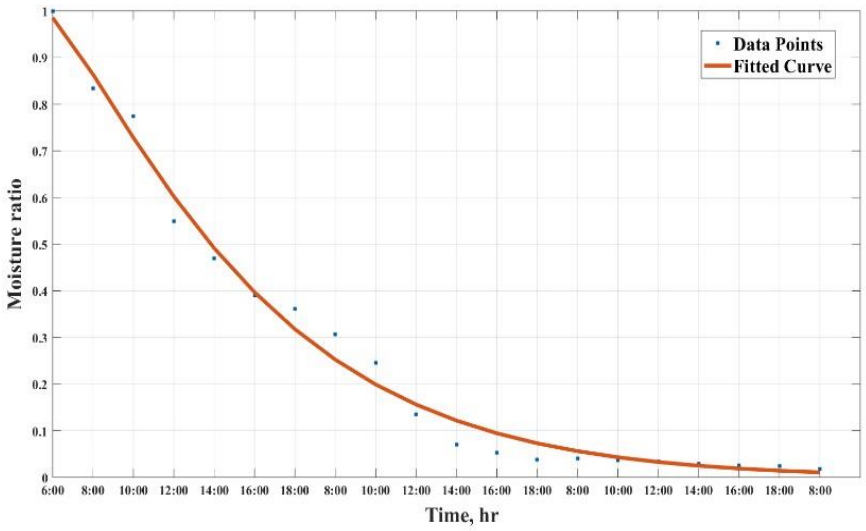

Figure 42: Experimental Midilli and Kucuk model curve for red pepper under PVGSD.

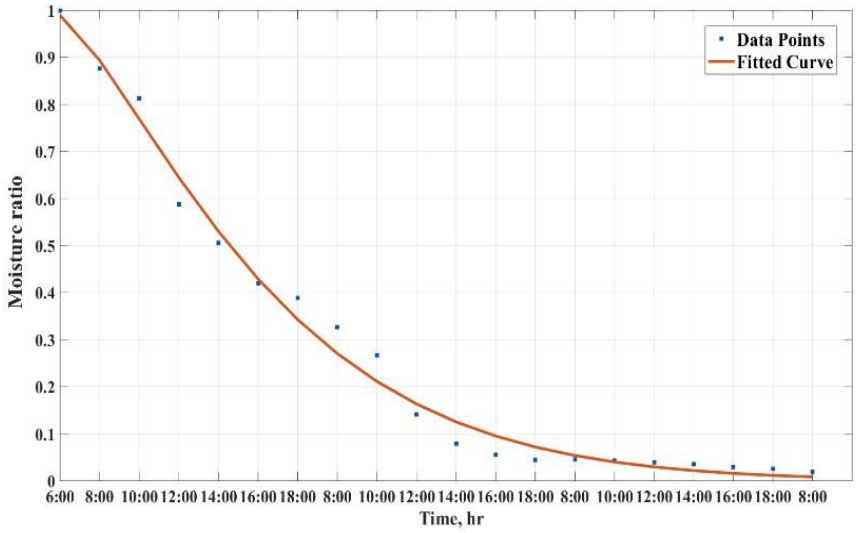

Figure 43: Experimental Midilli and Kucuk model curve for red pepper under GSD

University of Ghana http://ugspace.ug.edu.gh

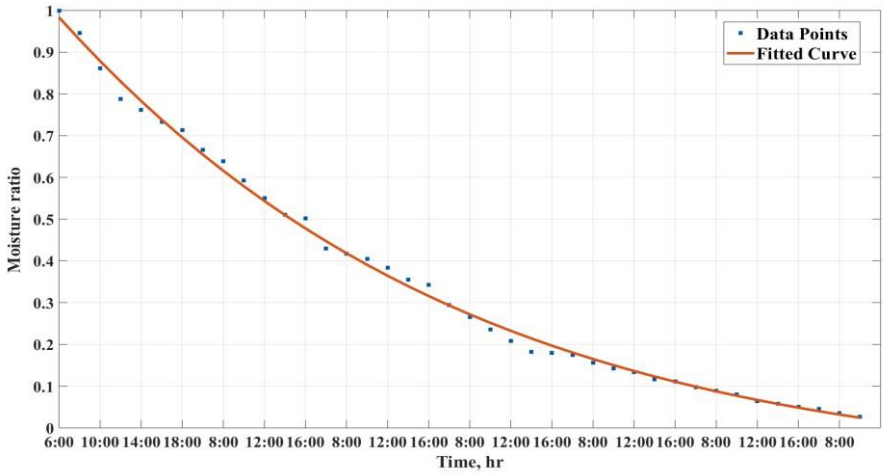

Figure 44: Experimental Logarithmic model curve for red pepper under OSD.

Table 24: Mathematical models and respective constants for PVGSD of Red Pepper.

Model no.	Model constants	R^2	χ^2	RMSE
1	k=1.9498	0.981425	0.001769	0.042066
2	k=2.0257; a=1.0417	0.983235	0.001685	0.041059
3	k=2.1217; n=1.1862	0.988706	0.001135	0.033700
4	k=1.8855; n=1.1861	0.988706	0.001135	0.033700
5	k_0=1.0658; k_1=1.0244; a=15.381; b=14.3855	0.986261	0.001554	0.039425
6	a=-1.3565; b=0.45816	0.984883	0.001520	0.038990
7	k=1.2596; a=5.4561; b=0.90962	0.987465	0.001334	0.036533
8	k=1.7844; a=1.0697; c=-0.046291	0.986721	0.001413	0.037601
9	k=2.5779; a=1.7098	0.988611	0.001145	0.033842
10	**k=2.0887; n=1.2011; a=0.98542 b=-0.0023488**	**0.988908**	**0.001262**	**0.035423**
11	k=1.7527; a=22.8042; g=1.7437	0.982099	0.001906	0.043658
12	k=1.385; a=1.4201; b=-5.9906; c=5.5755; g=0.19132; h=0.16639	0.988646	0.001467	0.038314

University of Ghana http://ugspace.ug.edu.gh

Table 25: Mathematical models and respective constants for GSD of Red Pepper.

Model no.	Model constants	R^2	χ^2	RMSE
1	k=1.8326	0.974762	0.002558	0.050581
2	k=1.9471; a=1.0677	0.979419	0.002202	0.046928
3	k=2.0572; n=1.2789	0.989329	0.001141	0.033791
4	k=1.7578; n=1.2789	0.989329	0.001141	0.033791
5	k_0=1.129; k_1=1.0508; a=8.2655; b=-7.2287	0.985696	0.001721	0.041496
6	a=-1.3077; b=0.42933	0.988832	0.001195	0.034570
7	k=1.0645; a=7.4813; b=0.92127	0.984155	0.001795	0.042370
8	k=1.6677; a=1.1058; c=-0.060221	0.984343	0.001773	0.042117
9	k=2.5851; a=1.8285	0.988795	0.001198	0.034626
10	**k=2.0694; n=1.3068; a=0.98947; b=0.0017757**	**0.989404**	**0.001279**	**0.035715**
11	k=1.5849; a=-13.6777; g=1.6016	0.976131	0.002704	0.052003
12	k=1.342; a=1.401; b=-5.1029; c=4.7359; g=0.065958; h=0.039317	0.9869978	0.001788	0.042295

University of Ghana http://ugspace.ug.edu.gh

Table 26: Mathematical models and respective constants for OSD of Red Pepper.

Model no.	Model constants	R^2	χ^2	RMSE
1	k=0.66265	0.987523	0.001008	0.031751
2	k=0.68181; a=1.0282	0.988581	0.000946	0.030772
3	k=0.61191; n=1.1446	0.993636	0.000527	0.022973
4	k=0.65108; n=1.1445	0.993636	0.000527	0.022973
5	k_0=0.66919; k_1=0.68117; a=-0.041498; b=1.0695	0.988582	0.000999	0.031615
6	a=-0.50243; b=0.066785	0.994804	0.000430	0.020758
7	k=1.0094; a=-22.9539; b=0.98021	0.994437	0.000473	0.021766
8	**k=0.49834; a=1.1317; c=-0.14417**	**0.997105**	**0.000268**	**0.016380**
9	k=0.66271; a=1.0086	0.987523	0.001034	0.032167
10	k=0.54895; n=1.0696; a=0.97604; b=-0.018525	0.996928	0.001588	0.016396
11	k=0.66368; a=1.0464; g=0.68172	0.987525	0.001062	0.032596
12	k=0.68602; a=15.7857; b=-14.6969; c=-0.10534; g=0.69961; h=0.0061187	0.996984	0.000256	0.016026

4.6.2 Mathematical modelling for Cassava root slices and chunks.

a. Cassava root drying to test the ability of the workstation to reduce humidity at night (with 80watts battery)

The result of the regression analysis and the values of the coefficients and constants for the three drying methods, PVGSD, GSD and OSD for the drying of cassava slices and chunks are shown in Tables 27, 28 and 29 for cassava slices and Tables 30, 31 and 32 for cassava chunks respectively. The mathematical models were assessed considering the highest R^2 value and lowest χ^2 and RMSE values describing the best model to predict the drying kinetics of the cassava with two sizes (Karthikeyan and Murugavelh, 2018).

University of Ghana http://ugspace.ug.edu.gh

Table 27: Mathematical models and respective constants for PVGSD of cassava root slices.

Model No.	Model constants	R^2	χ^2	RMSE
1	k=2.3613	0.906884	0.005037	0.070973
2	k=1.9861; a=0.87555	0.924321	0.004280	0.065422
3	k=1.8651; n=0.63068	0.980335	0.001112	0.033348
4	k=2.6868; n=0.63068	0.980335	0.001112	0.033348
5	K_0=1.9724; k_1=1.9688; a=2.9677; b=-2.0932	0.924313	0.004708	0.068619
6	a=-1.2822; b=0.40635	0.670619	0.018628	0.136486
7	**k=5.7083; a=0.63661; b=0.1493**	**0.990705**	**0.000550**	**0.023466**
8	k=3.2448; a=0.88284; c=0.089805	0.972452	0.001632	0.040399
9	k=6.5421; a=0.27075	0.950143	0.002819	0.053100
10	k=2.0218; n=0.67391; a=1.0149; b=0.013278	0.981894	0.001458	0.033561
11	k=5.7008; a=0.63713; g=0.85117	0.990705	0.000550	0.023466
12	k=2.0394; a=1.0272; b=0.46741; c=-0.60885; g=0.55553; h=0.68018	0.918948	0.005602	0.074850

University of Ghana http://ugspace.ug.edu.gh

Table 28: Mathematical models and respective constants for GSD of cassava root slices

Model No.	Model constants	R^2	χ^2	RMSE
1	k=2.7749	0.955725	0.002506	0.050067
2	k=2.5582; a=0.9344	0.960126	0.002360	0.048581
3	k=2.1747; n=0.70452	0.986247	0.000814	0.028530
4	k=3.0124; n=0.70455	0.986247	0.000814	0.028530
5	K_0=4.3553; k_1=0.66377; a=0.81005; b=0.19559	0.995661	0.000282	0.016807
6	a=-1.3739; b=0.45016	0.701472	0.017670	0.132929
7	**k=4.2948; a=0.80893; b=0.15138**	**0.995634**	**0.000270**	**0.016453**
8	k=3.4419; a=0.92275; c=0.064839	0.992892	0.000440	0.020993
9	k=6.9137; a=0.29808	0.977129	0.001353	0.036793
10	k=2.5815; n=0.81801; a=1.0104; b=0.02389	0.994069	0.001551	0.019650
11	k=4.2948; a=0.80894; g=0.65011	0.995634	0.000270	0.016453
12	k=1.7002; a=0.97772; b=-8.467; c=8.302; g=0.19644; h=0.18586	0.944144	0.004040	0.063568

Table 29: Mathematical models and respective constants for OSD of cassava root slices.

Model No.	Model constants	R^2	χ^2	RMSE
1	k=2.4626	0.961863	0.002257	0.047516
2	k=2.2554; a=0.92707	0.967589	0.002006	0.044788
3	k=2.0521; n=0.73317	0.988895	0.000687	0.026215
4	k=2.6657; n=0.73311	0.988895	0.000687	0.026215
5	K_0=4.2885; k_1=0.92395; a=0.70452; b=0.29586	0.992236	0.000528	0.022991
6	a=-1.3342; b=0.42953	0.773958	0.013990	0.118282
7	k=4.2786; a=0.70532; b=0.21534	0.992236	0.000503	0.022437
8	k=2.9402; a=0.91529; c=0.059554	0.989485	0.000681	0.026110
9	k=6.8295; a=0.27421	0.982614	0.001076	0.032803
10	**k=2.3073; n=0.81304; a=1.0071; b=0.018194**	**0.992708**	**0.001157**	**0.022280**
11	k=4.2811; a=0.70492; g=0.9223	0.992236	0.000503	0.022437
12	k=1.5639; a=1.3917; b=-17.0484; c=16.5119; g=0.57149; h=0.55744	0.966697	0.002519	0.050192

University of Ghana http://ugspace.ug.edu.gh

It was observed from the regression analysis of the MR data for cassava slices dried under PVGSD and GSD that Approximation of diffusion model obtained the higher value of R^2 = 0.99071 and lowest χ^2 =0.00055 and RMSE = 0.02347 and R^2 = 0.99563, χ^2 = 0.00027 and RMSE = 0.01645 respectively. While for OSD Midilli and Kucuk model best fit the drying curve with R^2 = 0.99271, χ^2 = 0.00116 and RMSE = 0.02228. Thus, the Approximation of diffusion model for cassava slices dried under PVGSD can be expressed as:

$$MR = 0.63661\exp(-5.7083t) + (1-0.63661)\exp(-5.7083\times0.1493\times t) \quad \text{Eq. (30)}$$

And Approximation of diffusion model for GSD can be expressed:

$$MR = 0.80893\exp(-4.2948t) + (1-0.80893)\exp(-4.2948\times0.15138\times t) \quad \text{Eq. (31)}$$

The Midilli and Kucuk model for OSD is expressed by:

$$MR = 1.0071\exp(-2.3073t^{0.81304}) + 0.018194t \quad \text{Eq. (32)}$$

The experimental moisture ratio using the Approximation of diffusion model and Midilli and Kucuk model for cassava slices under PVGSD, GSD and OSD are shown in Figures 45 to 47 respectively. These models can be used for the estimation of moisture ratio of cassava slices under the three drying methods.

University of Ghana http://ugspace.ug.edu.gh

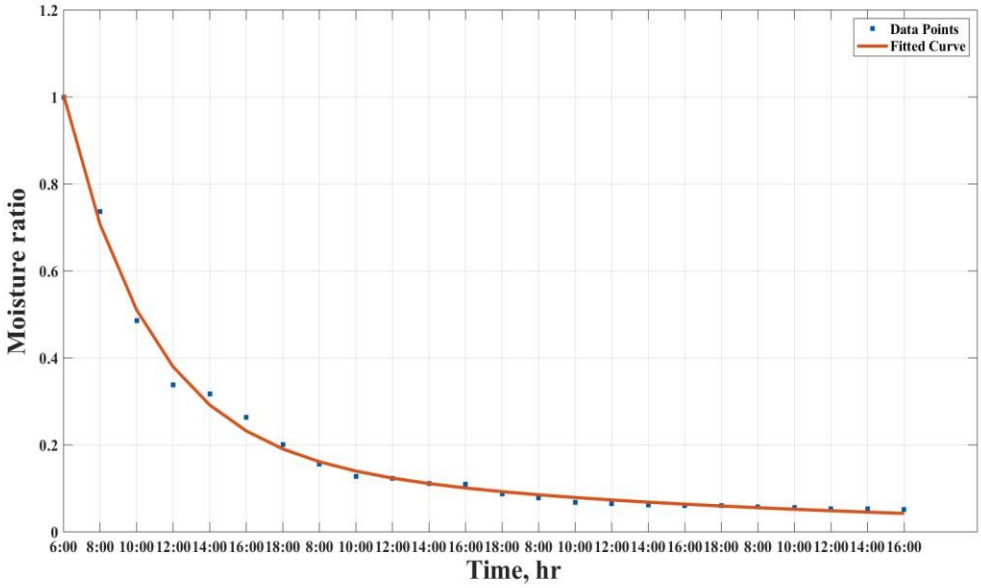

Figure 45: Experimental Approximation of diffusion model curve for Cassava slices under PVGSD.

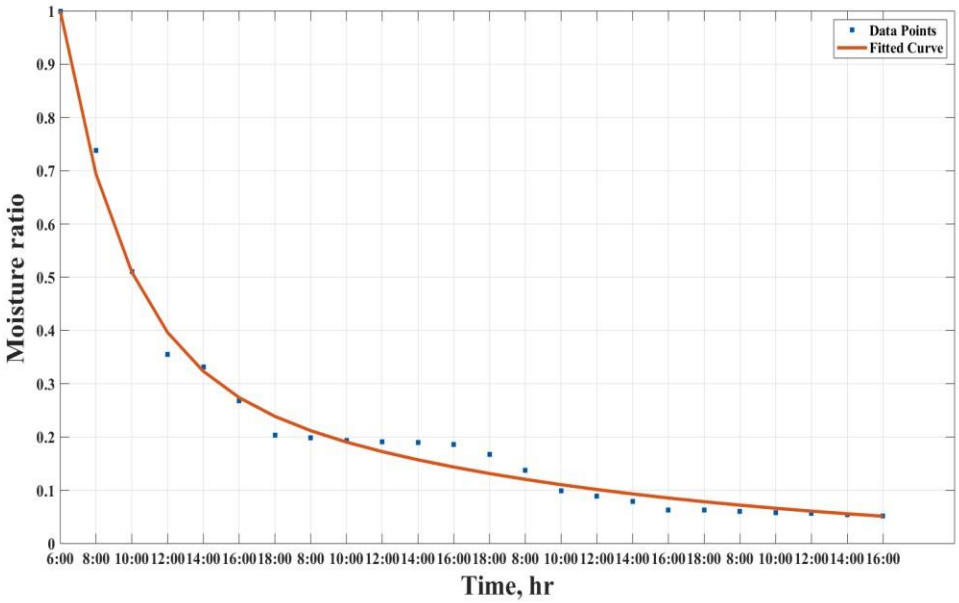

Figure 46: Experimental Approximation of diffusion model curve for Cassava slices under GSD

University of Ghana http://ugspace.ug.edu.gh

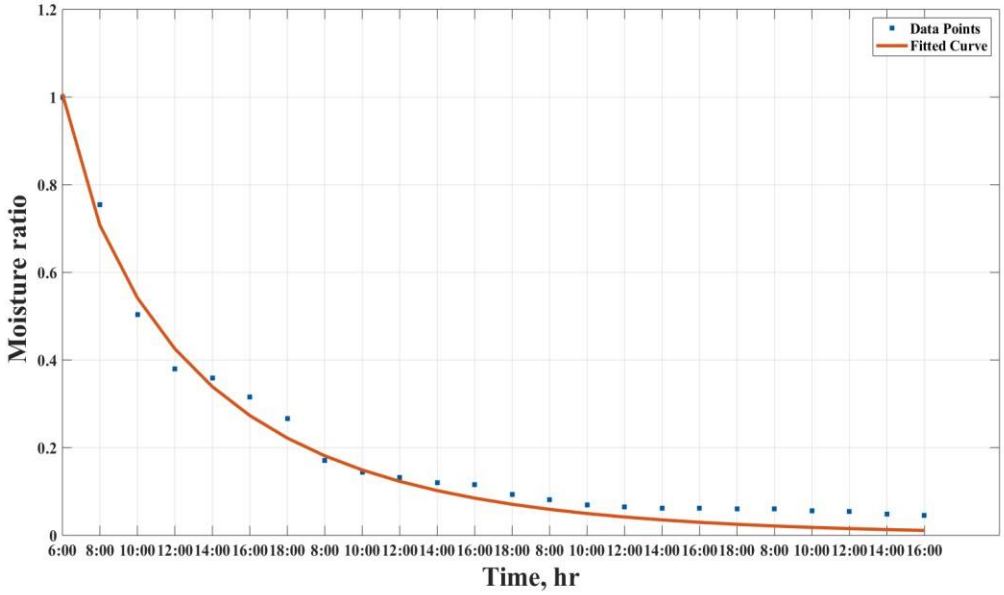

Figure 47: Experimental Midilli and Kucuk model curve for Cassava slices under OSD.

However, for the drying of cassava chunks under PVGSD, GSD and OSD, Verma et. al model, Midilli and Kucuk model and Logarithmic model respectively best fit the drying curves for these drying methods.

Thus, the Verma et. al. model for PVGSD is expressed as:

$$MR = 0.54761\exp(-3.5142t) + (1-0.54761)\exp(-0.96771t) \quad \text{Eq. (33)}$$

And Midilli and Kucuk model for GSD is expressed:

$$MR = 0.98772\exp(-1.8316t^{1.2001}) + 0.026882t \quad \text{Eq. (34)}$$

Similarly, the Logarithmic model for OSD can be expressed by:

$$MR = 0.96403\exp(-1.4289t) + 0.031937 \quad \text{Eq. (35)}$$

University of Ghana http://ugspace.ug.edu.gh

Table 30: Mathematical models and respective constants for PVGSD of cassava root chunks.

Model No.	Model constant	R^2	χ^2	RMSE
1	k=1.779	0.973723	0.001691	0.041129
2	k=1.6386; a=0.92882	0.980120	0.001337	0.036577
3	k=1.6488; n=0.79099	0.992986	0.000472	0.021725
4	k=1.8817; n=0.79098	0.992986	0.000472	0.021725
5	k_0=1.6373; k_1=1.6432; a=0.89392; b=0.03462	0.980120	0.001471	0.038363
6	a=-1.182; b=0.35629	0.887712	0.007557	0.086932
7	k=111.91; a=0.13804; b=0.013505	0.987016	0.000915	0.030256
8	k=2.0868; a=0.91032; c=0.060951	0.991534	0.000596	0.024430
9	k=4.8853; a=0.27794	0.991271	0.000587	0.024237
10	k=1.7439; n=0.83145; a=1.004; b=0.010711;	0.993718	0.000676	0.021564
11	**k=3.5142; a=0.54761; g=0.96771**	**0.994301**	**0.000401**	**0.020045**
12	k=1.0625; a=7.8898; b=0.015297; c=-6.9885; g=-0.84099; h=0.99426	0.981376	0.001531	0.039140

University of Ghana http://ugspace.ug.edu.gh

Table 31: Mathematical models and respective constants for GSD of cassava root chunks.

Model No.	Model constants	R^2	χ^2	RMSE
1	k=1.5725	0.985020	0.001207	0.034754
2	k=1.5994; a=1.0168	0.985337	0.001236	0.035157
3	k=1.5855; n=1.0279	0.985232	0.001244	0.035282
4	k=1.5657; n=1.0279	0.985232	0.001244	0.035282
5	k_0=1.2448; k_1=1.2707; a=-10.0079; b=11.0127	0.984185	0.001466	0.038294
6	a=-1.1311; b=0.32964	0.965741	0.002887	0.053739
7	k=9.3992; a=-0.05632; b=0.17616	0.985822	0.001252	0.035384
8	k=1.7438; a=1.0035; c=0.027518	0.986986	0.001149	0.033900
9	k=1.7815; a=0.68459	0.985163	0.001250	0.035364
10	**k=1.8316; n=1.2001; a=0.98772; b=0.026882**	**0.990440**	**0.002299**	**0.029772**
11	k=1.6032; a=0.99973; g=-2.1646	0.986993	0.001148	0.033891
12	k=1.2676; a=1.8519; b=0.0089431; c=-0.87407; g=-0.61838; h=1.0087	0.984797	0.001566	0.039577

University of Ghana http://ugspace.ug.edu.gh

Table 32: Mathematical models and respective constants for OSD of cassava root chunks.

Model No.	Model constants	R^2	χ^2	RMSE
1	k=1.3236	0.987293	0.000943	0.030723
2	k=1.2971; a=0.98114	0.987783	0.000948	0.030802
3	k=1.3148; n=0.94521	0.988410	0.000900	0.030001
4	k=1.3358; n=0.94523	0.988410	0.000900	0.030001
5	K_0=1.2396; k_1=1.2847; a=-0.23524; b=1.216	0.987775	0.001044	0.032316
6	a=-1.0126; b=0.27648	0.965790	0.002656	0.051543
7	k=77.3893; a=0.041798; b=0.016348	0.988069	0.000970	0.031155
8	**k=1.4289; a=0.96403; c=0.031937**	**0.989095**	**0.000887**	**0.029785**
9	k=1.877; a=0.51087	0.988904	0.000861	0.029355
10	k=1.3875; n=1.017; a=0.99049; b=0.014045	0.989080	0.001275	0.030542
11	k=1.2826; a=-0.97407; g=1.3028	0.987279	0.001034	0.032170
12	k=1.0953; a=1.3037; b=-0.3494; c=0.0020577; g=0.76347; h=-0.66999	0.986300	0.001300	0.036061

The experimental moisture ratio using the Verma et. al model, Midilli and Kucuk model and Logarithmic model for cassava chunks under PV- greenhouse solar drying (PVGSD), greenhouse solar drying (GSD) and open sun drying (OSD) are shown in Figures 48 to 50 respectively.

University of Ghana http://ugspace.ug.edu.gh

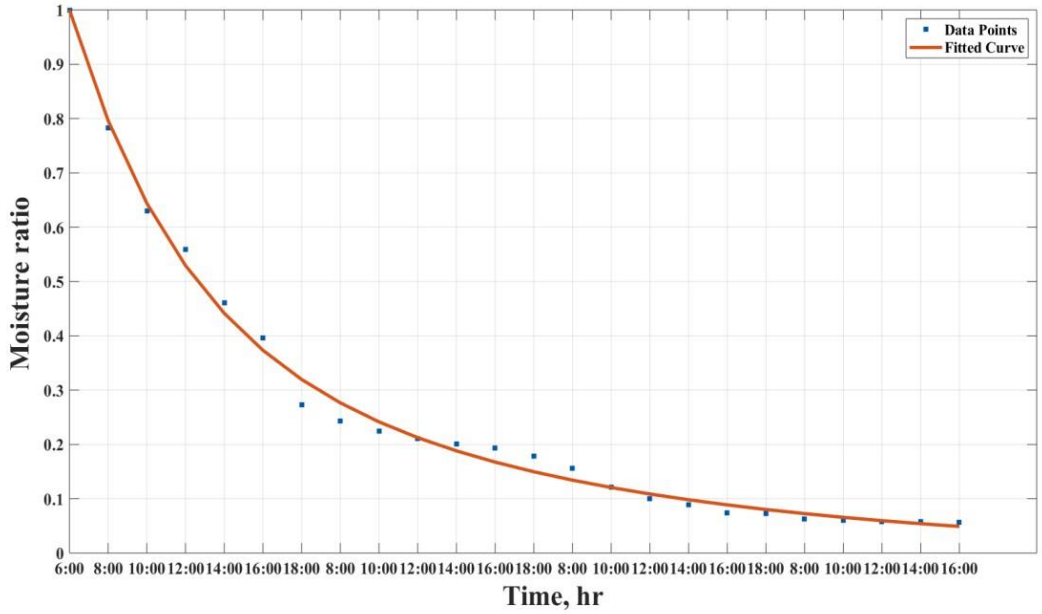

Figure 48: Experimental Verma et. al model curve for Cassava Chunks under PVGSD.

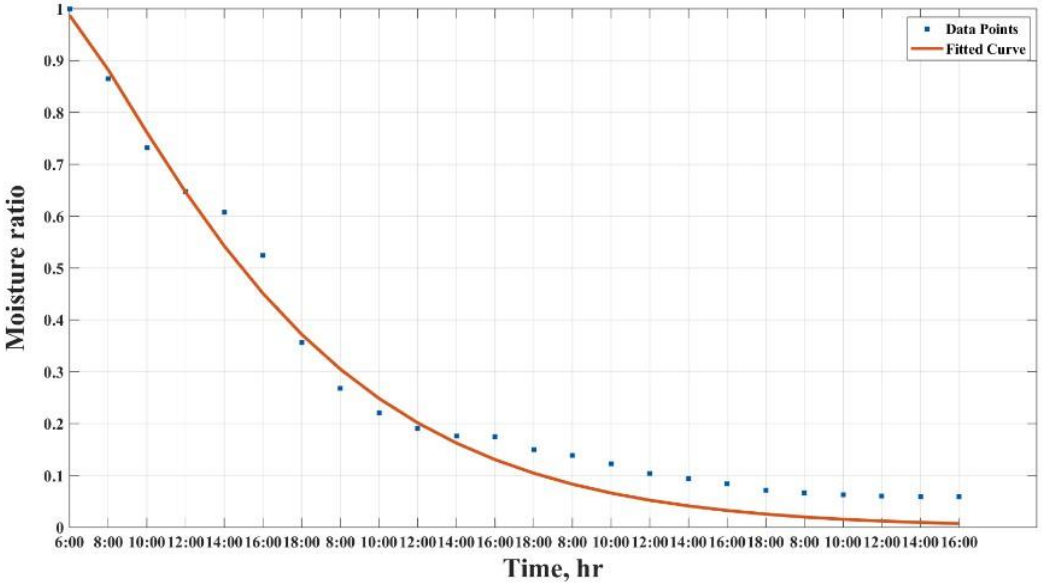

Figure 49: Experimental Midilli and Kucuk model curve for Cassava chunks under GSD.

University of Ghana http://ugspace.ug.edu.gh

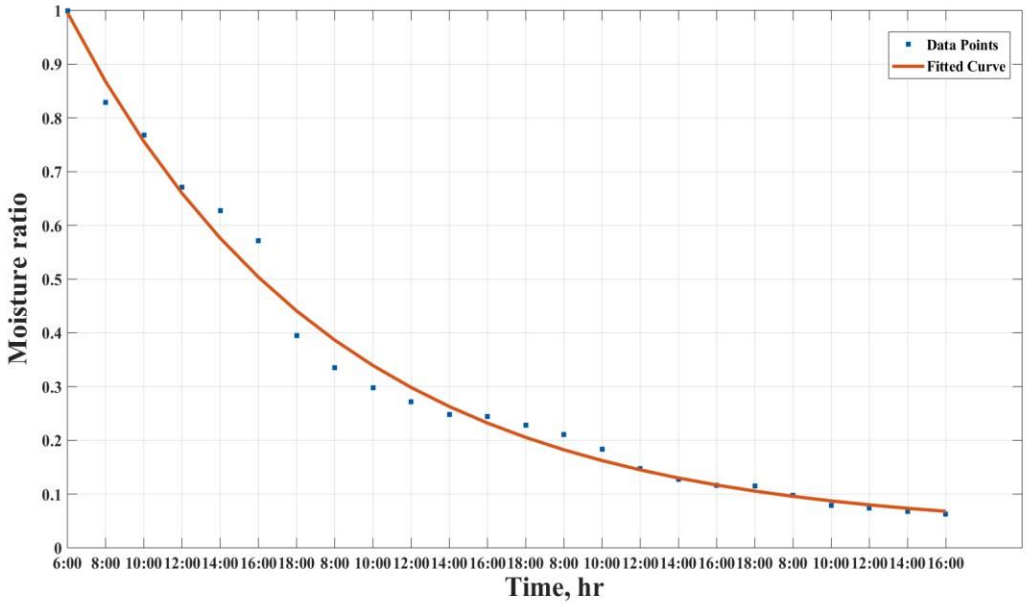

Figure 50: Experimental Logarithmic model curve for Cassava chunks under OSD.

b. Cassava drying to test the ability of the workstation to reduce humidity at night (with 1200watts battery)

The values of the coefficients and constants for the three drying methods, PVGSD, GSD and OSD for the drying of cassava slices are shown in Tables 33, 34 and 35 respectively.

University of Ghana http://ugspace.ug.edu.gh

Table 33: Mathematical models and respective constants for PVGSD of cassava root slices.

Model No.	Model constant	R^2	χ^2	RMSE
1	k=10.3427	0.964639	0.003533	0.059439
2	k=11.239;a=1.0898	0.973701	0.002732	0.052274
3	k=25.2161; n=1.4026	0.993778	0.000646	0.025425
4	k=9.9845; n=1.4025	0.993778	0.000646	0.025425
5	a=-114.1421, b=114.956, k_0=-0.38449, k_1=-0.35279	0.879847	0.013570	0.116493
6	a=-7.8637,b=16.1235	0.991024	0.000932	0.030539
7	a=57.9916,b=0.96198,k=2.0628	0.948109	0.005616	0.074943
8	a=1.185,b=8.4813,c=-0.13245	0.983474	0.001788	0.042293
9	a=-114.1421,b=114.956,k_0=-0.38449,k_1=-0.35279	0.879847	0.013570	0.116493
10	**a=0.94767, b=0.16047, k=45.8119, n=1.6639**	**0.996277**	**0.001018**	**0.020504**
11	a=29.9747,g=3.7864,k=3.9279	0.979865	0.002179	0.046683
12	a=9.0729, b=-15.7037 c=7.5147, g=0.4663, h=1.1437 k=0.37957	0.927898	0.008919	0.094441

University of Ghana http://ugspace.ug.edu.gh

Table 34: Mathematical models and respective constants for GSD of cassava root slices.

Model No.	Model constant	R^2	χ^2	RMSE
1	k=7.3813	0.928283	0.007821	0.088439
2	a=1.1448,k=8.4535	0.951919	0.005424	0.073651
3	k=24.0426,n=1.6055	0.984970	0.001695	0.041178
4	k=7.2469,n=1.6055	0.984970	0.001695	0.041178
5	a=-52.3953,b=53.2968,k_0=-0.58679,k_1=-0.52274	0.903644	0.011676	0.108057
6	a=-5.4648,b=7.2459	0.968341	0.003571	0.059764
7	a=11.0191,b=0.84898,k=2.176	0.963867	0.004222	0.064978
8	a=1.3831,b=5.1614,c=-0.29573	0.970863	0.003404	0.058349
9	a=2.0758,k=12.132	0.982497	0.001974	0.044438
10	**a=0.97678,b=0.15539,k=37.3683,n=1.799**	**0.986361**	**0.002332**	**0.040652**
11	a=41.7732,g=3.2877,k=3.3608	0.957804	0.004930	0.070218
12	a=19.9421,b=-19.3287,c=0.3868,g=0.83556,h=3.342,k=0.98626	0.955369	0.005841	0.076426

University of Ghana http://ugspace.ug.edu.gh

Table 35: Mathematical models and respective constants for OSD of cassava root slices.

Model No.	Model constant	R^2	χ^2	RMSE
1	k=5.8745	0.871264	0.015983	0.126424
2	a=1.2006,k=7.0889	0.915312	0.010853	0.104180
3	k=43.0474,n=2.1068	0.990195	0.001256	0.035447
4	k=5.9641,n=2.1068	0.990195	0.001256	0.035447
5	a=35.5969,b=-34.5547,k1=0.18643,k2=0.084767	0.950556	0.006773	0.082302
6	a=-3.7623,b=1.5181	0.948054	0.006657	0.081592
7	a=51.7378,b=1.0229,k=-3.0909	0.602868	0.052592	0.229331
8	a=2.0929,b=2.4835,c=-0.98023	0.960853	0.005184	0.072001
9	a=2.2483,k=10.6199	0.975191	0.003179	0.056386
10	**a=0.97168,b=0.20134,k=87.6514,n=2.4455**	**0.993243**	**0.002201**	**0.030424**
11	a=63.6988,g=2.0431,k=2.0879	0.925490	0.009867	0.099335
12	a=1.8446,b=-0.77733, c=0.036268, g=-0.49497,h=-0.6069,k=2.5202	0.960321	0.005838	0.076410

The data from the regression analysis for cassava slices dried under PVGSD, GSD and OSD show that Midilli and Kucuk model best describes the drying phenomena with higher value of R^2 = 0.99628 and lowest χ^2 =0.001018 and RMSE = 0.02050, R^2 = 0.986361, χ^2 = 0.002332 and RMSE = 0.040652 and R^2 = 0.99324 and lowest χ^2 =0.002201 and RMSE = 0.030424 respectively.

The experimental moisture ratio using the Midilli and Kucuk model for cassava slices under PV-greenhouse solar drying (PVGSD), greenhouse solar drying (GSD) and open sun drying (OSD)

University of Ghana http://ugspace.ug.edu.gh

are shown in Figures 51 to 53 respectively. These models can be used for the estimation of moisture ratio of cassava slices under the three drying methods.

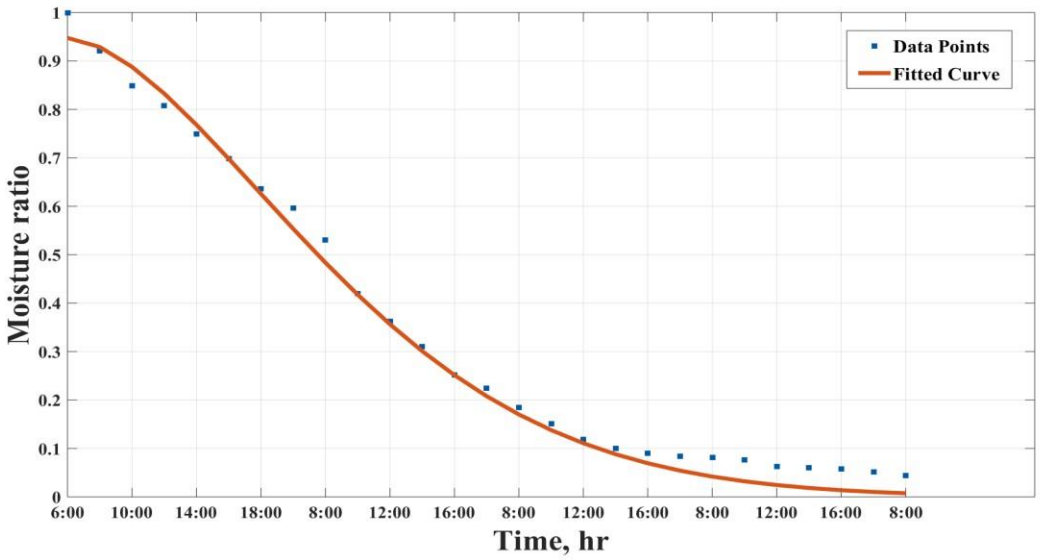

Figure 51: Experimental Midilli and Kucuk model curve for Cassava slices under PVGSD.

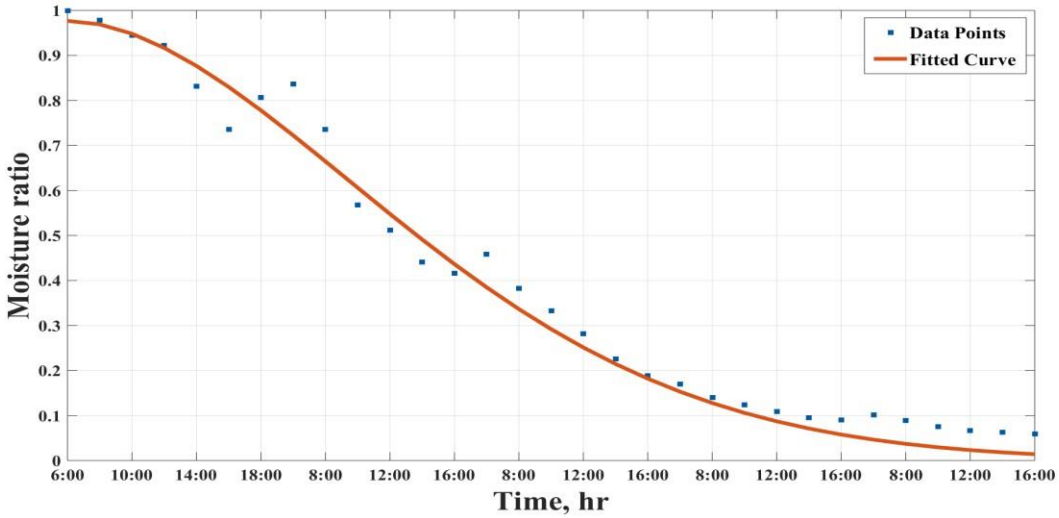

Figure 52: Experimental Midilli and Kucuk model curve for Cassava slices under GSD.

University of Ghana http://ugspace.ug.edu.gh

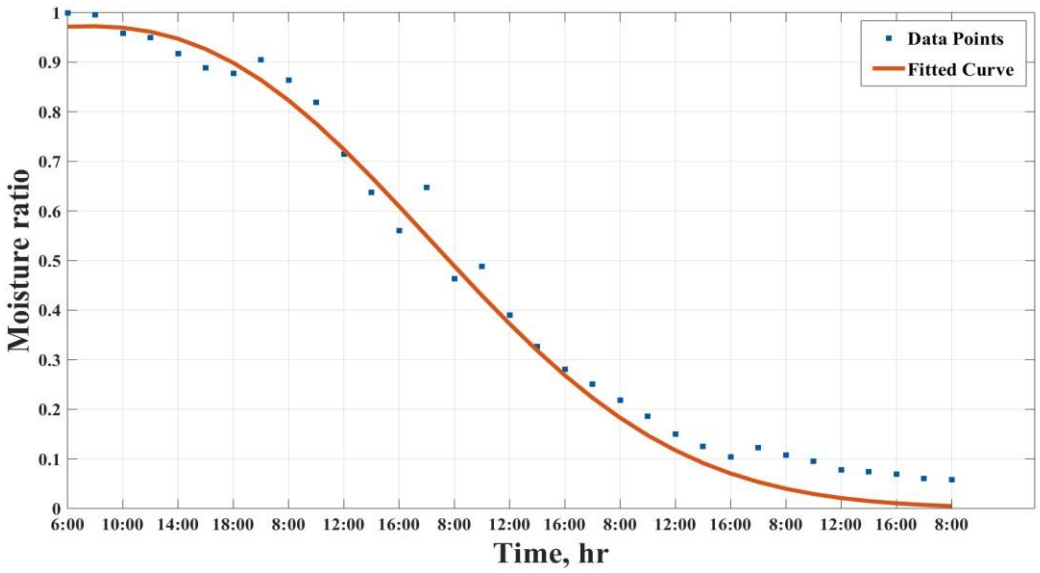

Figure 53: Experimental Midilli and Kucuk model curve for Cassava slices under OSD.

The drying of cassava chunks under PVGSD, GSD and OSD, Wang and Singh model best fit PVGSD and Midilli and Kucuk model best fit the drying curve both GSD and OSD. Thus, the Wang and Singh model for PVGSD is expressed as:

$$MR = 1 - 4.2017t + 3.8987t^2 \quad \text{Eq. (36)}$$

And Midilli and Kucuk model for GSD is expressed as:

$$MR = 0.96656\exp(5.4857t^{1.4953}) - 0.77568t \quad \text{Eq. (37)}$$

Similarly, the Midilli and Kucuk model for OSD is expressed as:

$$MR = 0.97564\exp(4.42375t^{2.6793}) + 0.043414t \quad \text{Eq. (38)}$$

The experimental moisture ratio using the Wang and Singh model and Midilli and Kucuk model for cassava chunks under PVGSD, GSD and OSD can be seen in Figures 54 to 56 respectively.

University of Ghana http://ugspace.ug.edu.gh

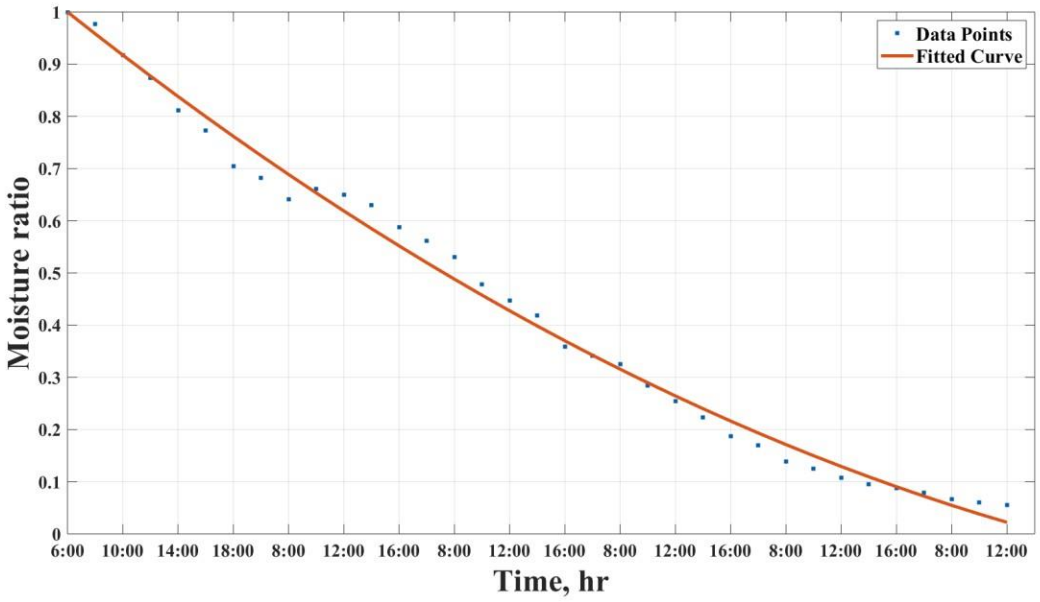

Figure 54: Experimental Wang and Singh model curve for Cassava chunks under PVGSD.

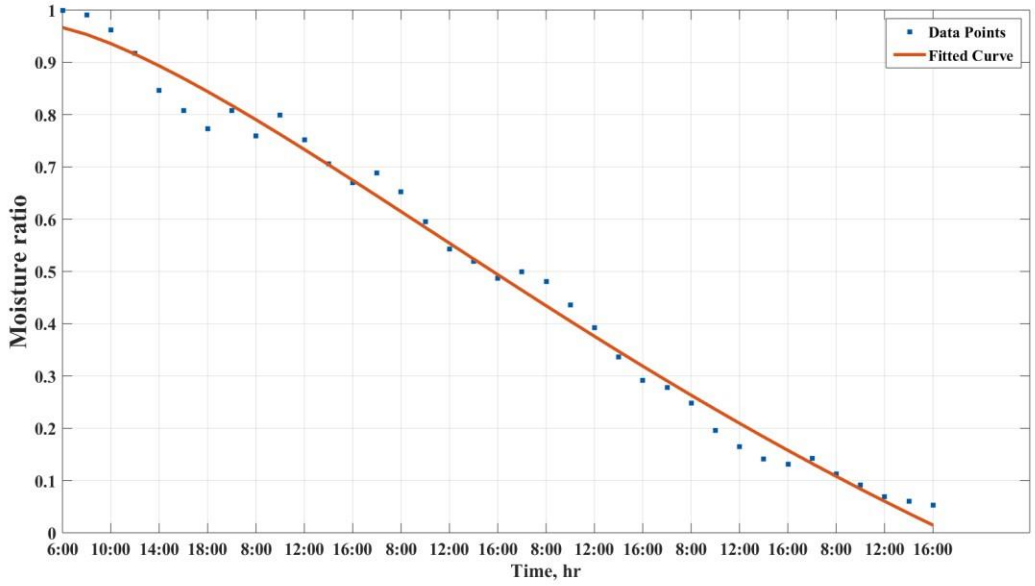

Figure 55: Experimental Midilli and Kucuk model curve for Cassava chunks under GSD.

University of Ghana http://ugspace.ug.edu.gh

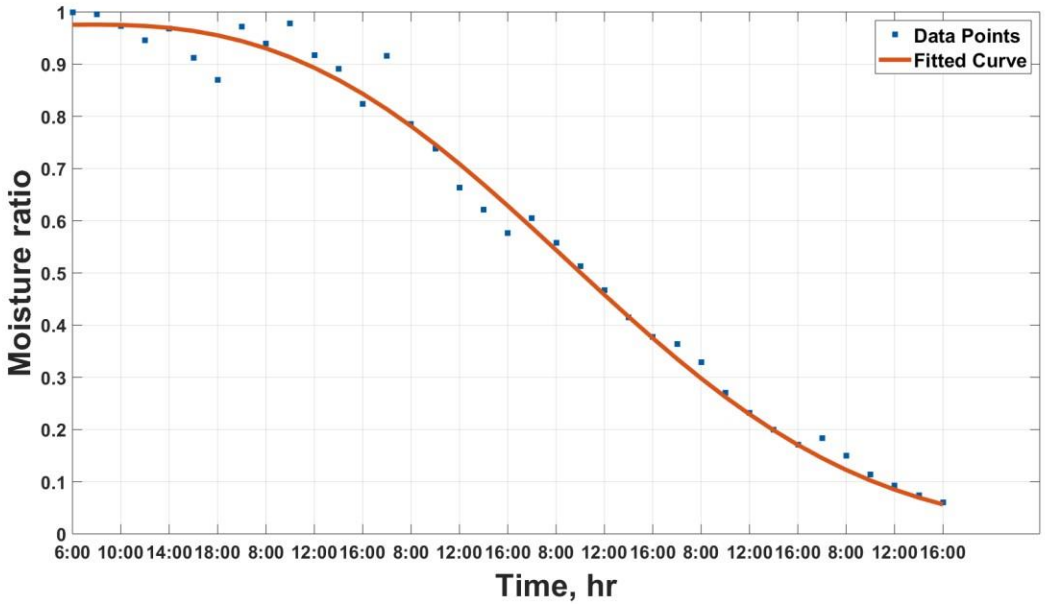

Figure 56: Experimental Midilli and Kucuk model curve for Cassava chunks under OSD.

4.7 Moisture effective diffusivity

Moisture evaporation from within the food materials to the surface depends on several combined mechanisms. During drying the falling rate period is mostly driven by diffusion of moisture through the product. This property depends on the moisture content, pressure and drying temperature of the samples and further implicates moisture in two states (liquid and vapor) (Koua *et al.*, 2009). This D_{eff} is typically evaluated by graphical method showing the logarithm of moisture ratio (*MR)* versus the drying time.

4.7.1 Moisture effective diffusivity of Red pepper

From the gradient of the graph of ln (*MR*) versus drying time (*t*), the moisture effective diffusivities of red pepper under PVGSD, GSD and OSD was calculated. The calculated values of the D_{eff} for the three drying methods can be seen in Table 36 and Figure 57 for PV-greenhouse solar drying (PVGSD). It was obtained that the D_{eff} of red pepper calculated from the Fick's diffusion model expressed by Equation 11 for PVGSD, GSD and OSD were 2.699 $\times 10^{-9}$ m^2/s, 2.647 $\times 10^{-9}$ m^2/s

University of Ghana http://ugspace.ug.edu.gh

and 9.944 $\times 10^{-10}$ m^2/s respectively over the drying period. The analysis of Table 36 indicates the effective diffusivity varies for the different drying methods with PV-greenhouse solar dryer been the highest and lowest for open sun drying. However, these values fall in the range of $10^{-8} - 10^{-12}$ m^2/s, which is reported for most food commodities (Wang *et al.*, 2018).

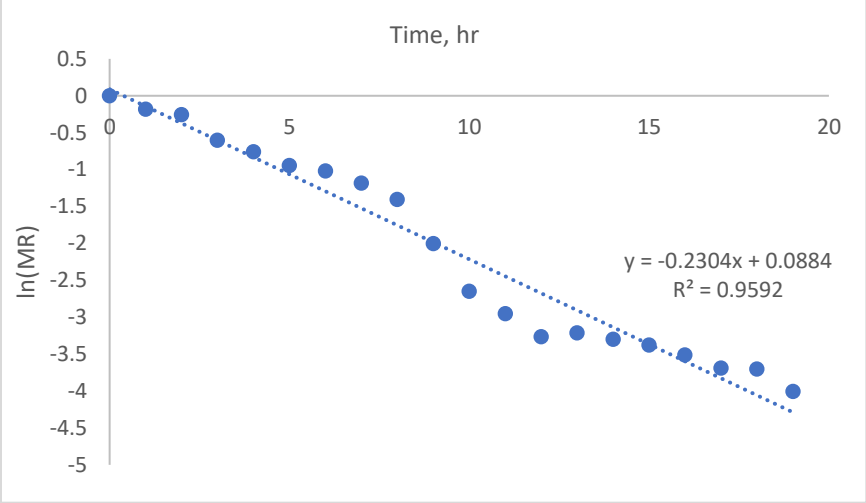

Figure 57: Variation of logarithm of red pepper moisture ratio with time for PVGSD.

Table 36: Values of moisture effective diffusivities for different drying methods of red pepper.

Drying method	Effective moisture diffusivity (m^2/s)	Correlation coefficient, R^2
PVGSD	2.699×10^{-9}	0.9592
GSD	2.647×10^{-9}	0.9607
OSD	9.944×10^{-10}	0.9744

4.7.2 Moisture effective diffusivity of Cassava slices and chunks

The moisture effective diffusivities of cassava samples under the different drying methods, PVGSD, GSD and OSD were calculated. The results of the D_{eff} for the three drying methods and two sizes of cassava are shown in Table 37 and Figure 58 and 59 for PV-greenhouse solar drying (PVGSD) slices and chunks respectively. The analysis of Table 37 indicates the moisture effective

University of Ghana http://ugspace.ug.edu.gh

diffusivity varies for the different drying methods with PV-greenhouse solar dryer been the highest and lowest for open sun drying. However, these values fall between 10^{-8} – 10^{-12} m^2/s, which is reported for most food materials (Wang *et al.*, 2018).

Table 37: Values of moisture effective diffusivities for different drying methods for cassava slices and chunks.

Drying method	Effective moisture diffusivity (m^2/s)	Correlation coefficient, R^2
PVGSD Slices	2.556×10^{-9}	0.9084
GSD Slices	2.419×10^{-9}	0.8780
OSD Slices	2.573×10^{-9}	0.9710
PVGSD Chunks	3.126×10^{-9}	0.9543
GSD Chunks	3.060×10^{-9}	0.9637
OSD Chunks	2.792×10^{-9}	0.9892

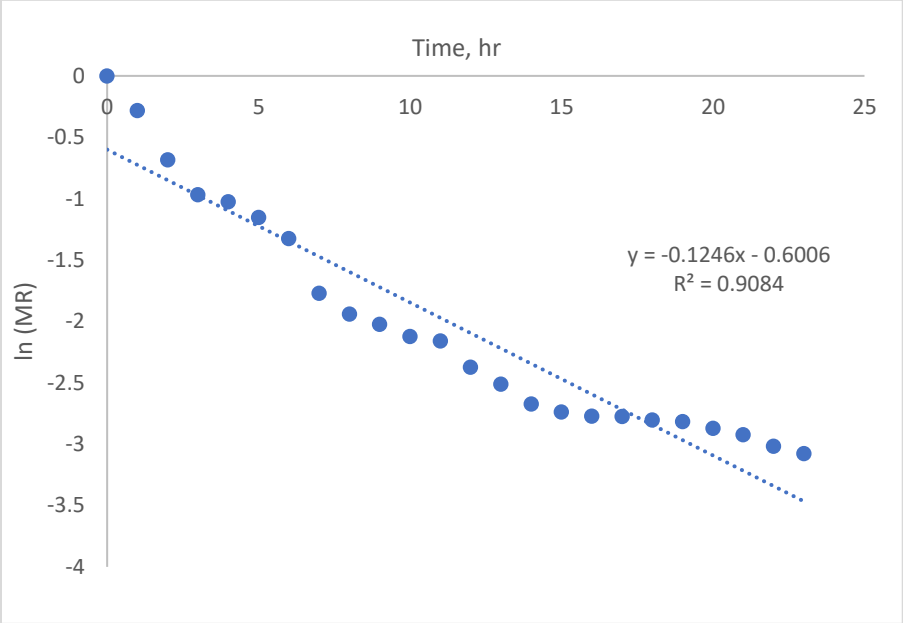

Figure 58: Variation of logarithm of cassava slices moisture ratio with drying time for PVGSD.

University of Ghana http://ugspace.ug.edu.gh

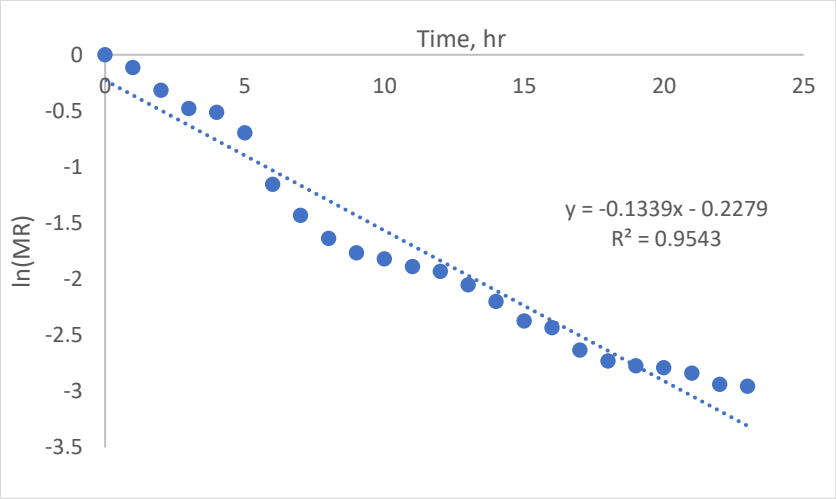

Figure 59: Variation of logarithm of cassava chunks moisture ratio with drying time for PVGSD.

4.8 Post drying evaluation by analyzing quality indices of the dried samples

4.8.1 Water Activity, α_w

Foods with similar moisture content vary in their perishability as a result of how water associates with other food constituents, hence moisture content alone as an indicator for food stability is not dependable. Furthermore, water bound with other food constituents is not easily accessible for microbial growth and deterioration to occur due to chemical reactions (Nielsen, 2010). Water activity of food however is a better indicator for food perishability as a measure of enzymatic and non-enzymatic browning, microbial growth, etc. (Belessiotis and Dalyannis, 2011) and can be used to predict the shelf stability of the food product. Every agricultural food has water activity limit below which microorganisms stop growing, the acceptable water activity for red pepper is 0.435 at 25°C (Peter, 2001) and that for high quality cassava flour (HQCF) is 0.1 - 0.8 at 25°C (Dziedzoave *et al.*, 2003).

The final water activity analysis determined for red pepper and cassava samples under the three drying methods are summarized in Table 38. The data showed that water activity decreases with

University of Ghana http://ugspace.ug.edu.gh

decrease in moisture content and the resultant dried red pepper and cassava samples demonstrated water activity within the acceptable limits to prevent microbial growth. However, it was observed for the second batch of cassava drying that all the OSD chunks and some of the OSD slices grew moldy as well as individual GSD chunks and slices among the lot sample, this can be attributed to high water activity levels and slow moisture removal.

This result indicates that the drying operation was efficient thus justifying that indeed solar energy plays a pivotal role during heat and mass transfer in a product undergoing dehydration. Also, analysis of variance performed delineating the effect of drying method, drying day and sample size on the two commodities indicated a significant effect of drying method and drying day on the water activity while sample size did not have an effect during the drying experiment (Table 39 and 40).

Table 38: Final average water activity of dried samples

Sample	Water activity / Temperature °C
Fresh red pepper	0.983 / 31.00
PVGSD dried red pepper	0.384 / 25.95
GSD dried red pepper	0.388 / 25.57
OSD dried red pepper	0.414 / 26.65
Fresh cassava	0.919 / 25.82
PVGSD cassava slices flour	0.361 / 25.62
GSD cassava slices flour	0.384 / 25.61
OSD cassava slices flour	0.421 / 25.25
PVGSD cassava chunks flour	0.415 / 25.31
GSD cassava chunks flour	0.446 / 25.59
OSD cassava chunks flour	0.490 / 25.44

University of Ghana http://ugspace.ug.edu.gh

Table 39: Analysis of Variance (ANOVA) of Water Activity changes for Red Pepper

Source	DF	SS	MS	F-Value	P-Value	F crit.
Drying days	1.040305	3	0.346768	32679.74	1.86E-43	3.008787
Drying method	0.699726	2	0.349863	32971.37	5.38E-42	3.402826
Interaction	0.311238	6	0.051873	4888.556	8.1E-36	2.508189
Error	0.000255	24	1.06E-05			
Total	2.051524	35				

Table 40: Analysis of Variance (ANOVA) of Water Activity changes for Cassava samples

Source	DF	SS	MS	F-Value	P-Value
Drying method	2	0.041465	0.020733	4.89	0.033
Sample size	1	0.017113	0.017113	4.04	0.072
Drying day	2	0.702035	0.351018	82.81	0.000
Interaction	2	0.003622	0.001811	0.43	0.664
Error	10	0.042387	0.004239		
Total	17	0.806622			

4.8.2 Color Profile

The extent of color degradation during thermal processing of food products is a factor attributing to dried food products stability and consumer acceptability. Color perception on food products is one of the basic indices looked out by consumers to determine a product acceptability. The color profile helps to recognize slight changes in overall appearance as well as alert potentially dangerous food contaminants or abnormalities or spoilage of the food product. The color indicators L^*, a^*, b^*, ΔE, BI and H^0 of the fresh and dried red pepper and cassava samples under the PVGSD, GSD and OSD are summarized in Tables 41 and 42.

University of Ghana http://ugspace.ug.edu.gh

The values for L^*, a^* and b^* of fresh red pepper were 41.38, 43.92 and 30.03 respectively. It was observed that L^*, a^* and b^* values reduced for all the drying methods. This occurrence may be caused by the increase in browning compounds as a results of Maillard reaction and the depletion of carotenoid pigment (Yang *et al.*, 2018). The L^* value showing whiteness, suffered the most for OSD with a value of 25.26 followed by GSD of 33.29, prompting a higher level of browning reaction for OSD. It was observed that yellowness suffered the most reduction for all systems, subsequently lightness and redness for red pepper drying. This also shows the yellowness is more easily affected by heat than redness. For redness of red pepper, PVGSD had the highest retention and OSD had the least.

The total color change ΔE, is used mostly to analysis the general color difference between the fresh and dried samples (Wang *et al.*, 2018). From the Table 38 dried red pepper showed significant color difference of 11.94, 16.43 and 25.50 respectively for PVGSD, GSD and OSD as compared to the fresh samples. From the Table 41 *BI* values increased from 87.75 to 107.76 with the different drying methods, signifying that the drying methods influences the browning index. For the hue angle (H^0), represent a more visual color than the other parameters. The H^0 value was lowest for PVGSD and highest for OSD

Analysis of variance done on the color coordinates L^*, a^* and b^* defining the drying method, drying time and sample size (Appendix 10), showed that for red pepper both the drying method and drying time have influence on the final color. On the other hand, cassava samples showed that both the drying method and drying time influence the color, the sample size did not have any effect on the final color (Appendix 11).

University of Ghana http://ugspace.ug.edu.gh

Table 41: The color indicators of fresh and dried red pepper under the PVGSD, GSD and OSD.

Color parameter	Fresh Sample	PV-GSD	GSD	OSD
L^*	41.38	36.80	33.29	25.26
a^*	43.25	38.20	34.38	29.40
b^*	30.03	20.23	18.81	15.94
ΔE	-	11.94	16.43	25.50
BI	-	87.75	91.57	107.76
H^0	-	27.90	28.68	28.47

Table 42: The color indicators of fresh and dried cassava slices and chunks under the PVGSD, GSD and OSD.

Drying method	Color parameter					
	L^*	a^*	b^*	ΔE	BI	H^0
Fresh cassava pulp	94.99	-0.88	16.81	-	-	-
PVGSD Slices	90.42	-0.42	7.38	10.49	21.79	93.26
GSD Slices	89.97	-0.52	7.21	10.84	21.98	94.13
OSD Slices	89.39	-0.26	6.68	11.59	22.2	92.23
PVGSD Chunks	88.65	-0.123	8.34	10.60	20.63	90.84
GSD Chunks	87.42	-0.197	7.41	12.09	21.40	91.52
OSD Chunks	87.5	-0.117	7.32	12.11	21.42	90.92

University of Ghana http://ugspace.ug.edu.gh

(a) (b) (c)

Illustration 22: Dried red pepper under PVGSD (a), GSD (b) and OSD (c).

(a) (b) (c)

Illustration 23: Dried red pepper powder under PVGSD (a), GSD (b) and OSD (c).

University of Ghana http://ugspace.ug.edu.gh

(a) (b) (c)

Illustration 24: Dried cassava slices under PVGSD (a), GSD (b) and OSD (c).

(a) (b) (c)

Illustration 25: Dried cassava slices flour under PVGSD (a), GSD (b) and OSD (c).

University of Ghana http://ugspace.ug.edu.gh

(a) (b) (c)

Illustration 26 Dried cassava chunks under PVGSD (a), GSD (b) and OSD (c).

4.8.3 Particle Size Distribution (PSD)

Traditionally cassava is used for local staples like *gari, fufu, kokonte* etc., including other products such as cassava flour and starch. High quality cassava flour can be used as a substitute for wheat flour in bakery products and in production of glucose syrups and alcohol (Dziedzoave *et al*., 2003). The desired particle size in flour industries is a very important factor in the production of flour. The granulation properties of flours affect the rate of hydration and swelling capacity as well as the textural characteristics of the finished product. The particle size distribution derived from the resultant flour of cassava slices and chunks under PVGSD, GSD and OSD can be seen in Appendix 12. A log-normal plot of the particle size distribution is shown in Figures 60 to 62.

University of Ghana http://ugspace.ug.edu.gh

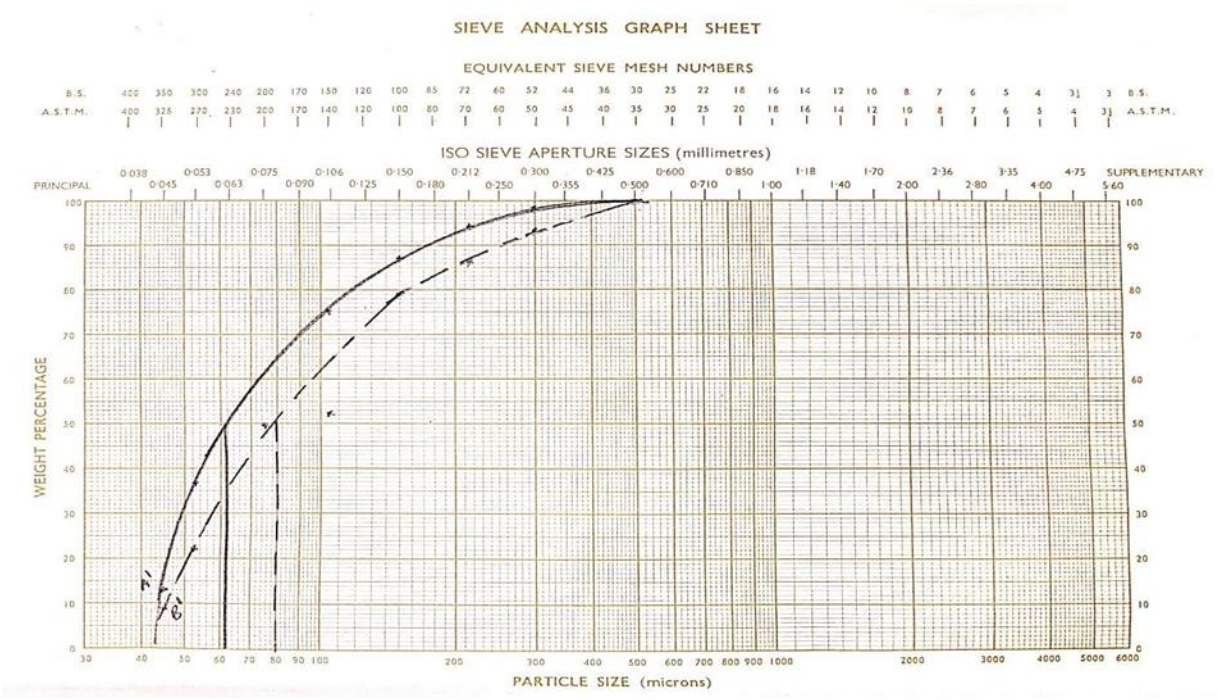

Figure 60: Cumulative frequency plot for PSD of PVGSD slices and chunks

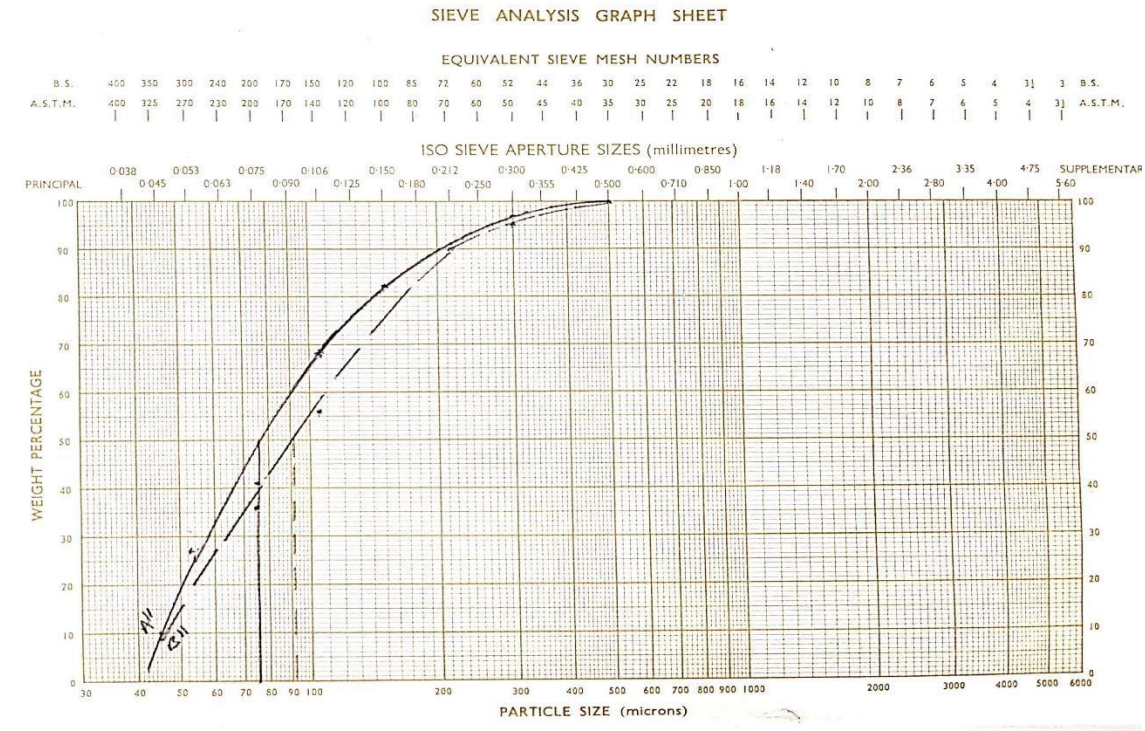

Figure 61: Cumulative frequency plot for PSD of GSD slices and chunks

University of Ghana http://ugspace.ug.edu.gh

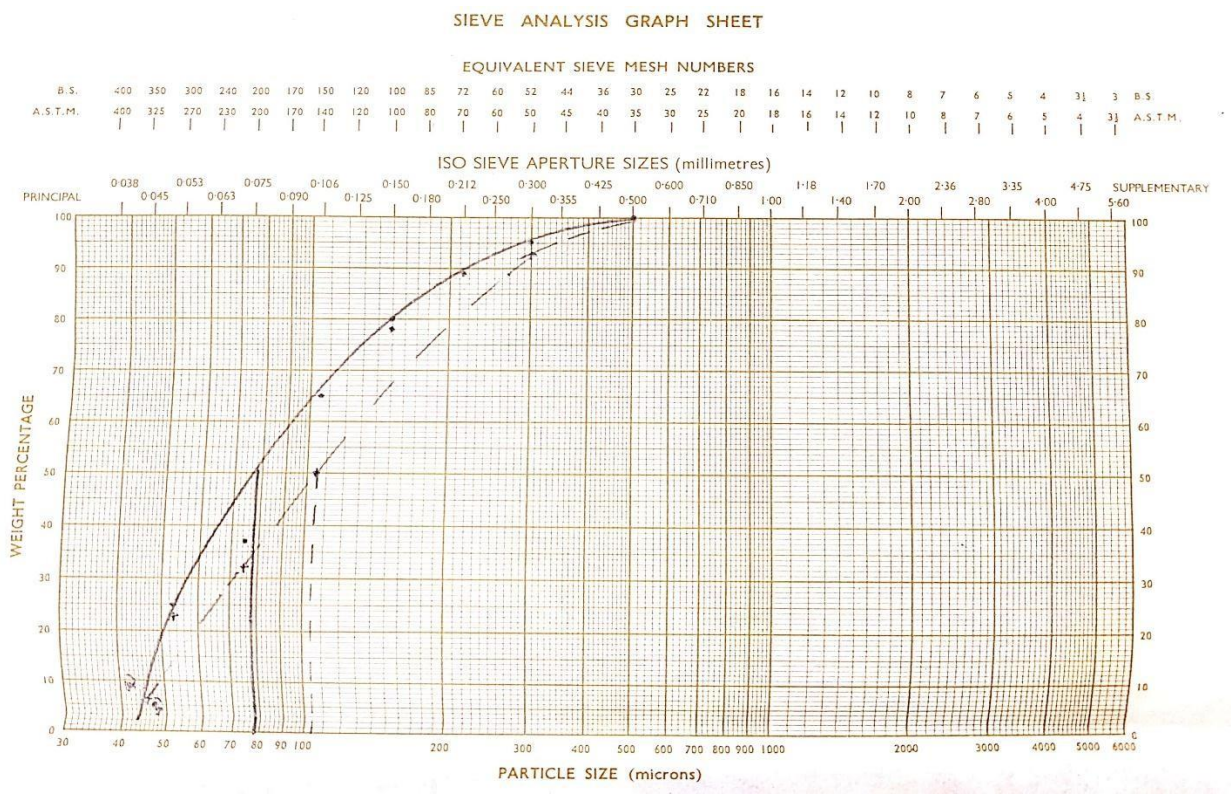

Figure 62: Cumulative frequency plot for PSD of OSD slices and chunks

The SD_{50} for PVGSD slices was recorded at 62 µm, indicating the potential of sieving through 80 µm which makes it a finer flour than the PVGSD chunks with SD_{50} of 80 µm (Figure 60). Also, the tendency of PVGSD slices having a greater hydration capacity than the chunks which is a desired functionality during processing (Hatcher *et al.*, 2009). The SD_{50} for GSD slices and chunks were recorded at 76 µm and 92 µm respectively showing a better fineness for the cassava slices than the chunks (Figure 61). And the SD_{50} for OSD slices and chunks were also determined at 78 µm and 106 µm and again the cassava slices depicting a finer particle size than the chunks (Figure 62). Thus, the sample size can be said to have influence on the particle size distribution of cassava flour.

University of Ghana http://ugspace.ug.edu.gh

CHAPTER FIVE

5.0 CONCLUSIONS AND RECOMMENDATIONS

5.1 CONCLUSIONS

1. A workstation with the capacity to provide a means to control the humidity in a PVGSD solar dryer was designed, built and effectively tested. The solar energy which is converted through the inverter made it possible to activate the fans in the dryer at night, the system therefore will be suitable for use in rural areas or off-grid areas.
2. The PVGSD operated with the control system provided the environment for the food samples to lose moisture continually without picking up moisture at night.
3. The introduction of racks with multiple shelves increased the load capacity of the greenhouse solar dryer.
4. The PVGSD is a much more efficient dryer with respect to the attainment of a high temperature, whilst the PCGSD attained a temperature of 69°C, the OSD attained 41.5°C. Generally, the PVGSD showed faster drying rate but this was influenced by the nature of the samples being dried. The cassava slices demonstrated faster drying rate than the cassava chunks for all the drying methods.
5. In drying cassava and red peppers, moisture removal was highest during the time of 12:00 and 14:00 GMT. The time of the day, drying method and sample type influence the drying of the cassava slices and chunks while the drying method and drying time affected the drying of red pepper.
6. From the characteristics of the flours produced from the dried cassava samples and red pepper, the Greenhouse Solar Dryers consistently gave products of relatively high quality comparing to the Open Sun drying.

University of Ghana http://ugspace.ug.edu.gh

7. The Midilli and Kucuk model best describe the drying phenomena of red pepper under both PVGSD and GSD while Logarithmic model describe best under OSD. Approximation of diffusion model best explains the drying of cassava slices under PVGSD and GSD, while Midilli and Kucuk model is best for drying under OSD.

5.2 RECOMMENDATIONS

1. The Workstation can be a beneficial research tool for the Department of Food Process Engineering. It is recommended that the Department should go through the appropriate process to patent the technology.
2. Due to the non-durability of wood and the plastic sheet, it is recommended that metal frames and possibly fiberglass or perplex be considered for future construction of the greenhouse solar dryer.
3. Further work should be done on the drying characteristics of other Ghanaian food commodities.

University of Ghana http://ugspace.ug.edu.gh

REFERENCES

Akpinar, K. E. (2006.). mathematical modelling of thin layer drying process under open sun of some aromatic plants. Retrieved from https://ac.els-cdn.com/S0260877405005650/1-s2.0-S0260877405005650-main.pdf?_tid=875f9a26-58a4-4051-bf46-4d2936fef7bc&acdnat=1548884916_415c4e3680f33b0a6ffb11705f8fcd33

AOAC 2005. Official Methods of analysis. 18th edition. Association of Official Analytical chemists; Arlington, VA, USA: 2005; method 930.15.

Belessiotis V. and Delyannis, E., (2011). Solar drying. *Solar Energy*, *85*(8), 1665–1691. https://doi.org/10.1201/b17208

Chauhan, P. S., Kumar, A., and Nuntadusit, C., (2018). Heat transfer analysis of PV integrated modified greenhouse dryer. *Renewable Energy*, *121*, 53–65. https://doi.org/10.1016/j.renene.2018.01.017

Chong, C. H., Law, C. L., Cloke, M., Hii, C. L., Abdullah, L. C., and Daud, W. R. W. (2008). Drying kinetics and product quality of dried Chempedak. *Journal of Food Engineering*, *88*(4), 522–527. https://doi.org/10.1016/j.jfoodeng.2008.03.013

Dangi, N. (2017). Monitoring environmental parameters: humidity and temperature using Arduino based microcontroller and sensors. Retrieved from https://www.theseus.fi/bitstream/handle/10024/142235/Dangi_Nagendra.pdf?sequence=1

Dziedzoave, N.T., Graffham, A.J., and Boateng, E.O. (2003). Training manual for the production of high-quality Cassava Flour. Food Research Institute, Accra- Ghana. pp 1-36

El Hage, H., Herez, A., Ramadan, M., Bazzi, H., and Khaled, M. (2018). An investigation on solar drying: A review with economic and environmental assessment. *Energy*, *157*, 815–829. https://doi.org/10.1016/j.energy.2018.05.197

University of Ghana http://ugspace.ug.edu.gh

Erbay, Z., and Icier, F. (2010). A review of thin layer drying of foods: Theory, modeling, and experimental results. *Critical Reviews in Food Science and Nutrition*, *50*(5), 441–464. https://doi.org/10.1080/10408390802437063

Fadhel, A., Kooli, S., Farhat, A., and Belghith, A. (2014). Experimental Study of the Drying of Hot Red Pepper in the Open Air, under Greenhouse and in a Solar Drier. *International Journal of Renewable Energy and Biofuels*, *2014*, 1–14. https://doi.org/10.5171/2014.515285

Jain, D., and Pathare, P. B. (2007). Study the drying kinetics of open sun drying of fish. *Journal of Food Engineering*, *78*(4), 1315–1319. https://doi.org/10.1016/j.jfoodeng.2005.12.044

Jerger, E. W. (1951). Mechanism of moisture movement in the drying of organic granular solids. *Energy Conversion and Management*, *40*(6), 551. https://doi.org/10.1007/BF00826517

Jumaat, S. A., and Othman, M. H. (2018). Solar Energy Measurement Using Arduino. *MATEC Web of Conferences*, *150*, 01007. https://doi.org/10.1051/matecconf/201815001007

Karthikeyan, A. K., and Murugavelh, S. (2018). Thin layer drying kinetics and exergy analysis of turmeric (Curcuma longa) in a mixed mode forced convection solar tunnel dryer. *Renewable Energy*, *128*, 305–312. https://doi.org/10.1016/j.renene.2018.05.061

Kemp, I. C. (2007). Humidity effects in solids drying processes. *Measurement and Control*, *40*(9), 268–271. https://doi.org/10.1177/002029400704000901

Koua, K. B., Fassinou, W. F., Gbaha, P., and Toure, S. (2009). Mathematical modelling of the thin layer solar drying of banana, mango and cassava. *Energy*, *34*(10), 1594–1602. https://doi.org/10.1016/j.energy.2009.07.005

Kumar, M., Sansaniwal, S. K., and Khatak, P. (2016). Progress in solar dryers for drying various commodities. *Renewable and Sustainable Energy Reviews*, *55*, 346–360.

University of Ghana http://ugspace.ug.edu.gh

https://doi.org/10.1016/j.rser.2015.10.158

Marques, L. G., Prado, M. M., and Freire, J. T. (2009). Rehydration characteristics of freeze-dried tropical fruits. *LWT - Food Science and Technology*, *42*(7), 1232–1237. https://doi.org/10.1016/j.lwt.2009.02.012

Mercer, D. G., (2014). *Drying of Specific Fruits and Vegetables An Introduction to the Dehydration and Drying of Fruits and Vegetables part 2: drying of specific fruits and vegetables*. Retrieved from http://iufost.org/wp-content/uploads/2017/08/Drying-Part-2.pdf

Mercer, D. G., (2018). *Food Processing Concepts for Entrepreneurs and Small-Scale Processors*.

Nielsen, S. S. (2010). *Food Analysis*. Food Science Texts Series, DOI 10.1007/978-1-4419-1478-1_6,

Obimpeh, L. O., (2018). The design and evaluation of a greenhouse type solar dryer and its performance on two food commodities: cassava and cocoa. Food science Mphil Thesis. Department of Nutrition and Food Science, University of Ghana. 120 pp.

Sigge, G. O., Hansmann, C. F., and Joubert, E. (1998). Effect of temperature and relative humidity on the drying rates and drying times of green bell peppers (*Capsicum annuum L.*). *Drying Technology*, *16*(8), 1703–1714. https://doi.org/10.1080/07373939808917487

Singh, P., Shrivastava, V., and Kumar, A. (2018). Recent developments in greenhouse solar drying: A review. *Renewable and Sustainable Energy Reviews*, *82*(October 2017), 3250–3262. https://doi.org/10.1016/j.rser.2017.10.020

Sonaye, S. Y., and Baxi, R. N. (2012). Particle size measurement and analysis of flour. *International Journal of Engineering Research and Applications*, *2*(3), 1839–1842.

Tiwari, S., Tiwari, G. N., and Al-Helal, I. M. (2016). Development and recent trends in

University of Ghana http://ugspace.ug.edu.gh

greenhouse dryer: A review. *Renewable and Sustainable Energy Reviews*, *65*, 1048–1064. https://doi.org/10.1016/j.rser.2016.07.070

Wang, J., Law, C. L., Nema, P. K., Zhao, J. H., Liu, Z. L., Deng, L. Z., and Xiao, H. W. (2018). Pulsed vacuum drying enhances drying kinetics and quality of lemon slices. *Journal of Food Engineering*, *224*, 129–138. https://doi.org/10.1016/j.jfoodeng.2018.01.002

Wang, J., Qian, J.-Y., Liu, Y.-H., Zhang, Q., Gao, Z.-J., Xiao, H.-W. and Mujumdar, A. S. (2017). Effect of high-humidity hot air impingement blanching (HHAIB) on drying and quality of red pepper (Capsicum annuum L.). *Food Chemistry*, *220*, 145–152. https://doi.org/10.1016/j.foodchem.2016.09.200

Wang, W., Li, M., Hassanien, R. H. E., Wang, Y., and Yang, L. (2018). Thermal performance of indirect forced convection solar dryer and kinetics analysis of mango. *Applied Thermal Engineering*, *134*(December 2017), 310–321. https://doi.org/10.1016/j.applthermaleng.2018.01.115

Yang, X. H., Deng, L. Z., Mujumdar, A. S., Xiao, H. W., Zhang, Q., and Kan, Z. (2018). Evolution and modeling of colour changes of red pepper (Capsicum annuum L.) during hot air drying. *Journal of Food Engineering*, *231*, 101–108. https://doi.org/10.1016/j.jfoodeng.2018.03.013

Zhang, X. L., Zhong, C. S., Mujumdar, A. S., Yang, X. H., Deng, L. Z., Wang, J., and Xiao, H. W. (2019). Cold plasma pretreatment enhances drying kinetics and quality attributes of chili pepper (Capsicum annuum L.). *Journal of Food Engineering*, *241*(July 2018), 51–57. https://doi.org/10.1016/j.jfoodeng.2018.08.002

University of Ghana http://ugspace.ug.edu.gh

APPENDICES

APPENDIX 1: Program code for the arduino uno

Program code:

```
#include <Wire.h>
#include <I2CIO.h>
#include <LCD.h>
#include <LiquidCrystal.h>
#include <LiquidCrystal_I2C.h>

#include <SPI.h>
#include <SD.h>
#include "DHT.h"
#include <Adafruit_Sensor.h>
#include <SoftwareSerial.h>

//I2C pins declaration
LiquidCrystal_I2C lcd(0x27, 2, 1, 0, 4, 5, 6, 7, 3, POSITIVE);

#include "DHT.h"
#define MOTOPIN 7
#define MOTOPIN2 8

#define PVPIN A0
float RESISTANCE =1; // Resistance in thousands of ohms
volatile float Area;
volatile float Power;
volatile float Radiation;
float voltage;
int THRESHOLD = 40;

DHT dht(2, DHT22);
SoftwareSerial SIM900(4, 5);
int ledPin = 9;
bool is_moto_running;
unsigned long startSensorReadMillis;
unsigned long startSensorLogMillis;
unsigned long currentSensorReadMillis;
unsigned long currentSensorLogMillis;
const unsigned long sensor_log_period = 600000;//TODO
float h = 0;
float t = 0;
float ah =0;
int tick = 1;
boolean is_sd_card_initialized;
boolean force_start_fan;
boolean force_stop_fan;
int sd_fail_count = 0;
int sensor_fail_count = 0;

void setup() {
  dht.begin();
  Serial.begin(19200);
  SIM900.begin(19200);
  Serial.println(F("Serial begin!"));
  pinMode(ledPin, OUTPUT);
  pinMode(MOTOPIN, OUTPUT);
  pinMode(MOTOPIN2,OUTPUT);
  digitalWrite(MOTOPIN, HIGH);
  digitalWrite(MOTOPIN2,HIGH);
  lcd.begin(16, 2);
  //initSDCard();
  lcd.setCursor(0, 0);
  lcd.print(F("WAITING FOR GSM"));
  Serial.println(F("WAITING FOR GSM"));
  delay(10000); //Give sometime to allow gsm to connect to network
```

University of Ghana http://ugspace.ug.edu.gh

```
  Serial.println(F("ready..."));
  // AT command to set SIM900 to SMS mode
  SIM900.print(F("AT+CMGF=1\r"));
  delay(100);
  // Set module to send SMS data to serial out upon receipt
  SIM900.print(F("AT+CNMI=2,2,0,0,0\r"));
  delay(100);
  lcd.clear();
  //lcd.print(F("PLEASE WAIT"));
  //SendDataToServer(F("t:20"));
  startSensorReadMillis = millis();
  startSensorLogMillis = millis();

}

void SendDataToServer(String data)
{
  connectGSM(F("AT+CGATT=1"),"OK");
  //connectGSM("AT+CIPSHUT","OK");
  connectGSM(F("AT+CGDCONT=1,\"IP\",\"internet\""),"OK");
  //connectGSM("AT+CSTT=\"internet\",\"\",\"\"",F("OK"));
  //connectGSM("AT+CIICR","OK");
  connectGSM(F("AT+CIFSR"),".");
  connectGSM(F("AT+CIPSTART=\"TCP\",\"35.225.49.222\",8090"),"OK");
  delay(5000);
  connectGSM(F("AT+CIPSEND"),">");
  delay(5000);
  SIM900.println("GET
/index.php?t="+String(t)+"&h="+String(h)+"&ah="+String(ah)+"&v="+String(voltage)+"&r="+String(Rad
iation)+"\r\n");
  SIM900.write(0x1A);    //0x1A
  delay(3000);
  if(SIM900.find(F("SEND OK"))||SIM900.find("E"))
  {
    //Sent Data Successfully
    Serial.println("Sent Data Successfully");
   }

  connectGSM(F("AT+CIPCLOSE"),"");
  connectGSM(F("AT+CIPSHUT=0"),"");
  delay(1000);
}

void connectGSM (String cmd, char *res)
{
  int i =0;
  while(i<5)
  {

    SIM900.println(cmd);
    SIM900.println(cmd);
     if(i>=5)return;
    delay(500);
    while(SIM900.available()>0)
    {
      if(i>=5)return;
      i++;
      if(SIM900.find(res))
      {
        Serial.println(cmd);
        Serial.print(" ok ");
        delay(100);
        return;
      }else{
        Serial.println(cmd);
        Serial.print(" not avail");

        }
    }
    delay(1000);
   }
```

University of Ghana http://ugspace.ug.edu.gh

```
 }

void loop() {
    if(SIM900.available() >0) {
    char incomingChar=SIM900.read();
    if(incomingChar=='S') {
      Serial.println(incomingChar);
      delay(10);
      incomingChar=SIM900.read();
      if(incomingChar=='A') {
      Serial.println(incomingChar);
      force_start_fan=true;
      }
      if(incomingChar=='B') {
      Serial.println(incomingChar);
      force_start_fan=false;
      }

      if(incomingChar=='D') {
      Serial.println(incomingChar);
      force_stop_fan=true;
      }
      if(incomingChar=='E') {
      Serial.println(incomingChar);
      force_stop_fan=false;
      }
      if(incomingChar=='C') {
      Serial.println(incomingChar);
      dht.begin();
      }
    }
    if(incomingChar=='H') {
      Serial.println(incomingChar);
      delay(10);
      incomingChar=SIM900.read();
      int upper = incomingChar-'0';
      Serial.println();
      delay(10);
      incomingChar=SIM900.read();
      int lower = incomingChar-'0';
      Serial.print(lower);
      if((upper*10+lower)<=60){//check for incorrect range of values
        THRESHOLD = upper*10+lower;
        Serial.println(F("Command received to change threshhold to: "));
        Serial.println(THRESHOLD);
      }
     }

   }
  // Wait a few seconds between measurements.

  currentSensorReadMillis = millis();
  currentSensorLogMillis = millis();
  if (currentSensorReadMillis - startSensorReadMillis >= 5000)  //test whether the period has
elapsed
  {

    if(sensor_fail_count>=5){
      SIM900.println(F("AT + CMGS = \"+233206657618\""));
      delay(100);
      SIM900.print(F("There might be problem reading from sensor"));
      delay(100);
      SIM900.println((char)26);//^Z
      delay(100);
      SIM900.println();
     sensor_fail_count=-1000;
     Serial.println(F("Sensor read error, Sending SMS to notify"));
    }

      Area = 3*(55.0 * 43.0) / (100*100); // we are dividing by 10000 get the area in square
meters
```

University of Ghana http://ugspace.ug.edu.gh

```
  float raw_read = analogRead(A0);
  //Serial.println(raw_read);
  voltage = 55*(raw_read/1023);//map(raw_read, 0, 1023, 0, 55);
  Power = pow(voltage, 2) / 1 ; // Calculating power
  Radiation = Power / (Area);
  //Serial.println(Area);
  //Serial.println(Power);
  //Radiation = 60;
  //char *msg;
  //sprintf(msg, " R %f W/M2 ", Radiation); // Generating message to be printed
  //lcd.setCursor(0, 0);
  lcd.setCursor(0, 1);
  lcd.print((int)voltage);
  lcd.print(F("V, "));
  lcd.print((int)Radiation);
  lcd.print(F("W/M2"));

    // Reading temperature or humidity takes about 250 milliseconds!
    // Sensor readings may also be up to 2 seconds 'old' (its a very slow sensor)

     h = dht.readHumidity();
    // Read temperature as Celsius (the default)
    t = dht.readTemperature();
    // Read temperature as Fahrenheit (isFahrenheit = true)
    //float f = dht.readTemperature(true);

    // Check if any reads failed and exit early (to try again).

    // Compute heat index in Fahrenheit (the default)
    //float hif = dht.computeHeatIndex(f, h);
    // Compute heat index in Celsius (isFahreheit = false)
    //float hic = dht.computeHeatIndex(t, h, false);
    ah = (6.112*pow(2.71828,(17.67*t/(t+243.5)))*h*2.1674)/(273.15+t);
    lcd.setCursor(0, 0);
    lcd.print(F("rH:"));
    lcd.print((int)h);
    lcd.print(F(" aH:"));
    lcd.print((int)ah);

    lcd.print(F(" T:"));
    lcd.print((int)t);
    Serial.println(h);
    if (isnan(h) || isnan(t)) {
      lcd.setCursor(0, 0);
      lcd.print(F("SENSOR FAILED   "));
      Serial.println(F("Failed to read from DHT sensor!"));
      sensor_fail_count++;
      //delay(1000);
      //startSensorLogMillis = currentSensorLogMillis;
      //return;

    }
    //sendDataToServer();
    if(is_sd_card_initialized && tick==1){

      tick++;

    }
    startSensorReadMillis = currentSensorReadMillis;
  }

  if (currentSensorLogMillis - startSensorLogMillis >= sensor_log_period)  //test whether the
period has elapsed
  {

      SIM900.println(F("AT + CMGS = \"+233206657618\""));
      delay(100);
      String dataMessage = ( "thr#"+String(h) + "," + String(ah) + ","+ String(t) + ","+
String(voltage) + ","+ String(Radiation));
      SIM900.print(dataMessage);
      delay(100);
```

University of Ghana http://ugspace.ug.edu.gh

```
      SIM900.println((char)26);
      delay(100);
      SIM900.println();
      SendDataToServer(dataMessage);


    startSensorLogMillis = currentSensorLogMillis;

   }

 if(ah>=THRESHOLD||force_start_fan){
   if(!is_moto_running){
  digitalWrite(MOTOPIN,LOW);//this will turn on fan1 since the relay is connected in normally
open mode
  digitalWrite(MOTOPIN2,LOW);//this will turn on fan2 since the relay is connected in normally
open mode
  digitalWrite(ledPin,HIGH);
   is_moto_running=true;
   }
  }
    else if(ah<THRESHOLD||force_stop_fan){
    if(is_moto_running){
     digitalWrite(MOTOPIN,HIGH);
     digitalWrite(MOTOPIN2,HIGH);
     digitalWrite(ledPin,LOW);
      is_moto_running=false;
    }
      }


}
```

University of Ghana http://ugspace.ug.edu.gh

APPENDIX 2: Temperature and Relative Humidity Profile

Comparison of the temperature and relative humidity of PV-Greenhouse Solar Dryer (PVGSD) and open sun (OSD)

		PVGSD			OSD			
Day	**Time, h**	**Temperature, °c**	**Relative humidity, %**	**Dew point, °c**	**Temperature, °c**	**Relative humidity, %**	**Dew point, °c**	**Comment**
1	6:00	29.5	65.5	22.3	26.5	53.0	16.1	Sunny
	8:00	29.5	65.5	22.3	27.0	55.0	17.2	
	10:00	42.0	53.0	30.4	32.5	62.5	24.4	
	12:00	63.0	26.5	36.4	35.0	57.5	25.3	
	14:00	66.5	23.5	37.0	39.0	47.0	25.5	
	16:00	56.0	27.0	30.9	36.5	54.5	25.8	
	18:00	41.5	40.0	25.1	31.0	69.0	24.6	
	20:00	38.5	45.0	24.4	30.5	66.5	23.5	
2	6:00	30.0	75.5	29.2	29.5	60.0	20.9	Very cloudy
	8:00	30.5	75.0	29.6	29.0	60.0	20.4	
	10:00	40.0	63.5	31.7	32.0	64.5	24.5	
	12:00	44.0	52.5	32.1	33.5	56.0	23.5	
	14:00	50.5	41.0	33.5	36.5	46.0	23.0	
	16:00	54.5	52.5	32.9	37.5	44.0	23.2	
	18:00	39.0	52.5	27.5	30.5	63.5	22.8	
	20:00	36.0	62.5	27.7	30.5	64.0	22.9	
3	6:00	31.0	73.5	25.7	29.0	60.0	20.4	Rained most part of the day
	8:00	35.5	64.0	27.6	29.5	72.5	24.0	
	10:00	42.5	51.5	30.4	31.5	65.5	24.2	
	12:00	50.0	76.0	25.3	35.5	73.5	24.0	
	14:00	54.0	70.0	27.7	34.5	70.5	24.0	
	16:00	38.5	81.5	25.0	26.5	80.0	25.0	
	18:00	28.0	73.0	22.7	26.3	81.0	25.0	
	20:00	28.0	74.0	22.9	26.2	81.0	25.0	
4	6:00	29.0	72.0	23.4	28.5	56.0	22.6	Sunny day
	8:00	30.5	78.0	26.2	29.0	47.0	20.0	
	10:00	41.0	58.5	31.2	33.0	56.0	23.0	
	12:00	61.0	25.0	33.7	38.5	48.5	25.7	
	14:00	68.5	17.5	33.3	39.5	46.5	25.9	
	16:00	55.0	23.5	27.6	33.5	60.5	24.8	
	18:00	39.5	40.0	23.4	32.0	65.5	24.7	
	20:00	38.0	50.0	25.8	30.5	71.5	24.8	

University of Ghana http://ugspace.ug.edu.gh

Comparison of the temperature and relative humidity of PV-Greenhouse Solar Dryer (PVGSD) and open sun (OSD)

		PVGSD			OSD			
Day	**Time, h**	**Temperature, °c**	**Relative humidity, %**	**Dew point, °c**	**Temperature, °c**	**Relative humidity, %**	**Dew point, °c**	**Comment**
5	6:00	34.5	58.5	25.5	30.5	75.0	25.6	Partly sunny
	8:00	37.0	54.5	26.3	34.5	61.0	25.9	
	10:00	38.0	57.0	28.0	35.5	57.0	25.7	
	12:00	54.0	30.0	31.0	35.0	57.0	25.2	
	14:00	56.0	25.0	29.5	36.5	53.0	25.4	
	16:00	48.0	30.0	25.9	33.5	60.5	24.8	
	18:00	35.0	49.5	22.8	30.5	71.5	24.8	
	20:00	31.5	60.0	22.8	28.5	52.5	17.8	
6	6:00	27.5	74.5	22.6	26.4	83.1	23.7	Partly sunny
	8:00	29.5	73.0	24.1	28.0	82.0	25.6	
	10:00	41.0	57.0	30.8	30.0	74.0	24.9	
	12:00	50.5	37.0	31.7	33.5	66.0	26.3	
	14:00	58.5	26.0	32.0	36.0	55.5	25.7	
	16:00	56.0	27.5	31.2	36.5	53.0	25.4	
	18:00	41.0	39.5	24.5	33.5	60.5	24.8	
	20:00	38.0	44.0	23.6	30.5	71.5	24.8	
7	6:00	30	74.0	24.9	28.0	67.5	21.4	Sunny
	8:00	32.5	66.0	25.3	30.5	66.5	23.5	
	10:00	43.5	51.0	31.1	34.5	59.0	25.3	
	12:00	61.0	26.5	34.7	36.5	51.0	24.7	
	14:00	66.0	21.5	35.0	37.5	48.5	24.8	
	16:00	57.0	24.5	30.0	35.5	56.0	25.4	
	18:00	41.5	37.0	23.8	33.0	63.0	25.0	
	20:00	34.0	49.0	21.8	30.5	71.5	24.8	
8	6:00	28.5	65.0	21.3	30.5	75.0	25.6	Sunny
	8:00	33.5	64.5	25.9	30.5	75.0	25.6	
	10:00	45.0	49.0	31.8	35.0	57.0	25.2	
	12:00	55.5	33.0	34.0	37.5	50.5	25.5	
	14:00	69.0	18.0	34.2	41.5	42.0	26	
	16:00	63.5	19.0	30.8	39.5	44.0	25	
	18:00	43.5	81.5	39.6	35.5	55.5	25.2	
	20:00	41.0	76.0	35.9	33.5	60.5	24.8	
9	6:00	33.5	72.0	32.0	30.5	69.5	24.3	Sunny
	8:00	36.0	71.0	34.3	33.5	66.0	26.3	
	10:00	49.0	52.5	36.7	35.0	57.0	25.2	
	12:00	67.0	26.5	39.7	38.5	49.5	26.0	
	14:00	69.0	20.0	36.1	41.5	42.0	26.0	
	16:00	54.0	28.0	29.8	38.5	48.0	25.5	
	18:00	40.5	40.0	24.3	31.5	68.5	25.0	
	20:00	30.5	52.0	20.6	31.5	61.0	23.1	

University of Ghana http://ugspace.ug.edu.gh

Comparison of the temperature and relative humidity of PV-Greenhouse Solar Dryer (PVGSD) and open sun (OSD)

		PVGSD			OSD			
Day	**Time, h**	**Temperature, °c**	**Relative humidity, %**	**Dew point, °c**	**Temperature, °c**	**Relative humidity, %**	**Dew point, °c**	**Comment**
10	6:00	30.0	71.5	24.3	29.5	63.0	21.7	Sunny
	8:00	38.0	54.5	27.8	30.0	65.5	22.8	
	10:00	50.0	41.0	33.1	36.5	56.0	26.3	
	12:00	55.5	29.0	31.7	37.0	53.0	25.8	
	14:00	67.0	19.5	34.1	40.5	43.5	25.7	
	16:00	57.5	23.0	29.3	38.5	48.0	25.5	
	18:00	42.0	41.0	19.9	33.5	60.5	24.8	
	20:00	39.5	47.5	19.7	31.0	70.0	24.9	
11	6:00	30.0	68.5	23.6	29.5	74.0	24.4	Sunny
	8:00	32.0	62.0	23.8	30.0	72.5	24.5	
	10:00	51.0	31.0	29.1	36.5	55.5	25.2	
	12:00	64.5	22.5	34.6	40.5	36.5	22.7	
	14:00	66.5	17.5	31.7	41.5	41.5	25.8	
	16:00	53.5	24.0	26.8	36.5	54.0	25.7	
	18:00	44.5	33.5	24.8	32.5	44.5	18.8	
	20:00	36.0	49.0	23.6	30.5	54.5	20.3	

University of Ghana http://ugspace.ug.edu.gh

APPENDIX 3: Temperature, Relative Humidity (Rh) And Solar Radiation Data for PVGSD, GSD and OSD.

Baseline Average of Temperature, Relative humidity and Solar radiation of PV-greenhouse solar dryer (PVGSD), Greenhouse solar dryer (GSD) and Open sun drying (OSD)

Day	Time, hr	PVGSD		GSD		OSD		Solar rad. W/m^2
		Temperature, °c	RH, %	Temperature, °c	RH, %	Temperature, °c	RH, %	
1	6:00	30.5	68	30.5	71	30	71.5	254.63
	9:00	45.5	40	42	44.5	33	63.5	356.95
	12:00	60.5	23	61	27	41	43	399.13
	15:00	68	18	65	20	44	36	688.19
	18:00	41	33	38	40.5	30.5	68	215.51
	21:00	28.5	60	28.5	65	29	66.5	52.95
2	00:00	30	60	30	65.5	29.5	41.5	44.06
	03:00	30	66.5	29	69	29	40.5	20.54
	06:00	30	69	29	73	28	59.5	140.94
	09:00	44.5	44	40.5	50.5	32	65	308.1
	12:00	66	20	62	23	40.5	42.5	359.36
	15:00	71	14	69	15	44.5	36.5	753.28
	18:00	41.5	35	38	42	32.5	59.5	109.57
	21:00	29	58	29	61.5	29.5	73	36.77
3	00:00	29	58	29	59.5	28.5	78	22.92
	03:00	27.5	60	27.5	65	28	81.5	44.06
	06:00	28.4	68	27.5	76.5	27	84.5	240.57
	09:00	35	74	33	79	30	67.5	27.39
	12:00	62.5	25	58	38.5	39	44.5	271.18
	15:00	65.5	19	63	20.5	42.5	38	394.04
	18:00	40	39	38	50	31.5	65.5	308.1
	21:00	32	58	30	63	29.5	73	340.27
4	00:00	29	76	29	79	28.5	78	333.24
	03:00	29	79	29	82	28	81.5	354.54
	06:00	30.5	82	30	84	28	84.5	273.29
	09:00	48	47	44	55.5	33.5	67.5	323.98
	12:00	68.5	23.5	65	33	46	34	401.68
	15:00	71	16	69	18.5	40.5	41	749.78
	18:00	39	33	36	40.5	31	66	109.57

University of Ghana http://ugspace.ug.edu.gh

APPENDIX 4: Moisture content variation of red pepper

Moisture content variation of Red Pepper

Drying time (hr)	Moisture Content (%±SD)		
	PVGSD	GSD	OSD
0	77.000 ± 1.00	77.000 ± 1.00	77.000 ± 1.00
12	54.711 ± 0.145	56.544 ± 0.566	70.475 ± 1.031
24	50.641 ± 0.194	52.194 ± 0.283	69.044 ± 0.331
36	11.891 ± 0.186	12.981 ± 0.126	62.682 ± 1.063
48	11.336 ± 0.345	13.262 ± 0.432	58.970 ± 0.755
60	7.624 ± 0.141	9.919 ± 0.129	53.381 ± 0.652
72	5.738 ± 0.198	6.045 ± 0.172	49.594 ± 1.011
84			37.565 ± 0.664
96			36.982 ± 0.305
108			27.065 ± 0.581
120			24.685 ± 0.431
132			14.363 ± 0.612
144			13.158 ± 0.330
150			10.740 ± 0.845
152			8.365 ± 0.158

University of Ghana http://ugspace.ug.edu.gh

APPENDIX 5: Drying rate of Red Pepper

Drying rate of Red Pepper (basis: initial moisture and 12 hours drying intervals)

Drying time (hr)	Drying rate (g/g h)		
	PVGSD	GSD	OSD
0			
12	0.178	0.170	0.080
24	0.097	0.094	0.047
36	0.067	0.089	0.046
48	0.089	0.067	0.039
60	0.054	0.054	0.037
72	0.046	0.046	0.033

University of Ghana http://ugspace.ug.edu.gh

APPENDIX 6: Moisture content of cassava using 80watts battery

Moisture content variation of Cassava using the 80watts battery

Drying time (hr)	Moisture Content (%±SD)					
	PVGSD Slices	**PVGSD Chunks**	**GSD Slices**	**GSD Chunks**	**OSD Slices**	**OSD Chunks**
0	64.00±0.580	64±0.580	64±0.580	64±0.580	64±0.580	64±0.580
12	37.58±1.160	52.42±0.448	40.33±0.750	53.52±0.379	49.84±0.198	54.40±0.688
24	31.91±0.762	46.99±0.554	35.94±0.861	48.27±0.712	41.32±0.476	50.41±0.856
36	17.87±0.542	23.33±0.843	19.01±0.431	25.31±0.209	27.23±0.759	32.54±0.397
48	16.31±0.581	21.22±1.012	17.03±0.766	23.72±0.403	25.62±0.668	30.29±0.570
60	10.00±0.732	13.52±0.315	10.02±0.356	14.25±0.397	13.61±0.466	18.53±0.976
72	9.71±0.225	10.40±0.812	9.72±0.501	11.23±0.460	11.44±0.421	16.99±1.010
84	7.45±0.422	8.48±0.765	7.57±0.230	9.43±0.226	9.13±0.789	10.09±0.299

University of Ghana http://ugspace.ug.edu.gh

APPENDIX 7: Drying rate of cassava using 80watts battery

Drying rates of Cassava using the 80watts battery (basis: initial moisture and 12 hours drying intervals)

Drying time (hr)	Drying rate (g/g h)					
	PVGSD Slices	**PVGSD Chunks**	**GSD Slices**	**GSD Chunks**	**OSD Slices**	**OSD Chunks**
0						
12	0.0979	0.0563	0.0918	0.0522	0.0653	0.0487
24	0.0545	0.0371	0.0507	0.0352	0.0447	0.0317
36	0.0433	0.0409	0.0428	0.0399	0.0389	0.0359
48	0.0330	0.0314	0.0328	0.0306	0.0298	0.0279
60	0.0278	0.0270	0.0278	0.0269	0.0270	0.0258
72	0.0232	0.0231	0.0232	0.0229	0.0228	0.0218
84	0.0202	0.0199	0.0200	0.0199	0.0120	0.0198

University of Ghana http://ugspace.ug.edu.gh

APPENDIX 8: Moisture content of cassava using 1200watts battery

Moisture content variation of Cassava using the 1200watts battery

Drying time (hr)	Moisture Content (%±SD)					
	PVGSD Slices	**PVGSD Chunks**	**GSD Slices**	**GSD Chunks**	**OSD Slices**	**OSD Chunks**
0	65.00±0.71	65.00±0.71	65.00±0.71	65.00±0.71	65.00±0.71	65.00±0.71
12	54.14±1.210	56.68±0.248	59.95±0.640	58.94±0.322	61.96±0.118	61.76±0.150
24	52.56±0.751	55.87±0.134	60.84±0.221	60.02±0.659	62.7±0.246	64.36±0.762
36	31.89±0.122	52.19±0.221	43.61±0.731	55.45±0.209	50.97±0.559	60.47±0.933
48	29.47±0.471	51.07±1.012	45.97±0.986	56.13±0.562	54.58±0.163	62.98±0.821
60	14.35±0.209	40.02±0.618	25.88±0.106	47.48±0.981	34.22±0.666	51.71±0.346
72	13.49±0.542	38.77±0.456	23.91±0.502	48.12±0.671	31.73±0.321	52.9±1.211
84	9.74±0.222	25.76±0.112	14.31±0.240	35.18±0.314	16.2±0.419	41.19±0.649
96		23.98±0.450	15.84±0.569	34.01±0.178	18.51±0.530	40.34±0.372
108		13.96±0.109	9.89±0.789	19.62±0.897	11.41±0.689	24.09±0.514
120		12.76±0.234		20.87±0.341	10.03±0.651	25.37±0.932

University of Ghana http://ugspace.ug.edu.gh

APPENDIX 9: Drying rates of cassava using 1200watts battery

Drying rates of Cassava using the 1200watts battery (basis: initial moisture and 12 hours drying intervals)

Drying time (hr)	Drying rate (g/g.h)					
	PVGSD Slices	**PVGSD Chunks**	**GSD Slices**	**GSD Chunks**	**OSD Slices**	**OSD Chunks**
0						
12	0.0563	0.0457	0.0300	0.0351	0.0190	0.0201
24	0.0312	0.0246	0.0126	0.0148	0.0073	0.0021
36	0.0385	0.0212	0.0301	0.0170	0.0227	0.0090
48	0.0299	0.0169	0.0209	0.0120	0.0136	0.0032
60	0.0281	0.0198	0.0251	0.0158	0.0222	0.0131
72	0.0236	0.0169	0.0214	0.0129	0.0193	0.0101
84	0.0208	0.0179	0.0201	0.0156	0.0198	0.0137
96		0.0160	0.0173	0.0139	0.0169	0.0123
108		0.0156	0.0161	0.0149	0.0160	0.0142
120		0.0142		0.0132	0.0145	0.0126

University of Ghana http://ugspace.ug.edu.gh

APPENDIX 10: Analysis of variance (ANOVA) on color profile for red pepper

Analysis of Variance (ANOVA) on the color profile (L^*) for Red Pepper

Source	DF	SS	MS	F-Value	P-Value	F crit.
Drying days	818.2912	3	272.7637	124.1445	9.49E-15	3.008787
Drying method	95.3173	2	47.65865	21.69116	4.17E-06	3.402826
Interaction	37.78482	6	6.297469	2.866204	0.02995	2.508189
Error	52.73152	24	2.197147			
Total	1004.125	35				

Analysis of Variance (ANOVA) on the color profile (a^*) for Red Pepper

Source	DF	SS	MS	F-Value	P-Value	F crit.
Drying days	774.2019	3	258.0673	247.3031	3.56E-18	3.008787
Drying methods	107.1656	2	53.58282	51.34783	2.13E-09	3.402826
Interaction	213.6637	6	35.61062	34.12527	1.32E-10	2.508189
Error	25.04463	24	1.043526			
Total	1120.076	35				

Analysis of Variance (ANOVA) on the color profile (b^*) for Red Pepper

Source	DF	SS	MS	F-Value	P-Value	F crit.
Drying days	982.6277	3	327.5426	945.8898	4.86E-25	3.008787
Drying method	74.60442	2	37.30221	107.7227	1.03E-12	3.402826
Interaction	33.3741	6	5.56235	16.06316	2.39E-07	2.508189
Error	8.310717	24	0.34628			
Total	1098.917	35				

University of Ghana http://ugspace.ug.edu.gh

APPENDIX 11: Analysis of variance (ANOVA) on color profile for cassava

Analysis of Variance (ANOVA) on the color profile (L^*) for Cassava samples

Source	DF	SS	MS	F-Value	P-Value
Drying method	2	3.913	1.9566	5.42	0.021
Sample size	1	0.612	0.6124	1.70	0.217
Drying day	2	184.932	92.4662	256.35	0.000
Error	12	4.328	0.3607		
Total	17	193.787			

Analysis of Variance (ANOVA) on the color profile (a^*) for Cassava samples

Source	DF	SS	MS	F-Value	P-Value
Drying method	2	0.05137	0.025683	2.46	0.135
Sample size	1	0.14169	0.141689	13.57	0.004
Drying day	2	1.15961	0.579803	55.54	0.000
Interaction	2	0.00582	0.002911	0.28	0.762
Error	10	0.10439	0.010439		
Total	17	1.46287			

Analysis of Variance (ANOVA) on the color profile (b^*) for Cassava samples

Source	DF	SS	MS	F-Value	P-Value
Drying method	2	2.695	1.348	5.09	0.030
Sample size	1	0.565	0.565	2.14	0.175
Drying day	2	282.085	141.042	532.83	0.000
Interaction	2	0.504	0.252	0.95	0.418
Error	10	2.647	0.265		
Total	17	288.496			

University of Ghana http://ugspace.ug.edu.gh

APPENDIX 12: Particle size distribution of cassava flour

Dried Cassava Slices and Chunks Flour Particle Size Distribution

Sieve size µm	PVGSD		GSD		OSD	
	Slices flour	Chunks flour	Slices Flour	Chunks flour	Slices flour	Chunks flour
	Weight Retained (%)					
500	1.97	7.29	2.65	4.34	4.55	7.37
300	3.97	6.75	5.91	5.51	5.94	7.07
212	6.79	7.29	8.96	7.27	9.87	7.28
150	11.89	27.05	14.90	27.2	14.90	28.52
106	25.65	18.68	26.15	19.5	27.59	17.45
75	12.57	10.61	10.10	9.63	12.54	9.07
53	24.01	13.56	21.02	17.26	16.88	15.87
45	12.91	8.7	10.22	9.2	7.62	7.27
Pan	0.12	0	0.00	0	0.00	0